



FRONT MOUNTING BICYCLE ATTACHMENT FOR IMPROVED ACCESSIBILITY OF  
ADULT PASSENGERS

A Major Qualifying Project Proposal  
Submitted to the Faculty  
of the  
WORCESTER POLYTECHNIC INSTITUTE  
in partial fulfillment of the requirements for the  
Degree of Bachelor of Science

Submitted by:

---

Victor Montero

---

Kelly Roberge

---

Brandon Stuczko

Submitted to:

Professor Holly Ault

Professor Allen Hoffman

April 28, 2011

## **ABSTRACT**

Current most bicycle attachments capable of transporting an adult passenger are limited to rear mounting products. Few available devices place the passenger in front of the existing bicycle which would significantly improve the passenger's range of vision and enjoyment. In addition, these current devices are purchased as stand-alone units that include both the bicycle and attachment which make them expensive and inconvenient. The goal of this project is to design a front mounting device capable of carrying an adult passenger that can be purchased separately and then attached to an existing bicycle. Two important design characteristics of this device were adaptability and accessibility; the device was designed to attach to different bicycle frames and accommodate a range of adult passengers, including those with limited mobility. After benchmarking current products, a design was developed satisfying this project goal. The steering system uses a parallelogram linkage to transfer rotational motion of the existing bicycle handlebars to two adjacent device wheels for a 1:1 steering ratio to maintain driver cycling instincts. The attachment mechanism consists of a compression device between the existing bicycle head tube and the space between the top and down tubes of the frame to maintain rigidity of the system while not harming the bicycle. Recommendations are made at the end of this report in order to provide solutions to problems discovered during the design and manufacturing processes.

## **ACKNOWLEDGEMENTS**

The team would like to thank Professors Allen Hoffman and Holly Ault for their guidance throughout this project. The team would also like to thank Neil Whitehouse for his extensive help with the manufacturing of the prototype. His expertise and advice were greatly appreciated.

# TABLE OF CONTENTS

ABSTRACT .....	i
ACKNOWLEDGEMENTS .....	ii
LIST OF FIGURES .....	vii
LIST OF TABLES .....	xiii
CHAPTER 1: INTRODUCTION .....	1
CHAPTER 2: BACKGROUND .....	3
2.1 Benchmarked Patents and Products .....	3
2.1.1 Rear Mounted Devices .....	3
2.1.2 Side-by-Side Devices .....	12
2.1.3 Front Mounted Devices .....	16
CHAPTER 3: PROJECT GOAL .....	31
CHAPTER 4: DESIGN SPECIFICATIONS .....	32
CHAPTER 5: FRAME DESIGN .....	35
5.1 Preliminary Frame Designs .....	35
5.2 Frame Selection .....	37
5.2.1 Sub-Frame Design Modifications .....	38
5.3 Free Body Diagrams and Stress Analysis .....	42
CHAPTER 6: STEERING DESIGN .....	51
6.1 Preliminary Steering Designs .....	51
6.1.1 Direct Attachment Steering .....	51
6.1.2 Cross Linkage Steering .....	53

6.1.3 Fork Replacement Steering.....	54
6.1.4 Long John Steering .....	55
6.1.5 Single Chain Driven Steering .....	57
6.1.6 Multiple Chain Driven Steering.....	58
6.1.7 Rack and Pinion Steering.....	59
6.2 Steering Selection .....	60
6.3 Steering System Design Variables.....	61
6.4 Zero-th Order Prototypes .....	62
6.4.1 Cross Linkage Steering System Prototype.....	62
6.4.2 Long John Style Steering System Prototype.....	64
6.5 Graphical Analysis.....	66
6.5.1 Cross Linkage Steering System .....	67
6.5.2 Long John Style Steering System .....	69
6.6 Computer Aided Kinematic Analysis .....	70
6.6.1 Cross Linkage Steering System .....	70
6.6.2 Long John Style Steering System .....	71
6.6.3 Steering System Re-Design .....	73
6.7 Steering Analysis .....	75
6.8 Stress Analysis .....	78
6.8.1 Horizontal Fork Analysis.....	78

CHAPTER 7: ATTACHMENT.....	83
7.1 Head Tube.....	83
7.2 Front Hub.....	84
7.3 Direct Fork Connection to Device.....	85
7.4 Attachment Decision.....	86
CHAPTER 8: FINAL DESIGN.....	91
8.1 Attachment.....	91
8.2 Steering.....	94
8.3 Device Frame.....	97
8.4 Safety Details.....	98
CHAPTER 9: MANUFACTURING.....	99
9.1 Purchased Parts.....	99
9.2 Reused Parts.....	103
9.3 Budget.....	104
9.4 Assembly.....	104
CHAPTER 10: TESTING.....	120
10.1 Device Frame Testing.....	120
10.1.1 Device Weight Test.....	120
10.2 Steering Testing.....	121
10.2.1 Force Transmission Test.....	121
10.2.2 Steering Angle Test.....	122

10.3 Parking Brake Test.....	122
10.4 Dynamic Testing.....	123
10.4.1 Braking Test.....	123
10.4.2 Steering Test .....	123
CHAPTER 11: RESULTS.....	125
CHAPTER 12: RECOMMENDATIONS.....	128
12.1 Device Frame .....	128
12.2 Attachment.....	129
12.3 Steering .....	129
CHAPTER 13: CONCLUSION .....	131
WORKS CITED .....	133
APPENDIX A: BICYCLE REGULATIONS.....	136
APPENDIX B: FRAME ANALYSIS .....	140
APPENDIX C: STEERING.....	173
APPENDIX D: ATTACHMENT MECHANISM.....	175
APPENDIX E .....	183

## LIST OF FIGURES

Figure 1: Pedicab Flatbed .....	4
Figure 2: Trailer Bicycle.....	4
Figure 3: Pedicab Shifter .....	5
Figure 4: Rear Differential Axle.....	5
Figure 5: Hydraulic Disc Brakes.....	6
Figure 6: Pedillac Pedicab .....	7
Figure 7: T.I.P.K.E Pedicab.....	7
Figure 8: Mains Street Pedicabs .....	8
Figure 9: Pedaltek Trailer .....	9
Figure 10: Chariot Carrier X-Country .....	10
Figure 11: Patent 4546992, the Sportcycle.....	11
Figure 12: Patent 4546992, Sportcycle Handlebar .....	12
Figure 13: Lightfoot Cycle Duos .....	13
Figure 14 - American Speedster Sidekick .....	14
Figure 15: Patent 4178008, Side by Side Bicycle.....	16
Figure 16: Bella Bike .....	17
Figure 17: Bella Bike Steering Mechanism.....	18
Figure 18: Bella Bike Steering Mechanism.....	19
Figure 19: Christiania Bike.....	20
Figure 20: Christiania Bike Cargo Frame.....	20
Figure 21: Nihola .....	21
Figure 22: Nihola Steering Mechanism .....	21
Figure 23: Taga.....	22



Figure 24: Taga Steering Linkage System.....	23
Figure 25: Trio Bike.....	23
Figure 26: Trio Steering Linkage System.....	24
Figure 27: The Zigo .....	24
Figure 28: Zigo Steering Linkage System .....	25
Figure 29: The Duet .....	26
Figure 30: Duet Steering Linkage System .....	27
Figure 31: Patent 4830388, Multi-Functional Wheelchair Assembly .....	29
Figure 32: Patent 4830388, U shaped adapter .....	29
Figure 33: US Patent 4,767,130, Foldable Pedicab .....	30
Figure 34: Self Supporting Chair.....	35
Figure 35: Chair on Sub-frame .....	36
Figure 36: Cargo Box with Seat.....	37
Figure 37: Sub-Frame Modification 1 .....	38
Figure 38: Free Body Diagram of Wheel Connection.....	39
Figure 39: Free Body Diagram of Wheel Connection Section 1 .....	40
Figure 40: Sub-Frame Modification 2 .....	41
Figure 41: Final Design .....	42
Figure 42: FBD of the Frame's Front View .....	43
Figure 43 : FBD of the Frame's Side View.....	44
Figure 44: Front View Shear Diagram.....	48
Figure 45: Front View Moment Diagram .....	48
Figure 46: Front View Deflection Diagram.....	49

Figure 47: Side View Deflection Diagram .....	49
Figure 48: Direct Attachment System.....	52
Figure 49: Cross Linkage Steering System.....	54
Figure 50: Fork Replacement Steering System .....	55
Figure 51: Long John Steering.....	56
Figure 52: Single Chain Steering System .....	57
Figure 53: Multiple Chain Design .....	58
Figure 54: Rack and Pinion Design .....	59
Figure 55: Steering System Design Variables .....	61
Figure 56: The Nihola.....	63
Figure 57: Nihola's Steering System.....	63
Figure 58: Cross Linkage Steering Zero-th Order Prototype.....	64
Figure 59: Long John.....	65
Figure 60: Long John Style Steering Zero-th Order Prototype.....	66
Figure 61: Cross Linkage Neutral and Toggle Positions .....	67
Figure 62: Cross Linkage Turned Position (revised).....	68
Figure 63: Long John Style Neutral Position.....	69
Figure 64: Long John Style Turned Position .....	70
Figure 65: Cross Linkage Four Bar Model.....	71
Figure 66: Long John Style Four Bar Model.....	72
Figure 67: Long John Style Four Bar Model Theta Values and Transmission Angle.....	73
Figure 68: Device Steering Kinematics .....	74
Figure 69: Detailed CAD Illustration of Steering System.....	75

Figure 70: Horizontal Fork Side View Free Body Diagram.....	76
Figure 71: Fork Arm Free Body Diagram .....	77
Figure 72: Fork Arm Connection Free Body Diagram.....	78
Figure 73: Input Horizontal Fork Displacement.....	79
Figure 74: Input Horizontal Fork Stress Analysis .....	80
Figure 75: Right Output Horizontal Fork Displacement .....	81
Figure 76: Right Output Horizontal Fork Stress Analysis.....	82
Figure 77: Head Tube Attachment.....	84
Figure 78: Front Hub Attachment.....	85
Figure 79: Direct Fork Connection .....	85
Figure 80: C Attachment Side View .....	88
Figure 81: C Attachment Top View.....	88
Figure 82: Elbow Joint Attachment .....	90
Figure 83: Final Design .....	91
Figure 84: Vertical Adjustment of Attachment Mechanism.....	92
Figure 85: Vertical Adjustment T Fitting .....	93
Figure 86: Angular Adjustment of Attachment Mechanism.....	94
Figure 87: CAD Illustration of Steering System.....	95
Figure 88: Middle Horizontal Fork Angle Adjustability .....	96
Figure 89: Design with New Wheel Placement.....	97
Figure 90: Device Wheel Attachment.....	98
Figure 91: Piece of tubing that will be bolted on the left and threaded on the right.....	99
Figure 92: T fitting with three bolt fits .....	100

Figure 93: Horizontal Fork Prototype.....	101
Figure 94: Steering System.....	102
Figure 95: Head Tube Attachment.....	103
Figure 96: Slip vs. Screw of Attachment.....	105
Figure 97: Slip vs. Screw for Bicycle Connection.....	105
Figure 98: Slip vs. Screw for Back of Device .....	106
Figure 99: Slip vs. Screw for Bottom of Device.....	107
Figure 100: Screw vs. Slip for Arms of Device.....	107
Figure 101: Wood Frame .....	109
Figure 102: Extension for Back Wheel Attachment.....	110
Figure 103: Large Device Wheel.....	110
Figure 104: Back View of the Device Showing Wheel Attachments.....	111
Figure 105: Vertical Adjustment of Attachment System.....	112
Figure 106: Side View of the Attachment System.....	113
Figure 107: Square Tubing and Head Tube Connection .....	114
Figure 108: Attachment System.....	115
Figure 109: Seat Attachment .....	116
Figure 110: Device Seatbelt.....	116
Figure 111: Seatbelt Attachment .....	117
Figure 112: Footrest.....	118
Figure 113: Parking Brake Control.....	118
Figure 114: Parking V-Brake on Device Wheel .....	119
Figure 115: Head Tube Attachment Mechanism.....	125

Figure 116: Horizontal Fork Attachment..... 126

## **LIST OF TABLES**

Table 1: Rear Mounting Products .....	10
Table 2: Comparison of Side by Side Devices .....	15
Table 3: Comparison of Front Mounting Systems.....	28
Table 4: Initial Values for FBD of the Front View.....	43
Table 5: Forces Acting on the Frame.....	45
Table 6: Summary of Singularity Functions.....	47

## **CHAPTER 1: INTRODUCTION**

The popularity of human-powered transportation, or active transportation, in the United States is primarily in recreational cycling. Recreational cyclists add modifications to their bicycles for either increased functionality or enjoyment. These modifications include suspension forks, mirrors, after market seats, and even cycling computers that can record and display statistics of the bike ride such as the distance traveled or the average speed. One common modification sought after by many cyclists is the ability to safely transport passengers.

The majority of the products on the market allowing bicycles or tricycles to transport passengers place the passenger behind the cyclist. This position is detrimental to the passenger's enjoyment of the ride because it severely limits their view. However, a device that places the passenger in front of the cyclist would give the passenger an unobstructed view and therefore a more enjoyable bike ride.

Currently, few products on the market place the passengers at the front of the bike, and are primarily designed to transport small children. Many of these devices are similar to a stroller and a number of them can be converted into a stroller or jogger. However, the product market for adult passengers is severely limited. In addition, many of these products are very expensive and a consumer would have to buy a complete system comprising both the bike and attachment.

The project goal is to create an attachable device allowing an adult passenger, including those with limited mobility, to sit in front of a cyclist. This device would address the needs of a target audience that is presently being overlooked: the elderly and adults with disabilities. This population is unable to use a number of the attachments currently on the market even though they may be the ones who could benefit from it the most, especially because they may not be able to ride a bicycle by themselves. In addition, this product would be desirable to more people because the consumer would not have to buy a whole new system, just an attachment to a bicycle

they already own; this option would be less expensive than many products currently on the market and therefore a more realistic option for many families.



## **CHAPTER 2: BACKGROUND**

The design team identified current products for passenger transportation that could serve as benchmarks for the device. These benchmarked devices aided in design and assisted with identifying related componentry which could potentially be useful.

### **2.1 Benchmarked Patents and Products**

The team researched numerous bicycle and tricycle variations designed for the purpose of passenger transportation, with emphasis placed towards devices capable of transporting adults. It was essential to identify the products that are currently on the market in order to understand the competition for this device. It is important to classify what types of products are available, their intended purpose, and their target audience. By looking into current designs the team was able to determine what items are well designed and what items are problematic; information helpful while designing the device.

Looking into patents was also necessary while benchmarking the product in order to determine related concepts to the design that may not have made it to the market yet. This provides a deeper understanding of designs that were created for passenger transportation. The team compared each product with other products in the same category: rear mounting systems, side by side, or front mounting systems.

#### **2.1.1 Rear Mounted Devices**

The most common method of transporting adult passengers on a bicycle is through a modification of the traditional rickshaw, a device consisting of a two-wheeled passenger cab pulled by a person. A cycle rickshaw is a passenger cab pulled by a bicycle and is also known as a Pedicab. The frame of a Pedicab is normally that of a large tricycle as seen in

Figure 1.



Figure 1: Pedicab Flatbed<sup>1</sup>

Pedicabs are available as direct modifications of bicycles, as seen in Figure 2. These Pedicabs are bicycles with a trailer attached to them. These types of Pedicabs are often referred to as trailer bicycles.



Figure 2: Trailer Bicycle<sup>2</sup>

### ***2.1.1.1 Mechanisms of Rear Mounted Rickshaws***

The pedal mechanisms for most Pedicabs are similar to those of normal bicycles in which the pedals are connected through the chain to a shifter. The shifter is then connected to a rear gear and differential. For the trailer bikes, the mechanism of the bicycle doesn't change; the trailer simply contains two free spinning wheels connected through an axle.

<sup>1</sup> Pedicab Flatbed (<http://www.cyclesmaximus.com/flatbed.htm#flat>)

<sup>2</sup> Trailer Bicycle (<http://i34.tinypic.com/21bssx1.jpg>)

Most bicycles, as well as Pedicabs, have different speed settings, meaning that the gearbox (Figure 3) can be shifted through various settings. Similar to bicycles, shifting in the Pedicabs is done through a shifter located on the handle bars (Main Street Pedicab). Most Pedicabs' gearboxes are 24 speeds.



Figure 3: Pedicab Shifter<sup>3</sup>

As previously mentioned, the shifter is connected to a differential axle (Figure 4). The differential is a mechanism that divides a single input torque into two outputs. The division of this torque allows each output to rotate at a different speed.



Figure 4: Rear Differential Axle<sup>4</sup>

Most Pedicabs utilize disc brakes as part of their braking system (Figure 5). The disc brakes work similarly to the caliper brakes, where the brake pads are squeezed against the wheel

<sup>3</sup> Pedicab Shifter (<http://www.cyclesmaximus.com/detailgearbox.htm>)

<sup>4</sup> Rear Differential Axle (<http://www.tartanrickshawcompany.co.uk/gpage6.html>)

rims. With disc brakes the pads are squeezed against the disc instead of the wheels with a force that is normally transmitted hydraulically.

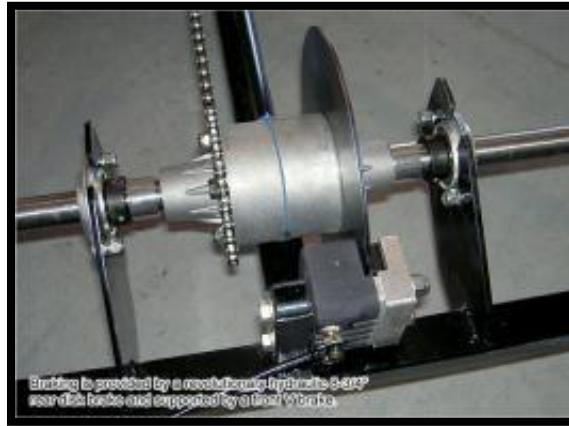


Figure 5: Hydraulic Disc Brakes<sup>5</sup>

Since the Pedicab doesn't bank when turning, it tends to be pulled towards the lower side while traveling on a slanted street. This can be compensated for by steering slightly uphill. The trailer bicycles are steered in the same manner as a regular bicycle with the only difference being the reduction of banking.

#### ***2.1.1.2 Rear Mounting Products and Patents***

Although most Pedicabs consist of a similar design, the design can be different depending on the manufacturer. An example is the Pedillac Pedicab (Figure 6); this Pedicab can either be powered by an electric motor or human power (Pedillac). This Pedicab is 93" X 44" with various heights depending on the cover used and weighs 205 lbs when pedal driven and 285 lbs with the electric system. The Pedicab has a capacity to hold 700lbs and contains dual hydraulic disc brakes. The Pedillac Pedicab is valued at \$2550.00 (Pedillac).

---

<sup>5</sup> Hydraulic Disc Brakes (<http://www.pedicab.com/images/broadway-hydraulic-brake.jpg>)



Figure 6: Pedillac Pedicab<sup>6</sup>

A second manufacturer of Pedicab is the Premier Pedicab, the manufacturer of T.I.P.K.E Pedicabs. This Pedicab contains a folding convertible canopy and is either powered by an electric motor or human power. It contains a differential system and a six speed Shimano Shifter. The T.I.P.K.E is valued at \$3,650.00. The T.I.P.K.E can be seen in Figure 7 (Premier Pedicab).



Figure 7: T.I.P.K.E Pedicab<sup>7</sup>

---

<sup>6</sup> Pedillac Pedicab ([http://maricopafreeclassifieds.com/img/ad\\_photos/p11140\\_fs.jpg](http://maricopafreeclassifieds.com/img/ad_photos/p11140_fs.jpg))

One of the largest manufacturers of Pedicabs in the United States is Main Street Pedicabs which produces five different products. These designs are the Boardwalk, Classic, Broadway, Pickup and Billboard Pedicabs, all seen in Figure 8. The only difference between these five designs is the bed. Although the bodies are designed differently, the steering and braking mechanisms are the same. Each Pedicab contains a 21 speed Shimano drive train with rear axle differential, rear hydraulic 8-3/4" disk brakes, and the option of being human powered or have an electric assist. Depending on the design, the Main Street Pedicabs can cost from \$2,895.00 to \$3,800.00 (Main Street Pedicab).



Figure 8: Mains Street Pedicabs <sup>8</sup>

<sup>7</sup> T.I.P.K.E Pedicab <http://www.premierpedicabs.com/Pedicab%20Gallery.htm>

<sup>8</sup> Mains Street Pedicabs (<http://www.pedicab.com/pedicabs.html>)

Similar to regular Pedicabs, bike trailers come in different models. The trailers are usually sold separately from the bike. One of the main manufacturers of trailers is PedalTek. PedalTek sells a base model for the trailers seen in Figure 9. This model can be customized as the client desires. The trailer is 350.5 square inches and is valued at \$1195 (Pedaltek).



Figure 9: Pedaltek Trailer<sup>9</sup>

A second manufacturer of bike trailers is Chariot Carriers Inc. This is the manufacturer of the Chariot Corsaire product line which is intended for children or small adults (Figure 10). The Chariot Corsaire is a foldable trailer with sitting dimensions of 25.6" X 25.2". The largest trailer has a weight capacity of 100 lbs. The overall dimensions are 39.2" X 33.3" X 38". This trailer is valued from \$675 to \$900 (Chariot Carriers).

---

<sup>9</sup> Pedaltek trailer (<http://pedaltek.com/plugins/albums/slideshow/slideshow.html?bgType=1&bgStyle=>)



Figure 10: Chariot Carrier X-Country<sup>10</sup>

Key design features of each rear mounting product can be seen in

Table 1.

Table 1: Rear Mounting Products

	<b>Pedicab</b>			<b>Bicycle Trailer</b>	
	<b>Pedillac</b>	<b>Premier Pedicab</b>	<b>Main Street Pedicab</b>	<b>Pedaltek</b>	<b>Chariot</b>
<b>Steering</b>	Front wheel Steering	Front wheel Steering	Front wheel Steering	Bicycle Front Wheel Steering	Bicycle Front Wheel Steering
<b>Braking</b>	Dual Hydraulic Disc Brakes	Rear Hydraulic Disc Brakes	Rear Hydraulic Disc Brakes	Dependent on Bicycle Brakes	Dependent on Bicycle Brakes
<b>Seating</b>	Up to 4 passengers	Up to 4 passengers	Up to 4 passengers	Up to 4 passengers	Up to 2 children
<b>Price</b>	\$2,550	\$3,650	\$2895-\$3800	\$1,195	\$675-\$900
<b>Electric motor</b>	Optional	Optional	Optional	No	No
<b>Reconfigurable System</b>	No	No	No	Yes (standalone bicycle)	(standalone bicycle)

<sup>10</sup> Chariot Carrier X-Country ([http://www.chariotcarriers.com/english/html/cx\\_specs.php?flaID=](http://www.chariotcarriers.com/english/html/cx_specs.php?flaID=))



Patent 4546992, the Sportcycle (Figure 11), also feature a Pedicab design. This patent was filed on September 10, 1984 by Harold S. R. Swartz, et al. and was issued on October 15, 1985. In this Pedicab a two wheeled cab is pivotally connected to the rear end of the frame. What makes this patent different from the current products on the market is the design of the trailer bike. Most modern bicycle trailers use a regular bicycle which pulls a trailer, but in this patent the front wheel and fork of the bicycle are missing. Steering is achieved by rotation of the handle bar, which is connected through links 18 and 23, seen in Figure 12, to the front wheel fork, which is located under the cyclist's feet.

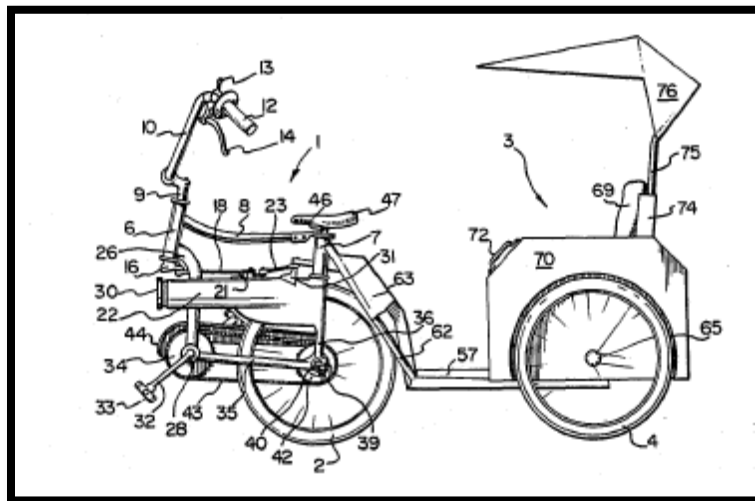


Figure 11: Patent 4546992, the Sportcycle<sup>11</sup>

<sup>11</sup> Swartz, Harold et al. "Sportcycle" Patent 4,546,992. 15 October, 1985

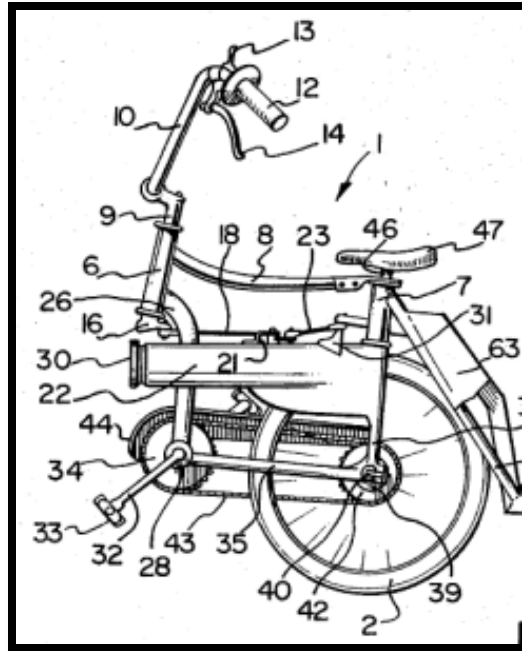


Figure 12: Patent 4546992, Sportcycle Handlebar<sup>12</sup>

### 2.1.2 Side-by-Side Devices

A side-by-side device is another bicycle-type device capable of carrying passengers. Each side-by-side device is constructed as a standalone unit, not as an attachment to an existing bicycle. The name “side-by-side” is used because it describes the seating arrangement of the riders where the riders are seated next to each other. Typically, these devices require power input from all occupants of the device and steering input from one passenger.

#### 2.1.2.1 Side-by-Side Products

One side-by-side device currently available is the Lightfoot Cycles Duo. This vehicle has a single chain drive train with one chain transferring the power of both the riders’ cranks to the solid axle connected to the rear wheels. Seating is similar to that of recumbent bicycle where the riders are seated with the pedals and crank in front of them. The riders’ legs use a primarily horizontal movement to transfer power into the crank. The brakes of the device are cable-

---

controlled mechanical discs controlled by the driver. An image of the Duo can be seen in Figure 13.



Figure 13: Lightfoot Cycle Duos<sup>13</sup>

Another side-by-side device available is the American Speedster Sidekick. The Sidekick is a single chain driven device where the driver provides the power input. The seating of this device is similar to that of a golf cart and the pedaling motion is primarily vertical, similar to a normal bicycle. Brakes on the Sidekick are only located on the rear wheels and are controlled through one hand lever on the handlebars. The steering of the Sidekick is achieved through a single input link rigidly connected to the handlebars. This input link is attached to the two front wheels via a coupler link which allow the two front wheels to turn in unison. An image of the Sidekick can be seen in Figure 14.

---

<sup>13</sup> Lightfoot Cycles (<http://lightfootcycles.com>)



Figure 14 - American Speedster Sidekick<sup>14</sup>

---

<sup>14</sup> American Speedster (<http://www.americanspeedster.com/side-kick.htm>)

A table containing key design features of each side-by-side benchmark device can be seen in Table 2.

Table 2: Comparison of Side by Side Devices

	<b>Lightfoot Cycles Duo</b>	<b>American Speedster Sidekick</b>
<b>Attachment</b>	N/A	N/A
<b>Steering</b>	Linkage System	Linkage System
<b>Braking</b>	Mechanical Disc on all four wheels	V-brake rim brakes on rear only
<b>Drivetrain</b>	Dual chain and dual power input	Single power input
<b>Seating</b>	Side-by-Side in Recumbent-type orientation	Side-by-Side in upright normal bicycling orientation

US patent 4178008, issued to Robert C. Barrett on December 11, 1979 is for a side-by-side bicycle frame (Figure 15). This patent consists of a frame with rear forks, a transverse crank tube, upright seat tube and upright steering tube. This design is interesting because it features two seats cantilevered off the bicycle frame and two sets of pedals, one on each end of the crankshaft. The pedals are connected to the rear wheels through a sprocket and chain mechanism. There are also two handlebars connected to the steering tube through a duplex yoke. One is connected rigidly and the other is able to steer the bike by rotating the bicycle's front fork through a linkage connected to the bottom of the head tube.

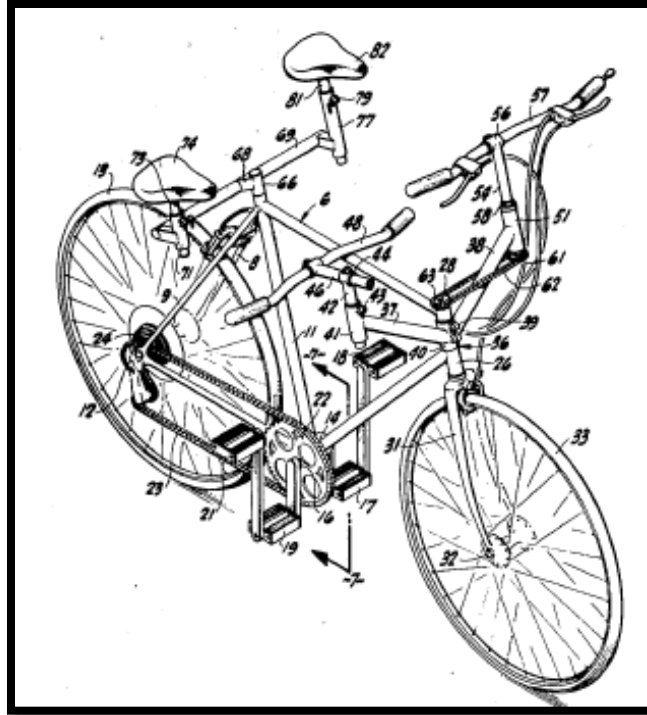


Figure 15: Patent 4178008, Side by Side Bicycle<sup>15</sup>

### 2.1.3 Front Mounted Devices

Front mounting systems, or reverse rickshaws, are a third option for cyclists who wish to carry passengers. These devices are designed for a variety of purposes including carrying cargo and transporting people. A prominent design feature in many of these reverse rickshaw devices is a large box in front of the handle bars supported by two large bicycle wheels. The front side of these compartments often can swing open on a hinge to facilitate loading. While a number of these devices are designed for carrying one or more children, there are options available for adult transportation.

<sup>15</sup> Barret, Robert. "Side by Side Bicycle" Patent 4,178,008. 11 December 1979

### ***2.1.3.1 Mechanisms of Front Mounting Devices***

The drive train of front mounting devices consists of a crank and pedals connected to the rear drive wheel through a chain. The steering is controlled by the rotation of the handlebars; however this rotational motion is transferred into the two front wheels.

### ***2.1.3.2 Front Mounting Products***

Front mounting devices on bicycles are very popular in Denmark. Two Danish companies, Bella Bikes and Christiania Bikes produce this type of product. Bella Bikes has designed their bicycle specifically to cater to the transportation of children; their compartments can hold up to four children at once and the consumer can choose from a variety of seating arrangements, including some that feature reclining seats. The outside of the compartment can also be personalized with bold colors or graphics. An attachable cover can also be added to protect the passengers from rain or sun.

The mechanisms of Bella Bike's design are unique because it reverses a standard bicycle. Instead of rear wheel propulsion, the drive train is connected to the two front wheels of the product. The steering rotation of the handlebars is transferred into the rear wheel of the tricycle. An example of a Bella Bike can be seen in Figure 16.



Figure 16: Bella Bike<sup>16</sup>

---

<sup>16</sup> Bella Bikes (<http://bellabike.dk/>)

The Bella Bike steers through a direct link from the handle bar to the rear fork. The steering mechanism is when the driver turns the handlebar [2] counter clockwise the steering bar [3] is pushed back. When this bar is pushed back the wheel turns right which pushes the Bella Bike to make a wide turn towards the left. This can be seen in Figure 17.

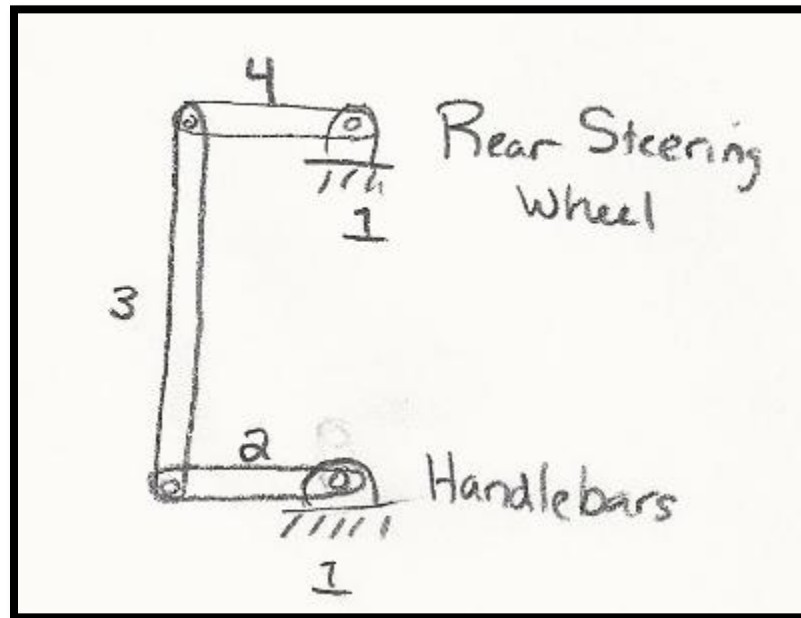


Figure 17: Bella Bike Steering Mechanism





Figure 18: Bella Bike Steering Mechanism<sup>17</sup>

Christiania Bikes offers more diversity in the shape of their compartments to cater towards a larger variety of tasks including transporting children, wheelchair users, or cargo. They also allow the consumer to customize their purchase with a variety of extras including a seat or a cover. Their website claims that their devices are able to carry up to 220 lbs and have dimensions of 82” long and 34” wide.

The mechanisms of the Christiania Bikes are very similar to that of a bicycle. The only difference is that instead of being steered by normal bicycle handlebars, the handlebar of Christiania’s products resembles that of a lawnmower, as seen in Figure 19. This product has disc brakes attached to the front wheels as well as parking brakes.

---

<sup>17</sup> Bella bike Steering Mechanism (<http://carrierbike.com/2009/10/28/jernhesten-carrier-bike-from-denmark/>)



Figure 19: Christiania Bike<sup>18</sup>

In order to steer the Christiania Bike the rider must use the frame of the box as the steering mechanism. For this design the front wheels are mounted on the front of the frame which is attached to the box. The driver steers by rotating the box on a pivot which is positioned underneath the box, near the center of the bicycle frame.



Figure 20: Christiania Bike Cargo Frame<sup>19</sup>

Two companies in the Netherlands manufacture similar design, Nihola and Feetz. Nihola's product appears to feature a smaller compartment than those in Denmark and is

---

<sup>18</sup> Christiania Bikes ([http://www.christianiabikes.com/english/uk\\_main.htm](http://www.christianiabikes.com/english/uk_main.htm))

<sup>19</sup> Christiania Bike Steering Mechanism (<http://www.ped-hl.com/christiania-bikes/>)

advertised to carry a small individual or as many as three very small children. An image of the Nihola can be seen in Figure 21.



Figure 21: Nihola

The Nihola cargo bike steers through a linkage system which works as follows: when the handle bar [2] is rotated counterclockwise, link [3] pushes the left wheel link [6] while link [4] pulls the right wheel link [5].

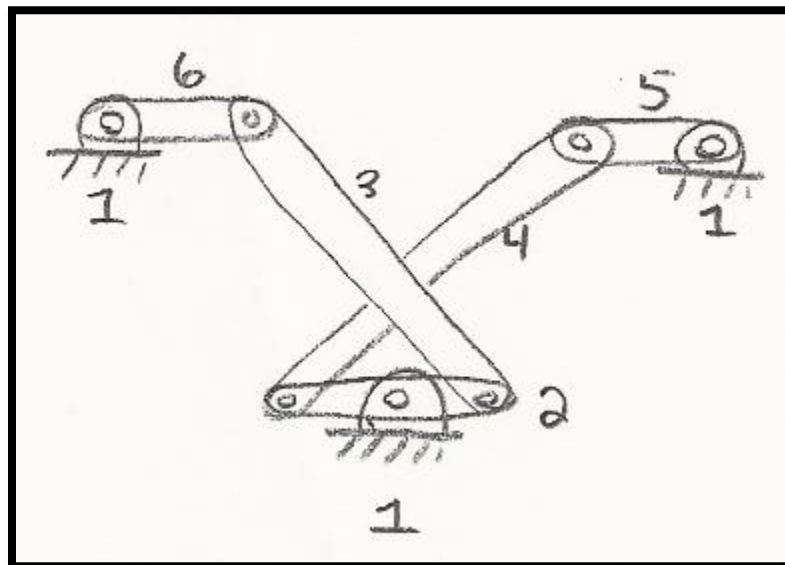


Figure 22: Nihola Steering Mechanism

<sup>20</sup> Nihola Bikes (<http://www.nihola.info/>)

Another category of reverse rickshaws is reconfigurable systems intended for families with infants or very young children. One attribute to these bikes is that the passenger compartment is detachable and can be converted into another configuration; the user has the options of having a bike, a bike with a child carrier on the front, a stroller, and, in at least one design, a jogger. Although these devices are fairly expensive, they are desirable because of the multiplicity of the system and the reduced need for multiple products.

A company from the Netherlands, Taga, produces a bike within this category in which the compartment is very similar to a child's car seat. This particular product is advertised to convert from a bike with a child carrier in the front to a stroller within 20 seconds. The product can also be folded so that it can be transported in the back of a car.

This product steers like a normal bicycle but has an enhanced braking system; there are disc brakes on each of the front wheels, a V-brake on the rear wheel and an additional parking brake. This bike weighs 64 lbs and has 28.7" w x 64.9" l x 40.1" h dimensions. An image of the Taga can be seen in Figure 23.



Figure 23: Taga<sup>21</sup>

---

<sup>21</sup> Taga Bikes (<http://www.tagabikes.com/>)

The Taga steering system uses two separate handles to transfer rotational motion into the steering of the front wheels. To ensure that the wheels turn in unison, a four bar linkage is used, seen in Figure 24. The two front wheels are mechanically forced to rotate in unison.

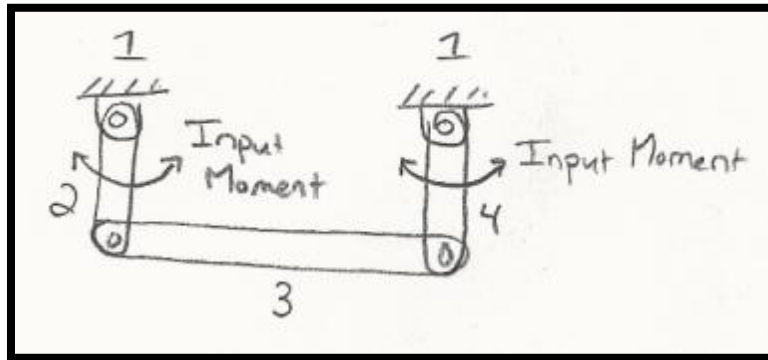


Figure 24: Taga Steering Linkage System

Trio bike of the UK has a bike with pod compartment on the front that can carry up to two children. This product comes in two options; one in which the front compartment is permanently attached and another, more expensive option in which the compartment can be detached and converted into a stroller. An image of the Trio Bike can be seen in Figure 25.



Figure 25: Trio Bike<sup>22</sup>

<sup>22</sup> Trio Bikes (<http://www.triobike.co.uk/>)

The Trio's steering seen in Figure 26 uses an input link rigidly connected to the front fork of the bicycle to transfer rotation of the fork and handlebars into rotation of the rigid front axle.

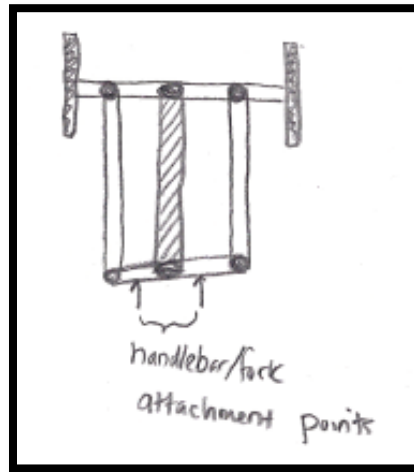


Figure 26: Trio Steering Linkage System

There is another reconfigurable system, the Zigo that is from the United States. The Zigo is a system that can be converted into a regular bicycle, a bicycle with a child compartment on the front, a stroller, or a jogger. The Zigo offers the greatest number of configurations and can fulfill a broader variety of consumer's needs. An image of the Zigo can be seen in Figure 27.



Figure 27: The Zigo<sup>23</sup>

---

<sup>23</sup> Zigo (<http://www.myzigo.com/>)

The Zigo steering system uses two separate four bar linkages, seen in Figure 28, to transfer the output of one system to the output of the other. The input link [6] is the handlebars of the device, which rotate to select direction. The input link [6] is connected with a coupler link [5] to the output link [4]. This system's purpose is to transfer the rotation of the handlebars to the steering of the left front wheel. To transfer this motion to the right front wheel, a second four bar linkage is used with the input link being the output of the first system [4]. The input link [4] is connected with a coupler link [2] to the output link [3]. This system allows links [3] and [4] to rotate in unison about pivot points [e] and [d] respectively.

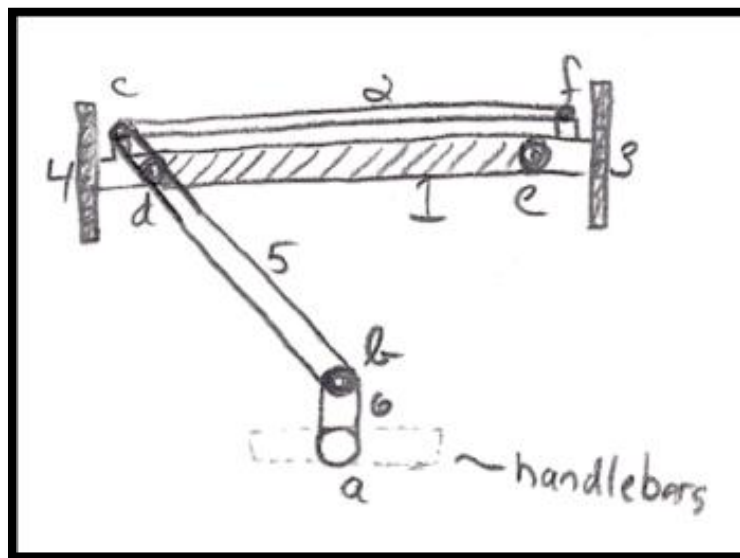


Figure 28: Zigo Steering Linkage System

A company located in Pennsylvania, Frank Mobility Systems, Inc. offers a reverse rickshaw design that is significantly different than the other designs on the market. Instead of having a compartment attached to the front of the bicycle, this design, known as the Duet, incorporates a wheelchair. This special wheelchair is attached to the front end of a bicycle to create a functioning tricycle where the cyclist pushes the passenger in the wheelchair in front of them. However, there is also a quick release, which allows the front to separate and function as a

working wheelchair. This product is designed for all ages and can hold up to 275 lbs. The Duet has dimensions of 105”l x 26”w x 43”h and weights 87 lbs. An image of the Duet can be seen in Figure 29.



Figure 29: The Duet<sup>24</sup>

The steering mechanism on the Duet can be seen in Figure 30. Steering is achieved by using a rigid axle [1] between the device’s wheels (left wheel and right wheel in Figure 30) and pivot point [a] in the center of this rigid axle. Pivot point [a] connects to the device’s frame [2], which may be considered to be the ground link. The input link [3] has input forces from the driver’s arms, which create clockwise or counterclockwise motion of the pivot point [a]. This rotation causes movement of the front wheels in the direction of rotation.

---

<sup>24</sup> Frank Mobility Systems (<http://www.frankmobility.com/duet.php>)



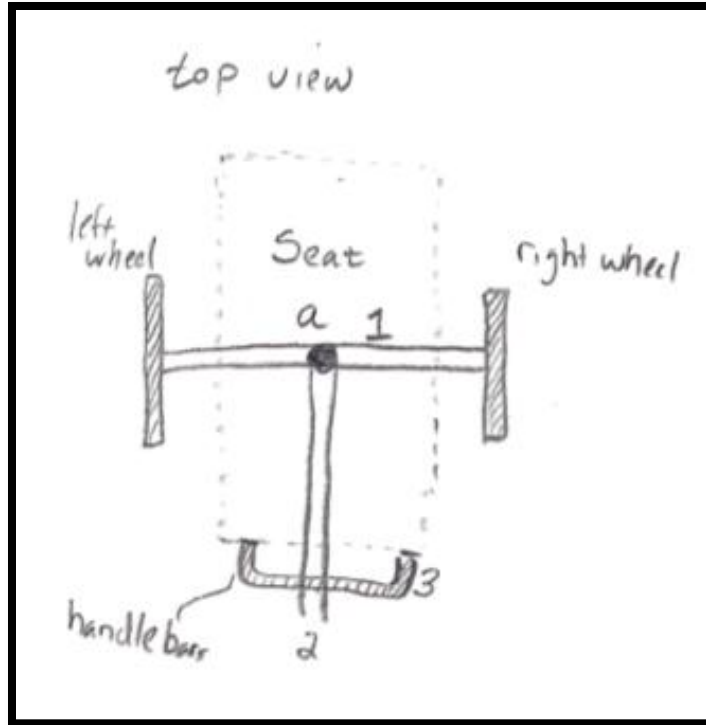


Figure 30: Duet Steering Linkage System

All of these front mounting systems are compared in Table 3.

Table 3: Comparison of Front Mounting Systems

	<b>Bella Bike</b>	<b>Christiania Bikes</b>	<b>Nihola</b>	<b>Feetz</b>	<b>Taga</b>	<b>Trio Bike</b>	<b>Zigo</b>	<b>DUET</b>
<b>Steering</b>	Rear wheel	Front wheels	Front wheels	Front wheels	Front wheels	Front wheels	Front wheels	Front wheels
<b>Propulsion</b>	Front wheels	Rear wheel	Rear wheel	Rear wheel	Rear wheel	Rear wheel	Rear wheel	Rear wheel
<b>Braking</b>	N/A	Disc brakes and parking brake	Parking brake, either coaster brake or v brake	N/A	Disc brakes on front wheels, roller brake on rear wheel and parking brake	Disc brakes and parking brake	Drum brakes and parking brake	N/A
<b>Reconfigurable System</b>	No	No	No	No	Yes (bike with child carrier, stroller)	Yes (bike with child carrier, stroller)	Yes (bike with child carrier, bike, stroller, jogger)	Yes (bike with seat, wheelchair)
<b>Footprint</b>	N/A	82" x 34"	? x 35"	N/A	64" x 28.7"	88.6" x 310.5"	? x <32"	105" x 26"
<b>Price</b>	N/A	N/A	N/A	N/A	\$1,500	\$3500	\$1,400	\$4500
<b>Weight</b>	N/A	N/A	N/A	N/A	64 lbs	80.4 lbs	N/A	87 lbs
<b>Carrying Capacity</b>	N/A	220 lbs.	220 lbs.	N/A	N/A	198 lbs.	100 lbs.	275 lbs.

A different type of mounting mechanism is the front mounting rickshaw mechanism. One of these mechanisms is US Patent 4830388. This patent was issued on May 16, 1989 to Allen S. P. Wang for a Multi-Functional Wheelchair Assembly seen in Figure 31. This invention is basically a wheelchair with a removable bicycle assembly. The bicycle assembly contains a hollow sleeve which is attached to the wheelchair through a U-shaped adapter [Numbers 221 and 223] seen in Figure 32.

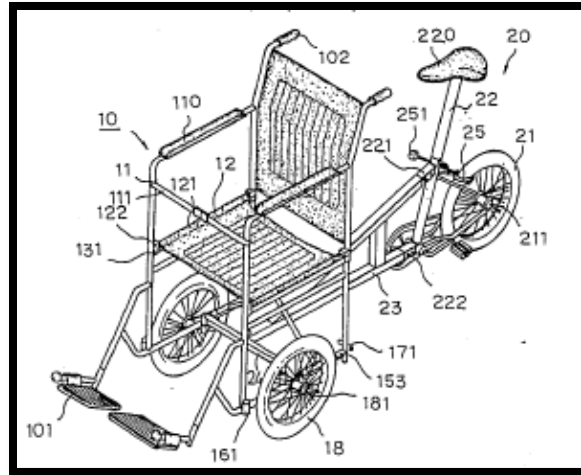


Figure 31: Patent 4830388, Multi-Functional Wheelchair Assembly<sup>25</sup>

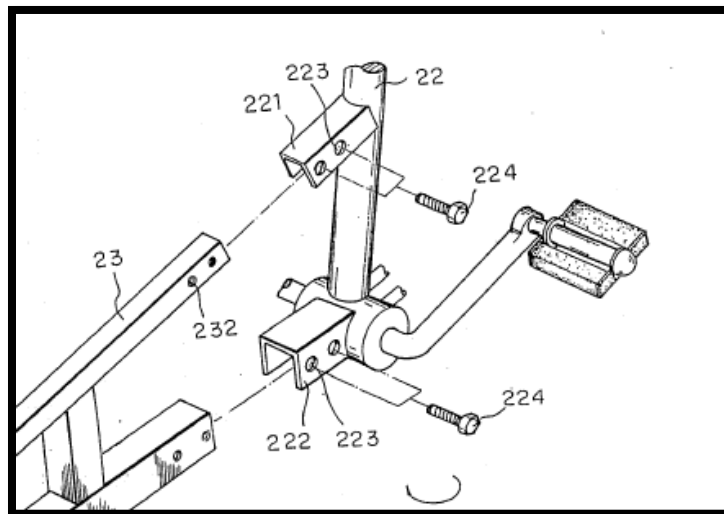


Figure 32: Patent 4830388, U shaped adapter<sup>26</sup>

A similar design is US Patent 4,767,130 issued on August 30, 1988 to Wang Fu-Chao (Figure 33). This patent describes a reverse rickshaw device with 4 wheels, 3 positioned in a similar position to the other reverse rickshaw devices described and the fourth located in the front, under the middle of the footrest.

<sup>25, 36</sup> Wang, Allen. "Ridable Multi-Functional Wheelchair Assembly" Patent 4,830,388. 16 May, 1989

This device is a modular system. The back wheel and seat can be removed and the rest of the device can be used like a normal wheel chair. When the rear seat and wheel are attached, they propel the wheelchair. The rear wheel is both the driving wheel and contains the brake. The benefit of this particular design is that it can be folded into an extremely compact area for ease of transportation.

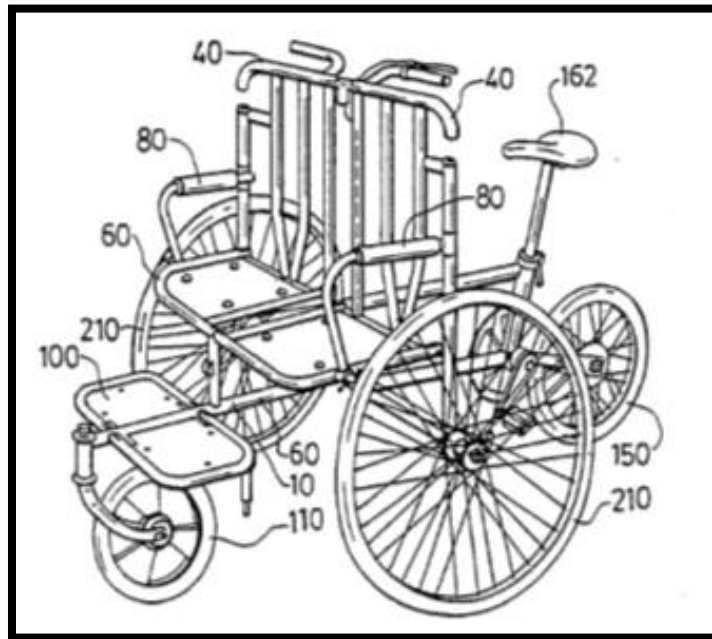


Figure 33: US Patent 4,767,130, Foldable Pedicab<sup>27</sup>

---

<sup>27</sup> Fu-Chao, Wang. "Foldable Pedicab" Patent 4,767,130. 30 August 1988

## **CHAPTER 3: PROJECT GOAL**

Although there are many successful products on the market, there are still a number of obstacles that restrict the widespread usage of these types of passenger transportation devices. One major concern is performance limitations like steering ability, continuous stability, and cost to consumers. Even the products that are well designed have drawbacks; for example, side by side devices are typically too wide for bike trails and common sidewalks, and rear mounted systems normally result in a restricted view for the passenger. Front mounted systems offer a solution to both of these concerns, but the majority of those currently on the market are targeted towards families with babies or small children. Options for adult passenger transportation are limited in comparison to options available for transportation of children, and options for adult passengers in front mounted systems are even less common. This excludes the elderly and the persons with disabilities that could benefit from this type of system.

The team's goal is to create a device that will be accessible for adults with limited mobility; a target audience that is currently not being reached by product on the market. The design will attach to the front of a bicycle so that an adult passenger will be able to enjoy a bike ride with an unobstructed view. The device will be able to be attached to a pre-purchased bicycle, and will exhibit an ease of steering as well as adequate braking and stability. Additionally, the product will be reasonably priced so that it will be affordable for more families.

## **CHAPTER 4: DESIGN SPECIFICATIONS**

### **GENERAL**

1. The device must be able to attach to an existing bicycle.
2. The attachment of the device must be able to accommodate bicycles with a range of heights and frame styles.
3. The device's seating must be accessible by an adult casual ambulant or an adult of limited mobility.
4. Adults capable of riding a bicycle should be capable of operating this device.
5. The device should support a 250 lbs passenger.

### **STEERING**

6. The device will be steered through the bicycle's handlebars and a 1:1 steering ratio will be maintained so that the bicycle will be steered the same with or without the attachment.

### **BRAKING**

7. The device must either:
  - a. Allow both the front and rear brakes of the existing bicycle to function normally,  
or
  - b. Use the existing rear brake and provide an additional braking system to replace the bicycle's front brake.
8. The device must be able to stop within 35 feet while holding a total load of 350 lbs (driver and passenger weight) starting at a speed of 15 mph.
9. The device will contain a parking brake.

## SAFETY

10. The device must include footrest for added support and safety for the passenger while the bicycle is in motion.
11. When seated the passenger must not interfere with the driver's line of sight.
12. A seatbelt will be used to ensure the passenger is secure during braking or deceleration.
13. Protection devices around moving parts of the device will be used to protect the passenger from any injuries (particularly additional wheels and brake rotors and calipers) if the said devices are within reach of the passenger.
14. Armrests or similar side supports will be incorporated into the passenger seating of the device to ensure minimal lateral motion of the passenger during turning.
15. The device must not contain any sharp edges that could harm the passenger.

## MAINTENANCE

16. Maintenance will only require common knowledge of bicycles.
17. A wrench set, screwdriver, and set of pliers are the only tools required to maintain and attach the device.

## SIZE

18. The device must weigh less than 100 lbs.
19. The maximum width of the device must be less than 4 feet, which is the size of the smallest bicycle lanes.
20. The device's seating must accommodate an average sized adult (5'10").
21. The ground clearance of the device must be greater than 5 inches defined as the height from the ground to the lowest horizontal component of the device which would be the footrests for the passenger.

## ASSEMBLY

22. The device should be able to be attached to a bicycle within 10 minutes.

## ENVIRONMENT

23. The device must be designed to travel on mildly undulating, smooth paved roadways or rail trails with packed gravel trail surface.
24. The device will be able to endure high moisture weather conditions.
25. The device must be stored in a dry area.

## COST

26. The overall cost of the device must be less than USD\$1500.

## AESTHETICS

27. The device will not resemble a wheelchair so not to deter people from using it based on the stigma of wheelchair dependence.

## PASSENGER

28. The passenger must not weigh over 250 lbs.
29. The passenger must be able to transfer between seats of similar heights with limited assistance.
30. The passenger must be able to sit for the duration of the intended bike ride.
31. The passenger must be capable of maintaining an upright seated posture with minimal lateral motion.



## CHAPTER 5: FRAME DESIGN

This chapter will cover the various design stages of the frame design as well as the different analyses performed on these designs. When referring to the frame of the design the team will cover the structure of the frame, the location of the seat, and placement of the wheels.

### 5.1 Preliminary Frame Designs

After researching the different types of mobility devices, the team developed three different preliminary frame designs. These designs were referred to as Self Supporting Chair, Chair on Sub-Frame, and Cargo Box with Seat.

The Self Supporting Chair, Figure 34, consists of a chair on support wheels connected to the bicycle through the Direct Attachment system, which will be explained later. The two outside device wheels are used as the steering system and a smaller wheel is positioned under the existing bicycle fork to reduce moments exerted on the bicycle head tube. The front two wheels are trailing casters to prevent the device from tilting forward under loading or unloading of the passenger and to reduce forces on the device wheels.

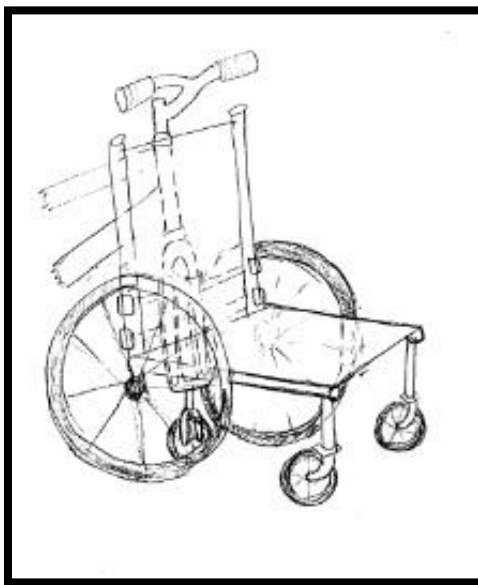


Figure 34: Self Supporting Chair

The next design, Chair on Sub-Frame, consisted of a sub-frame that is connected to the bicycle and acts as a supportive base for the passenger seat. This design can be seen in Figure 35. The attachment mechanism would allow the existing bicycle and the device frame to remain rigid while turning. The smaller wheel positioned under the existing bicycle fork is a trailing caster to reduce moments acting on the attachment mechanism from driver and passenger weight. The larger diameter device wheels are the steering wheels pivoting about a pin joint grounded on the device frame. The front wheel is a trailing caster to prevent the device from tilting forward under braking and while loading or unloading the passenger.

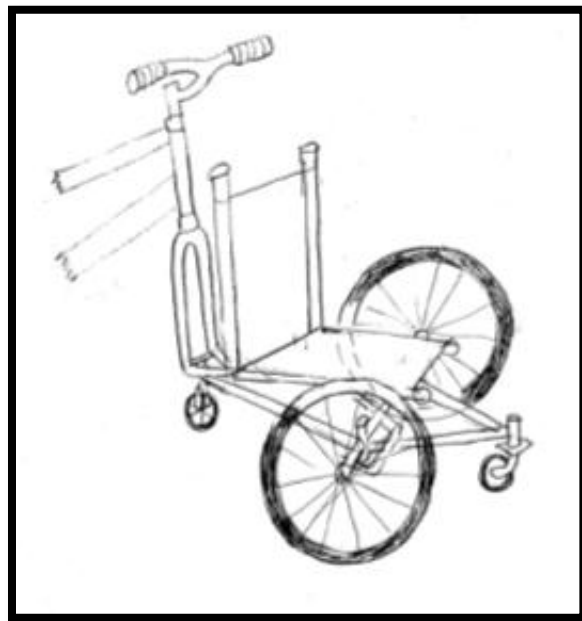


Figure 35: Chair on Sub-frame

The third design was the Cargo Box with Seat (Figure 36), consisted of a large cargo box attached to the front of a bicycle. This design features a seat for the passenger, and a hinged door that swings down for ease of access for the passenger. Two trailing casters are located in the rear of the cargo box to support passenger weight. The front two device wheels are used for steering via a steering linkage mechanism that transfers handlebar rotation to both device wheels.

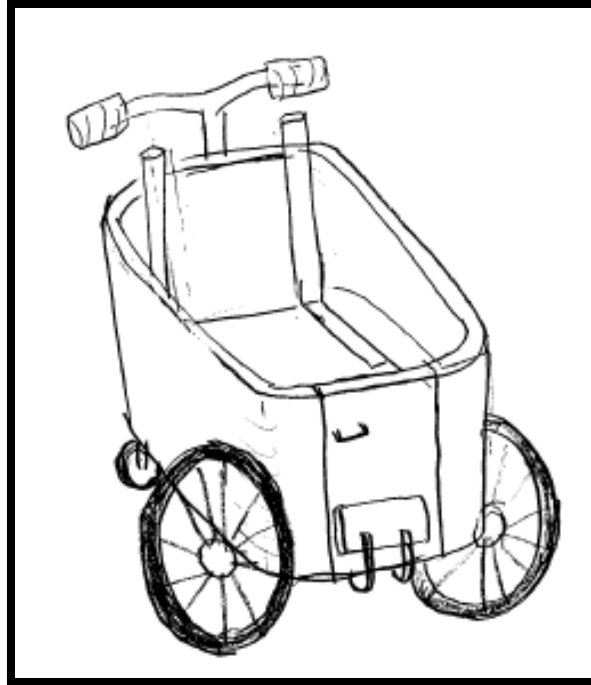


Figure 36: Cargo Box with Seat

## 5.2 Frame Selection

The design team was able to rule out the Self Supporting Chair for two reasons. The first of these reasons is the steering mechanism for this design. The self-supporting chair relies on using Direct Attachment steering mechanism, an option that was deemed insufficient in the steering analysis section. The second reason was purely aesthetics; the self-supporting chair too closely resembles a wheel chair. The stigma surrounding a wheelchair may affect how often the device will be used in public.

The Cargo Box was temporarily ruled out due to functionality. Although a passenger may feel safer in an enclosed space, the fact that the passenger has to climb up into the cargo box that is not ideal for someone with limited mobility. Most of the designs on the market having this type of frame are intended for children or mobile adults. Additionally, even if the passenger

received help from the driver in loading or unloading, it would be difficult to assist someone into the seat in such a small space.

Due to these reasons the design team decided to move forward with the sub-frame design. The team needed to determine the appropriate shape and measurements of the frame. To do so, structural analysis was completed to correctly determine the details of the design. Because the frame is the support system for the weight of the passenger and partially for the weight of the driver and bicycle, the applied loads will be considered in the design analysis.

### 5.2.1 Sub-Frame Design Modifications

After selecting the sub-frame, the team took other factors into consideration, one being the safety of the passenger. As designed, the passenger was at risk of falling off the sides if the device turns sharply or hits a bump. Due to this the team decided to combine the sub-frame design with the box design. This new design would have two walls, one on either side of the seating area while the front remains open; the walls will ensure that the passenger doesn't fall from the device and the open front makes it easier for the passenger to get in or out of the seat. The preliminary sketch for this design can be seen in Figure 37.

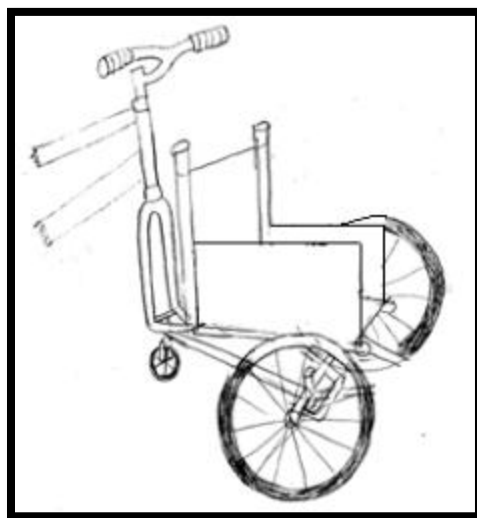


Figure 37: Sub-Frame Modification 1

This design added an extra safety factor and seemed appropriate for the design objectives. An analysis of the design was performed to the wheel connections of this design to determine if output links were feasible. For this analysis it was assumed that the weight of the passenger and the weight of the device would be equally distributed between the two front wheels. A Free Body Diagram (Figure 38) was drawn of one of the wheel connections. Since it was assumed that the forces would be equally distributed between the two front wheels, the force on this Free Body Diagram was 50% of the maximum design load.

In this Free Body Diagram the distance is 4" and distance b is 8". The weight of the passenger is originally assumed to be 250lbf, but will be placed with a magnitude of 125lbf because only half of the frame is being analyzed. The weight of the frame is 100lbf but will be analyzed at 50lbf. The analysis can be seen below.

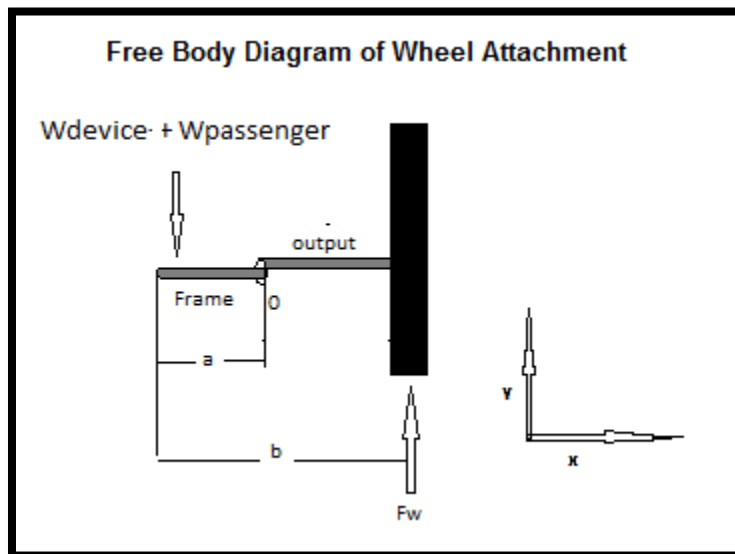


Figure 38: Free Body Diagram of Wheel Connection

$$\sum F(y) = -W_{\text{device}} - W_{\text{passenger}} + F_w$$

$$F_w := W_{\text{device}} + W_{\text{passenger}} = 175 \text{ lbf}$$

After creating the free body diagram, a section cut will be placed at the rotary link where the wheel is connected (Figure 39). With this analysis, we can now examine the internal forces acting upon this link.

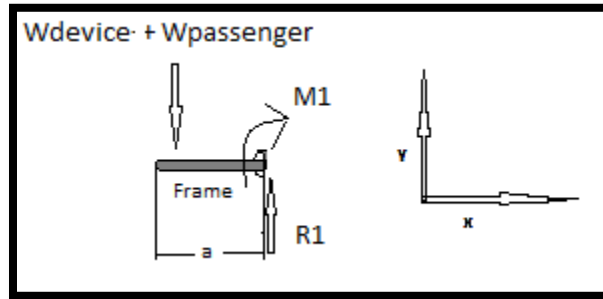


Figure 39: Free Body Diagram of Wheel Connection Section 1

$$\sum F(y) = -W_{\text{device}} - W_{\text{passenger}} + R_1$$

$$R_1 := W_{\text{device}} + W_{\text{passenger}}$$

$$\sum M(y) = -M_1 + R_1 \cdot a$$

$$M_1 := R_1 \cdot a = 700 \text{ lbf} \cdot \text{in}$$

Through this analysis it was determined that there would be approximately 700lbf-in acting on the rotary link. This magnitude is too large for the moment acting on the rotary link and therefore the design had to be modified. In order to remove this moment, the wheels needed to rotate about their own axis. To do this, the first step was modifying the walls around the passenger. An extra frame section was added (1 on Figure 40) to the wall which extended perpendicular to each wall and the wheels were mounted on it. The wheels are connected to bicycle forks, the forks are mounted on the extended frame by using two shaft collars. The design can be seen in Figure 40.

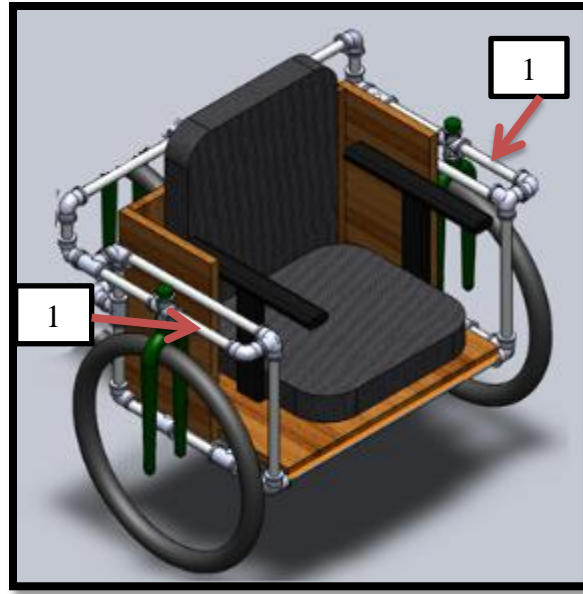


Figure 40: Sub-Frame Modification 2

This design was analyzed and was determined capable of meeting the design specifications. However, the current steering system and attachment mechanism both proved to be insufficient and the new changes required modifications to be made to the frame. The steering system and attachment changes will be described in detail in their designated sections, and the frame changes will be described below.

In order to accommodate changes in steering and attachment designs, the wheels of the frame had to be pushed back so that they are parallel to the wheel of the attached bicycle. Since the device wheels were pushed back, the two load bearing caster wheels were added underneath the front of the frame. The new design can now be seen in Figure 41.

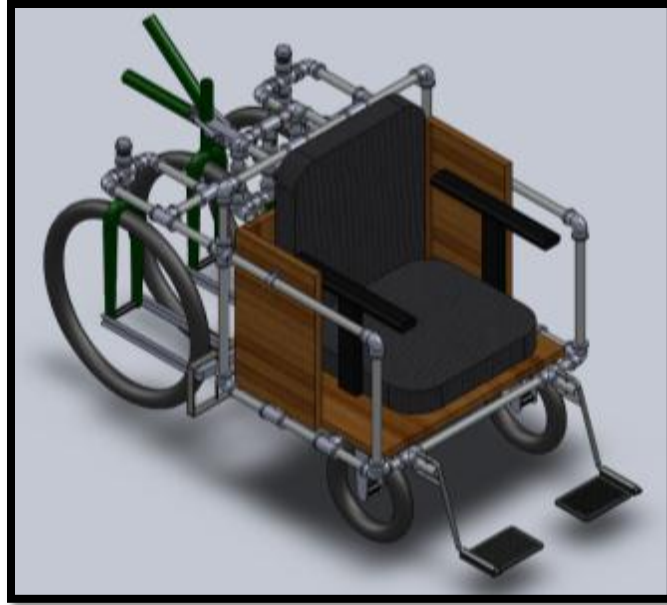


Figure 41: Final Design

With the final frame design completed it is necessary to conduct a structural analysis.

### 5.3 Free Body Diagrams and Stress Analysis

To analyze the frame of this device, various free body diagrams were created. The device was analyzed under static conditions from which a stress analysis was performed. Since the device frame is a three-dimensional problem, two Free Body Diagrams (FBDs) were used to create the equations necessary to calculate the forces. The calculated forces were used to determine the stresses on the device frame. A three dimensional stress analysis was performed to determine the Von Misses stress which compared to the yield strength of the device would tell us if the frame will fail. If the Von Misses stress is larger than the yield strength the device fails. The Free Body Diagrams used to perform these analyses can be seen in Figure 42 and Figure 43. Figure 42 represents the front view of the frame, while Figure 43 is a side view.



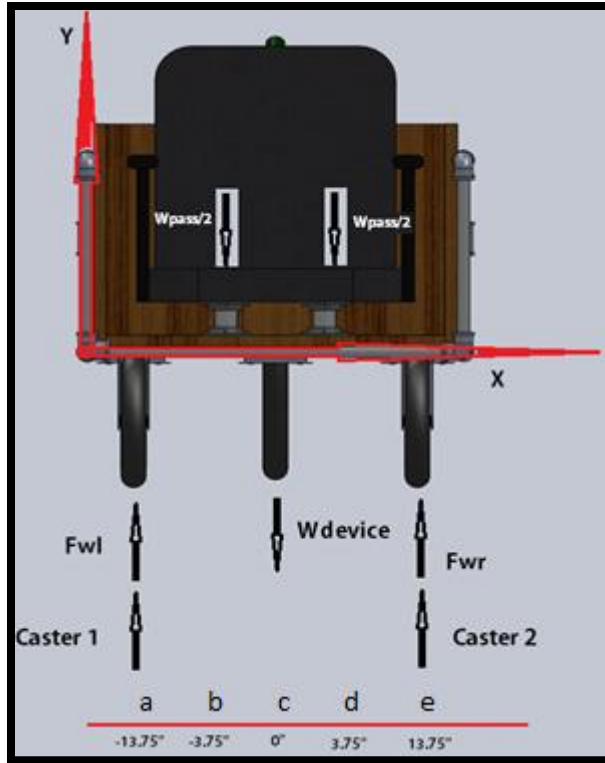


Figure 42: FBD of the Frame's Front View

From this FBD, a set of equations was created to generate shear, deflection and moment diagrams for the frame. Unfortunately, this FBD alone would not be enough to solve for these diagrams because there are only two equations with five unknowns as seen in Table 4.

Table 4: Initial Values for FBD of the Front View

<b>FBD of the Frame's Front View</b>	
<b>Variables</b>	<b>Value</b>
a	-13.75 in
b	-3.75 in
c	0 in
d	3.75 in
e	13.75 in
Wpassweight	250 lbf
Wdevice	100 lbf
Fwl	unknown
Fwr	unknown
Caster 1	unknown
Caster 2	unknown

Knowing these values and having the FBD of the front view the following equations were formed:

$$\sum F(y) = F_{wr} + F_{wl} - W_{device} - Caster1 + Caster2 - W_{Passweight} = 0$$

$$F_{wl} = -F_{wr} + W_{device} + Caster1 - Caster2 + \frac{W_{Passweight}}{2} + \frac{W_{Passweight}}{2}$$

$$\sum M(a) = \frac{-W_{Passweight}}{2} \cdot (b - a) - (c - a) - \frac{W_{Passweight}}{2} \cdot (d - a) - (W_{device}(c - a) + F_{wl}) \cdot (e - a) + Caster2 \cdot (e - a) = 0$$

After forming these equations, analysis of the side view of the frame was performed. For the side view analysis, the unknowns have not changed; now the FBD analyses have three equations and five unknowns. Only three equations exist since the sum of the forces for this FBD is the same as the sum of the forces for the FBD of the front view of the frame. For this FBD there are three new variables defined as constants, f is -22", g is 0", and h is 10".

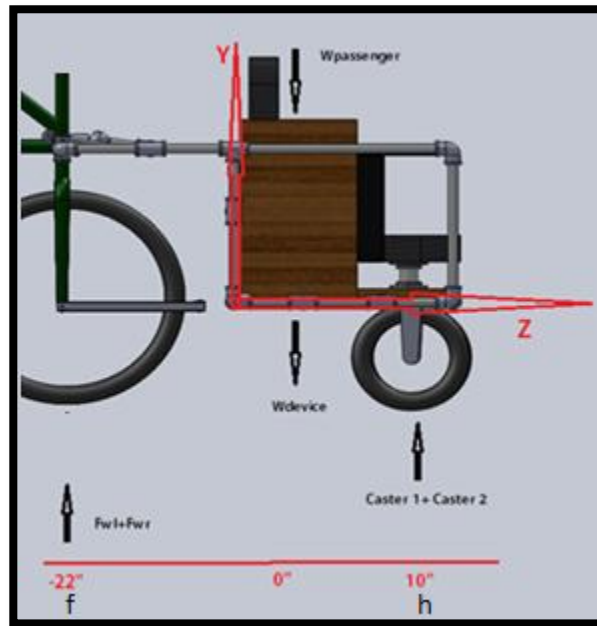


Figure 43 : FBD of the Frame's Side View

$$\sum F(y) = F_{wr} + F_{wl} - W_{device} + Caster1 + Caster2 - W_{Passweight} = 0$$

$$\sum M(f) = -W_{device} \cdot (g - f) - W_{Passweight} \cdot (g - f) + Caster1(h - f) + Caster2(h - f)$$

After these analyses there are still more unknowns than equations, so a section analysis of each frame is required to solve for the rest of the unknowns. The first section analysis will be that of the front view of the frame. For this analysis the frame will be divided into three different sections. The first section will be from -13.75" to -4", the second section will be from -4" to 4", and the third will be from 4" to 13.75". The equations determined by this analysis can be found on pages 3-6 of Appendix A.

After analyzing the Free Body Diagrams and retrieving the set of equations it is possible to calculate the forces acting on the frame. In order to do this, the equations developed in the front and side view FBDs combined in order to calculate for the individual forces. The full calculations can be seen in page 6 of Appendix A. After combining these equations, the forces calculated can be seen in Table 5.

Table 5: Forces Acting on the Frame

<b>Forces</b>	
<b>Variables</b>	<b>Value</b>
Wpassweight	250.0 lbf
Wdevice	100.0 lbf
Fwl	270.0 lbf
Fwr	270.0 lbf
Caster 1	120.0 lbf
Caster 2	120.0 lbf

Once all the forces had been calculated, accurate shear and moment diagrams were developed. In order to create these diagrams, singularity functions were used. To create the

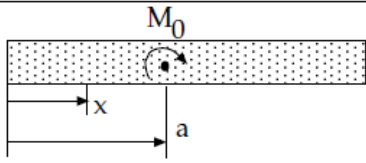
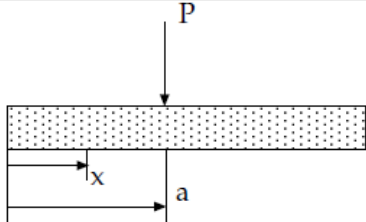
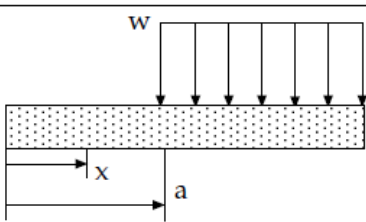
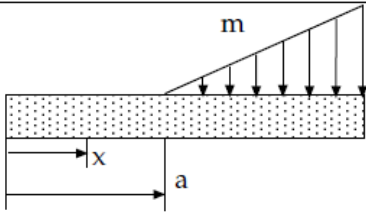
singularity functions the following functions were used.  $V(x)$  represents the shear forces,  $M(x)$  represents the moments,  $\theta(x)$  is the slope and  $y(x)$  represents deflection.

$$\begin{aligned}V(x) &= \int -q(x) + C_1 \\M(x) &= \int V(x) + C_1 \cdot x + C_2 \\ \theta(x) &= \int M(x) + \frac{C_1 \cdot x^2}{2} + C_2 \cdot x + C_3 \\ y(x) &= \int \theta(x) + \frac{C_1 \cdot x^3}{6} + \frac{C_2 \cdot x^2}{2} + C_3 \cdot x + C_4\end{aligned}$$

To determine how to express the forces, the diagram in

Table 6 was used. This diagram shows how the forces and moments are written for the shear and moment diagram as well as the form of their integration. The same example was followed for slope and deflection.

Table 6: Summary of Singularity Functions<sup>28</sup>

Loading	Distribution $q(x)$	Shear = $-\int q(x)dx$	Moment = $-\int q(x)dx$
	$q = M_0 \langle x - a \rangle^{-2}$	$V = -M_0 \langle x - a \rangle^{-1}$	$M = M_0 \langle x - a \rangle^0$
	$q = -P \langle x - a \rangle^{-1}$	$V = P \langle x - a \rangle^0$	$M = -P \langle x - a \rangle^1$
	$q = -w \langle x - a \rangle^0$	$V = w \langle x - a \rangle^1$	$M = -\frac{w}{2} \langle x - a \rangle^2$
	$q = -m \langle x - a \rangle^1$	$V = \frac{m}{2} \langle x - a \rangle^2$	$M = -\frac{m}{6} \langle x - a \rangle^3$

From these diagrams it is possible to write the singularity functions for the two main Free Body Diagrams, the front and side view. These functions give the Shear Diagram seen in Figure 44, and Moment Diagram in Figure 45.

<sup>28</sup> <http://www.cgl.uwaterloo.ca/~tjlahey/sfunctions.pdf>

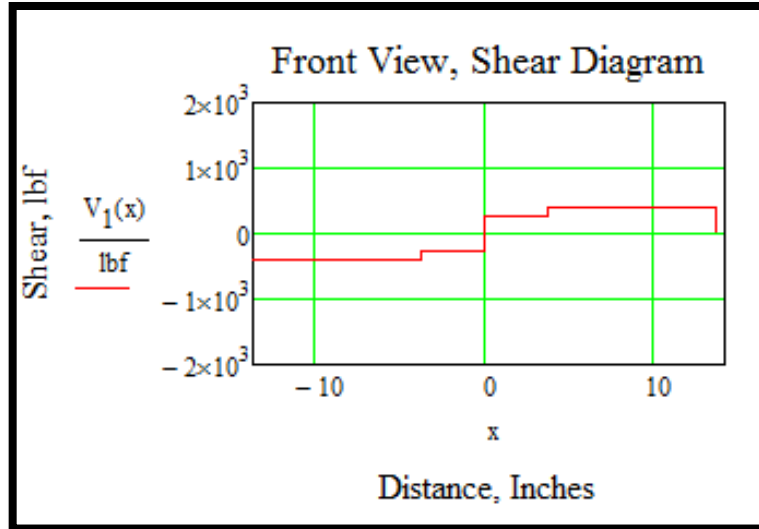


Figure 44: Front View Shear Diagram

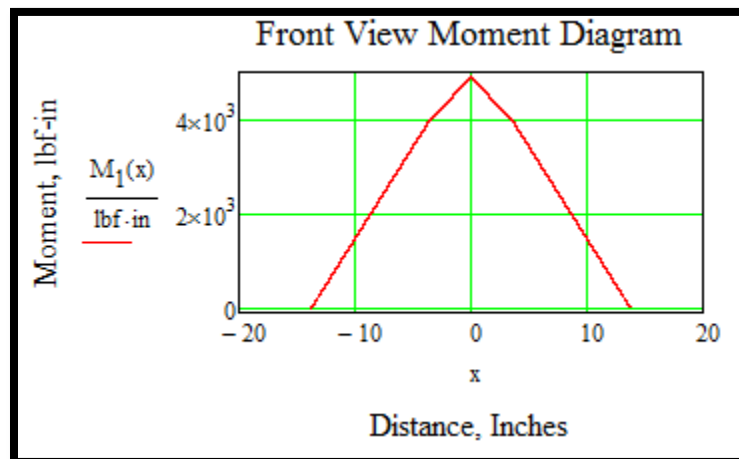


Figure 45: Front View Moment Diagram

From these equations it was also possible to create a deflection diagram, seen in Figure 46.

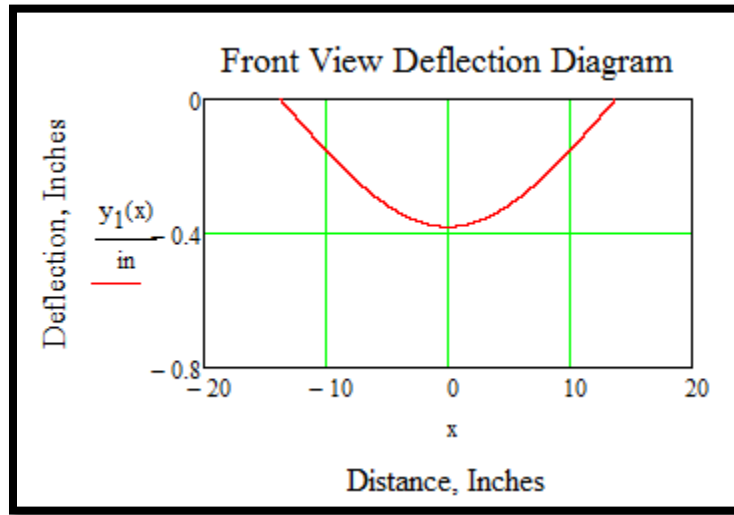


Figure 46: Front View Deflection Diagram

The same method to analyze the front view was applied for the side view. Singularity equations were created based on the sum of the forces and moments. The full analysis for the front and side view can be seen on pages 10 to 13 of Appendix A. The deflection Diagram for the side view can be seen in Figure 47.

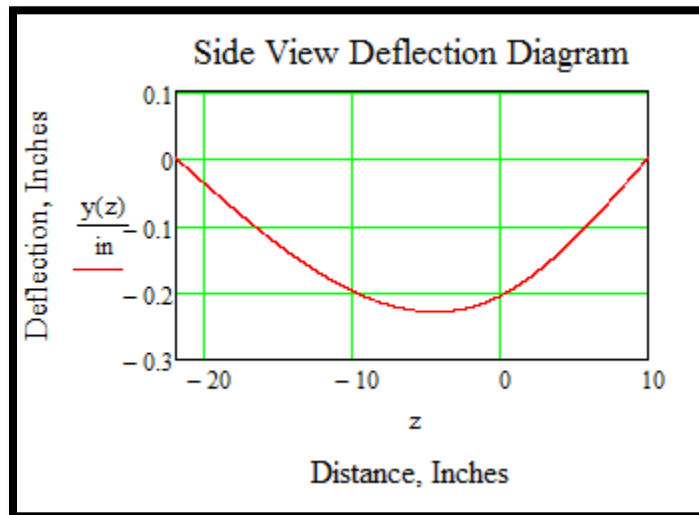


Figure 47: Side View Deflection Diagram

These two diagrams show that the deflection from both views will be less than half an inch.



From the moment diagram the maximum moment in the frame can be calculated. Using this maximum moment value the normal bending stress and the torsional shear stress on each member of the frame can be determined. To calculate the normal bending stress, the moment of inertia of the structure will be necessary. To calculate the moment of inertia, the dimensions of a schedule 40, 1 inch nominal diameter tube will be used. This will give an outer diameter of 1.315 inches and inner diameter of 1.049 inches. Knowing this the moment of inertia is calculated as:

$$I := \frac{\pi}{64} \cdot (OD^4 - ID^4) = 0.087 \text{ in}^4$$

After all torsional and bending stresses have been calculated a 3D stress analysis is performed to calculate the Von Mises stresses of the frame. Von Mises stresses are found using the stress cubic equation to calculate the principal stresses. The full calculations can be found on pages 14 and 15 of Appendix A.

The Von Mises stress was calculated to be 16.8 kpsi meaning that a material with the yield strength of less than 16.8 kpsi would fail under these conditions. The yield strength of the aluminum tubing is 45 kpsi, which means that the frame should not fail. This analysis does not take into consideration the use of different materials in different portions of the frame. The tubing used to build the frame is aluminum, but all fasteners will be made out of galvanized steel which has higher yield strength than aluminum. The galvanized steel fasteners are used at all points in the device frame subjected to the greatest forces and moments. For these reasons we believe that the frame will not fail.

## **CHAPTER 6: STEERING DESIGN**

When considering mounting a device to the front of a bicycle, the issue arises of how the device and bicycle will steer. As defined by the design specifications, steering will remain controlled by the existing bicycle's handlebars. The manner by which the rotational motion of the handlebars can be transferred to steering of the device consists of many possible solutions.

Other design specifications taken into consideration for steering systems were steering angle and transmission angles. An ideal maximum steering angle is as close to  $45^\circ$  as possible without going over  $45^\circ$  or hitting the frame of the device. An ideal transmission angle is as close to  $90^\circ$  as possible without altering a 1:1 steering ratio between the input and output links. The 1:1 ratio allows the rotation of the handlebars to be equivalent to the rotation of the device wheels, a feature of regular bicycles. It is desired to keep the same steering ratio so that the driver will be able to steer the bicycle and attachment in the same manner that the bicycle would be steered without the attachment. This way it will be significantly easier for the cyclist and they won't have a learning curve when the bicycle attachment is used.

### **6.1 Preliminary Steering Designs**

The preliminary steering designs are detailed in the remainder of this section.

#### **6.1.1 Direct Attachment Steering**

Steering for this design is achieved through direct attachment of the device to the rear section of a self-supporting seat or wheelchair. The rigid attachment of the existing bicycle's fork to the frame of the passenger compartment allows for the use of the steering abilities of the device as seen in Figure 48. The ease of steering of a similarly structured wheelchair was the main focus of this concept and this ease should potentially translate to the steering of the bicycle with the wheelchair attached. Using a wheelchair-type steering system presents the issue of potential skidding of the outside wheel in a turn caused by differing velocities between the

outside and inside wheels. Also, steering with the passenger's weight directly over the steering wheels creates greater resistance to handlebar rotation by the driver resulting in steering difficulty and degradation of occupant safety.

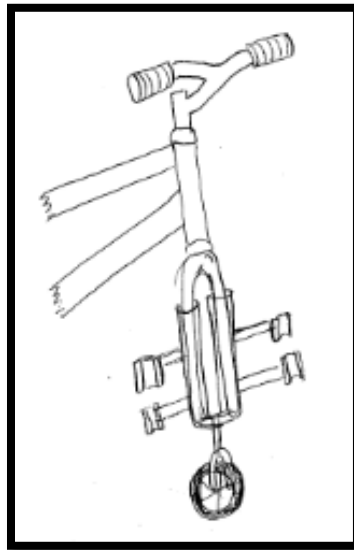


Figure 48: Direct Attachment System

The way that the Direct Attachment differs from the other designs is that instead of acting as a steering system that turns the wheels independently of the frame, it turns the frame itself. However, a test was performed in Europe on transport bikes (bicycle systems with a passenger compartment on the front) claiming that the Nihola Bike was the best, particularly because it was not a direct attachment system. Their website claims “On normal transport bikes you have to swivel the whole load when you steer. But on the Nihola the front wheels turn independently, the same way as a car’s. The great benefit of this is that it makes the bike comfortable to ride. That was also the clear result of our test: the Nihola transport bike is the fastest and the most

comfortable to steer and ride.”<sup>29</sup> From this statement, it becomes clear the use of steering systems acting independently of the entire frame will provide improved operating performance.

### **6.1.2 Cross Linkage Steering**

The Cross Linkage Steering concept developed for steering of this device was the use of a four bar linkage system with the coupler links crossing each other seen in Figure 49. Link [2] is considered ground because it is rigidly connected to the sub frame. The input link [6] transfers motion via coupler links [4] and [5] to output links [1] and [3] respectively. The output links [1] and [3] then rotate about ground on pivot points [b] and [c] respectively. When the input link is rotated counterclockwise, a compressive force is exerted on link [4] and link [1] and a tensile force is exerted on links [5] and [3]. The inverse of this system occurs when the input link is rotated clockwise.

---

<sup>29</sup> <http://nihola.info/en/nihola+bikes/The+best+for+you!+Test+winner+Nihola/>

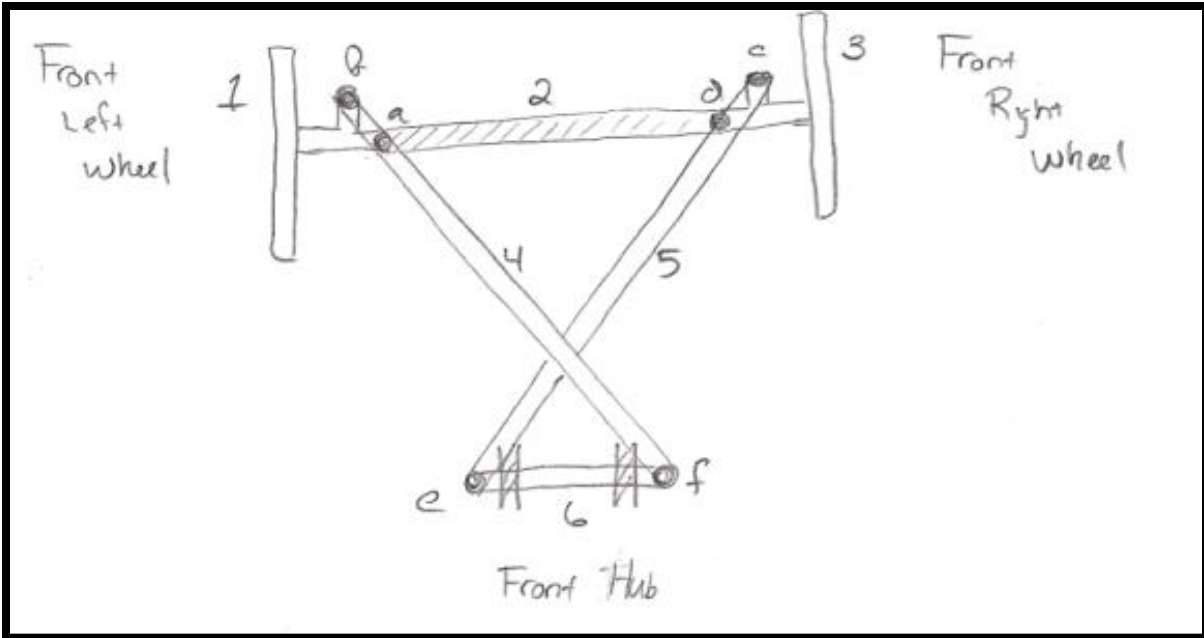


Figure 49: Cross Linkage Steering System

### 6.1.3 Fork Replacement Steering

The steering for the Fork Replacement concept, seen in Figure 50, is achieved by using a rotating steering tube rigidly connected to the bicycle's handlebars. This steering tube is then connected to the input link [2] and the coupler link [3] translates steering motion into the front wheels via output links [4] and [5].

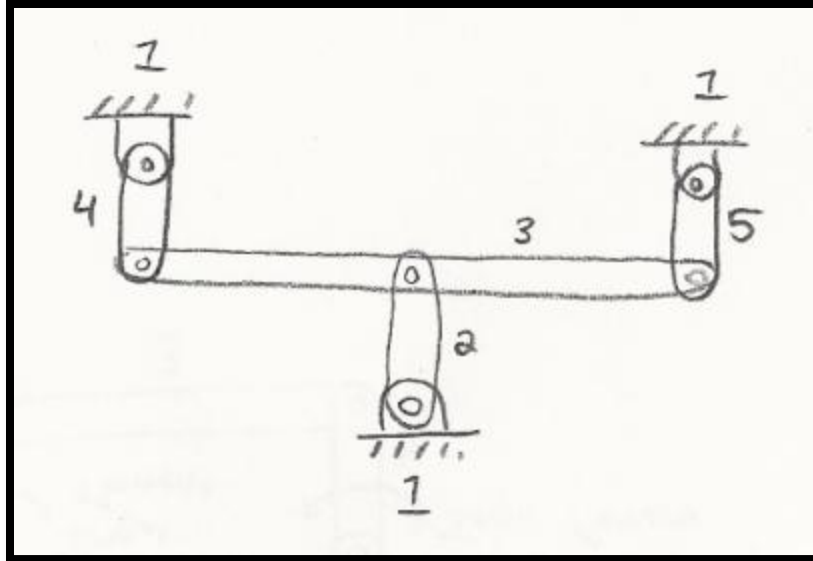


Figure 50: Fork Replacement Steering System

#### 6.1.4 Long John Steering

Using the Long John bicycle as a reference, a similar design was created to accommodate the two steering wheels used in this design, seen in Figure 51. Link [3] and pivot point [f] are considered ground and pivoting about ground respectively. The input link of this system is the front hub link [7], which rotates with the handlebars of the bicycle. This rotation is transferred via coupler link [6] to output link [5], which converts the y-direction movement to an x-direction movement. The output link [5] is then used as an input to create rotation of the front wheels links [1] and [2] via coupler link [4].

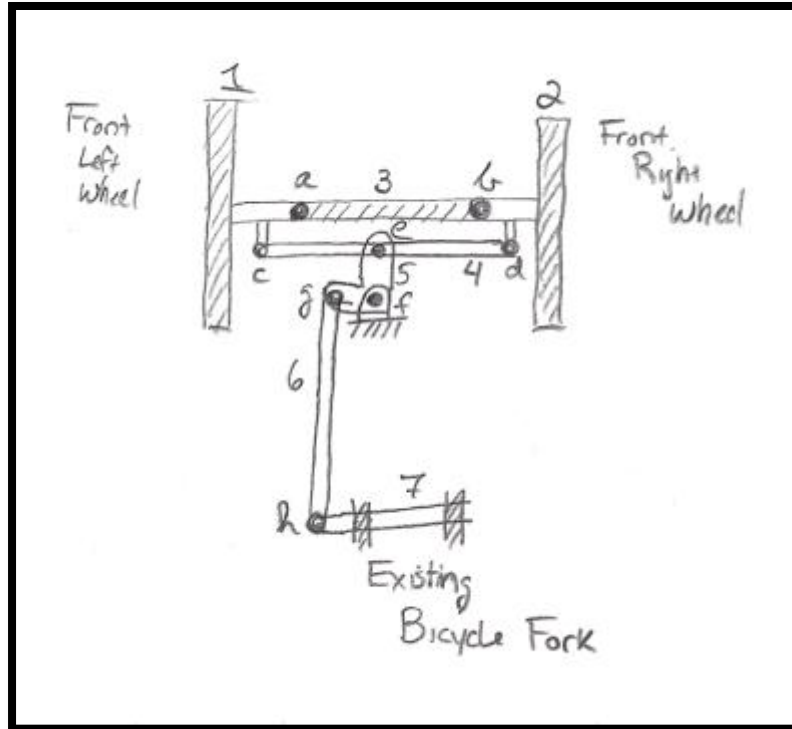


Figure 51: Long John Steering

### 6.1.5 Single Chain Driven Steering

A chain driven concept was also created to steer dual front wheels via the rotational motion of the existing bicycle's handlebars, as shown in Figure 53. Link [6] is considered to be rigidly connected to ground. The existing bicycle's fork is affixed with two near semi-circular gears on either side shown as Half Sprockets [2] and [3]. Sprockets [4] and [5] rotate about pivot point [c] and [d] respectively and are rigidly connected to output links [7] and [8] respectively. A single chain is fixed at point [a] and runs around gears [4] and [5], and then the opposite end is fixed to point [b].

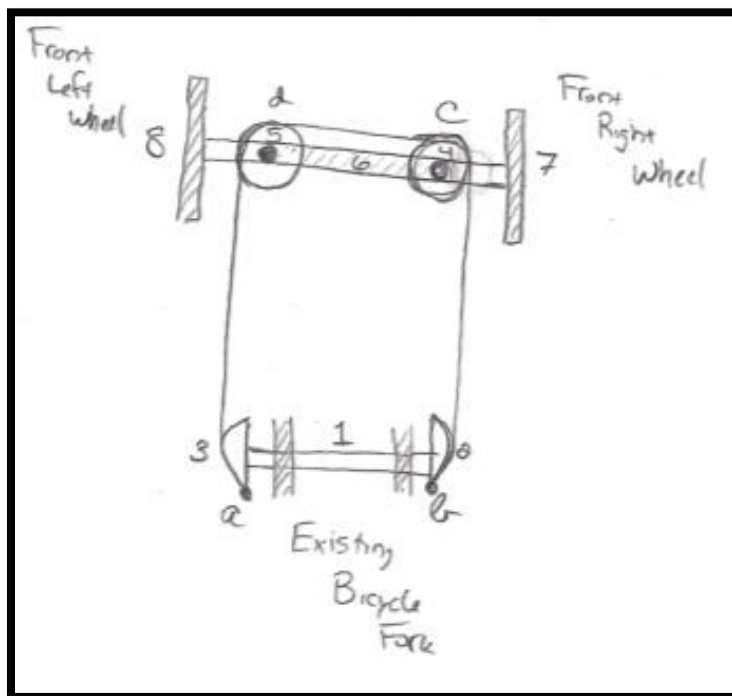


Figure 52: Single Chain Steering System



### 6.1.6 Multiple Chain Driven Steering

A second chain driven concept was created to similarly steer dual front wheels via the rotational motion of the existing bicycle's handlebars. The handlebar will be directly connected to a sprocket as seen in Figure 53. The frame for this design will be rectangular with sprockets at each corner. The sprockets will be fixedly mounted on a shaft located at each corner, for the front. The chain will be driven across these sprockets all the way to the forks. The forks will also have a sprocket attached to their ends; these sprockets will allow the forks to rotate as the handlebars are turned. All sprockets and chains will have a frame covering them for safety. The rear wheels in Figure 53 are trailing casters used to reduce the bending load on the existing bicycle head tube and the front device wheels.

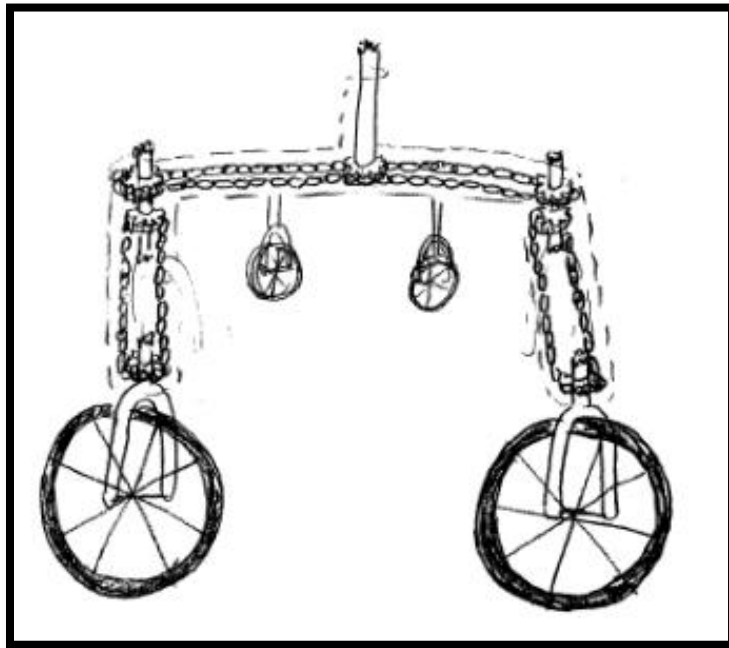


Figure 53: Multiple Chain Design

### 6.1.7 Rack and Pinion Steering

Similar to the steering in most automobiles, this preliminary design uses a rack and pinion mechanism to steer the front wheels. For this design the fork will be modified to fit a pinion gear attached to the handlebar. When the cyclist turns the handlebar, the gear spins, moving the rack in the direction the handlebar is turned. The rack will have a tie rod attached at both ends; this tie rod connects to the steering arm on the spindle of the wheel. This rack and pinion gear set converts the rotational motion of the handlebar into a linear motion to turn the wheel.

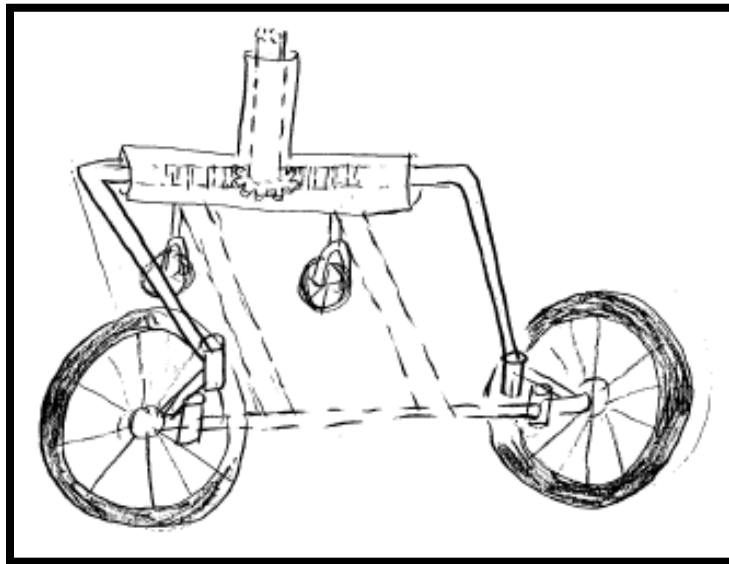


Figure 54: Rack and Pinion Design

## 6.2 Steering Selection

Choice of a final steering design was based on the following criteria derived from the design specifications set at the beginning of the project:

**Ease of Installation** – the amount of technical knowledge required to install the steering mechanism on the existing bicycle. Higher ratings were given to the mechanisms requiring the least technical knowledge because more people would be able to install the device.

**Efficiency of Transferring Motion** – the reliability of the system to transfer the handlebar rotation to rotation of the front wheels during steering. Higher ratings were given to the mechanisms with reliable motion transfer and minimal lag time between input and output reactions.

**Profile of the System** – the overall size of the system and number of moving parts included. Higher rankings were given to lower profile mechanisms.

**Safety to Passenger** – the location of moving parts relative to the location of the passengers. Higher rankings were given to devices that have reasonable distances between the passenger and moving parts or can be shielded.

The team was able to eliminate four of these designs based on the criteria mentioned above. In addition, these eliminated designs required significantly more work in installation and maintenance and did not offer improved performance over the other designs. The design team also valued designs that offered minimal to no modification to the bicycle. The designs eliminated using these criteria were the Direct Attachment, Fork Replacement, Single Chain, Multiple Chain, and Rack and Pinion steering systems.

After the unsatisfactory designs were eliminated, the remaining designs were the Cross Linkage and Long John Style systems.

### 6.3 Steering System Design Variables

As alterations were made to the steering systems to fit the device, the true effects of these changes required consideration. The following list illustrates how changing the link lengths in device will affect the bicycle's performance. In Figure 55 the input link is labeled [g] and the output link is labeled [h].

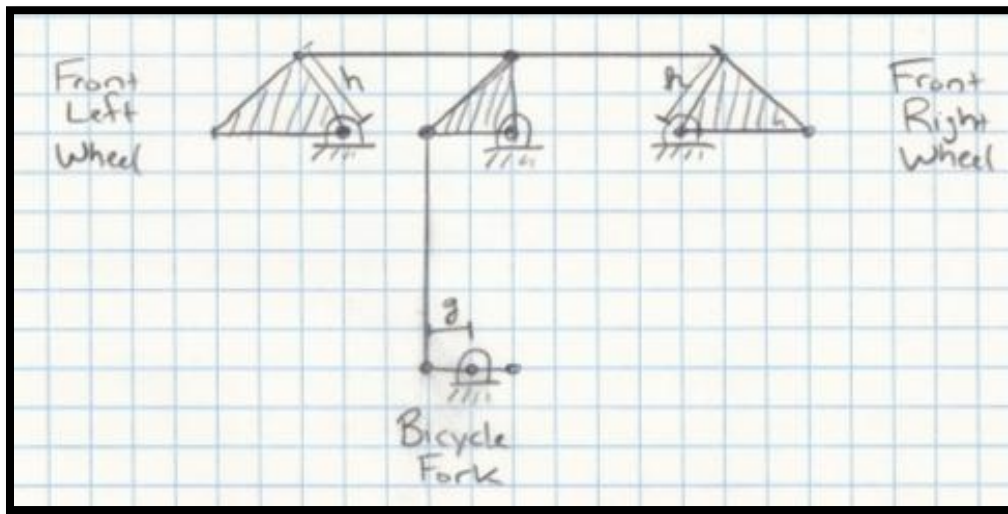


Figure 55: Steering System Design Variables

1. Input Link length [g in Figure 55]
  - a. Shorten
    - i. Greater handlebar rotation required for steering of device wheels
    - ii. Increase modification if shortened below the width of the existing bicycle's front hub
  - b. Lengthen
    - i. Smaller handlebar rotation required for steering of device wheels
    - ii. Confliction with driver's pedaling stroke if too wide
    - iii. May cause changes in attachment time
2. Output Link length [h Figure 55]

- a. Shorten
  - i. For an input, the steering wheels will rotate more.
  - ii. May increase modification if shortened too much and clearance around the steering wheels becomes an issue
- b. Lengthen
  - i. For an input, the steering wheels will rotate less.
  - ii. May conflict with the passenger's footrest/legs if lengthened too far.

The design team developed steering systems focusing on satisfying the task specifications of the project by altering the steering with respect to the design variables.

## **6.4 Zero-th Order Prototypes**

To develop a further understanding of these steering systems, a zero-th order prototype of each system was created. The prototypes helped with visualization of the systems and showed design flaws in the systems that weren't apparent in diagrams.

### **6.4.1 Cross Linkage Steering System Prototype**

The first steering design concept developed is similar to a benchmarked device researched called the Nihola bicycle, as seen in Figure 56 and Figure 57. The cross linkage system of the Nihola bike can be seen in Figure 57.



Figure 56: The Nihola<sup>30</sup>

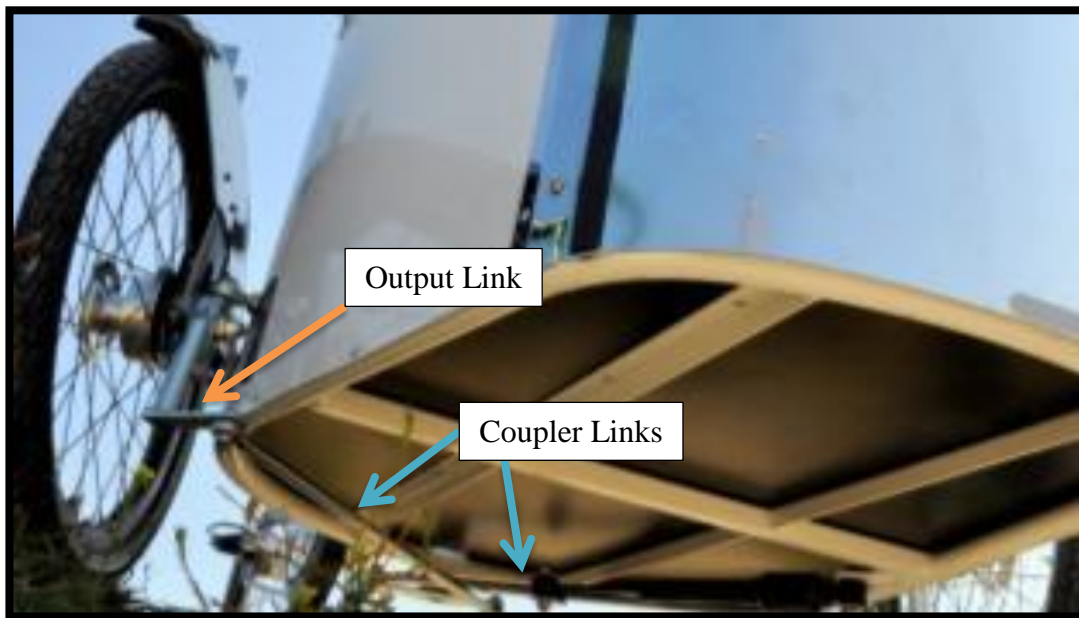


Figure 57: Nihola's Steering System<sup>31</sup>

The Nihola bike is a stand-alone bicycle that carries passengers in a large compartment located in front of the driver. The zero-th order prototype of the Cross Linkage system can be

<sup>30</sup> [http://www.nihola.de/en/nihola\\_bikes](http://www.nihola.de/en/nihola_bikes)

<sup>31</sup> <http://www.nihola.de/en/news/848.a-niholas-global-adventure-40.000-kilometres-through-south-america..html>

seen in Figure 58. The system can be regarded as two four bar linkage systems transferring motion of the handlebars [input link] to the output links via two coupler links.



Figure 58: Cross Linkage Steering Zero-th Order Prototype

#### 6.4.2 Long John Style Steering System Prototype

The Long John Style steering system was created using a Danish Long John bicycle as a model. The Danish Long John bicycle uses a single coupler link to transfer the rotation of the handlebars to a front wheel placed approximately four feet forward of the handlebars, as seen in Figure 59.



Figure 59: Long John<sup>32</sup>

However, for the bicycle attachment device, the linkage systems would need to transfer rotational motion of the handlebars into rotation of two device wheels. Using two coupled parallelogram linkages, the Long John Style steering system is capable of transferring the motion into two device wheels as seen in Figure 60.

---

<sup>32</sup> [http://www.longjohn.org/galerie/galerie\\_de.html#26](http://www.longjohn.org/galerie/galerie_de.html#26)



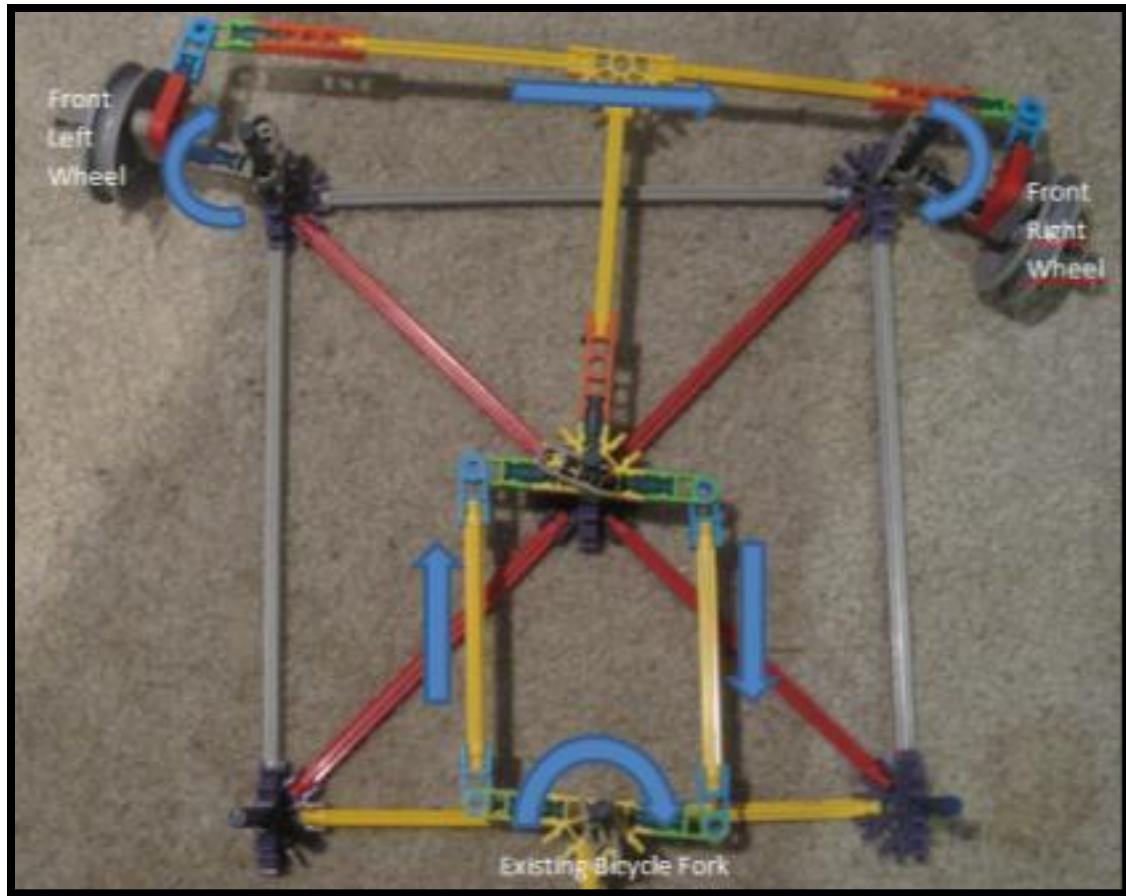


Figure 60: Long John Style Steering Zero-th Order Prototype

## 6.5 Graphical Analysis

Using these zero-th order prototypes, the steering systems were then drawn to scale in two positions: neutral (straight steering) and fully turned to the left. These diagrams were used to measure transmission angles and link lengths.

The following are the assumptions of the device:

- 1) Distance from front fork to device wheels (y axis) = 16 inches
- 2) Front hub width = 4 inches
- 3) Distance between device wheels (x axis) = 36 inches

### 6.5.1 Cross Linkage Steering System

Using these assumptions and the drawing seen in Figure 61 of the Cross Linkage system, the following values were calculated:

Coupler Link length = 24 inches

When the Cross Linkage system is drawn with a  $45^\circ$  steering angle, the linkage enters a toggle position and continues movement through toggle as seen in Figure 61. This condition is unsatisfactory for a steering system and could potentially be very harmful to the cyclist and passenger because the system enters a state where multiple different paths are possible and therefore could result in the device steering unpredictably. As the steering of this device should follow a single path through its range of motion, toggle positions within this range are unacceptable.

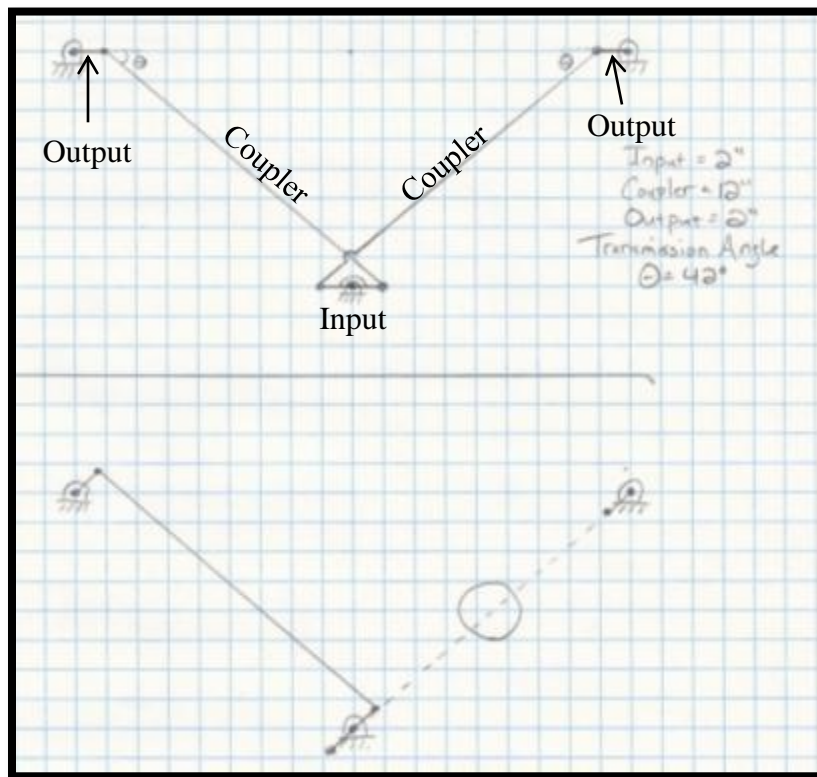


Figure 61: Cross Linkage Neutral and Toggle Positions

In order to operate this steering system without reaching toggle, the steering angle must be reduced to approximately  $30^\circ$ . This altered version of this steering system can be seen in Figure 62. The decreased steering angle would ultimately cause greater difficulty for the driver when attempting to turn, and especially in situations with a sharp turn, like a U-turn. Decreasing the steering angle will reduce the maneuverability of the device as well as increase the turning radius. In addition, this  $30^\circ$  steering angle is below the original design specification of a maximum steering angle of  $45^\circ$ . The transmission angles for this design also proved to be a concern; the left and right sides have transmission angles of  $65^\circ$  and  $13^\circ$  respectively. The left transmission angle is acceptable for this device's purposes, but the right steering angle is far below the efficient operating transmission angles for any four bar linkage system. Therefore, a greater force must be exerted by the driver while rotating the handlebars to steer the system from neutral to the maximum turning position. While at a fully turned position, the steering system will not respond as quickly as the other systems because it is so close to a toggle position.

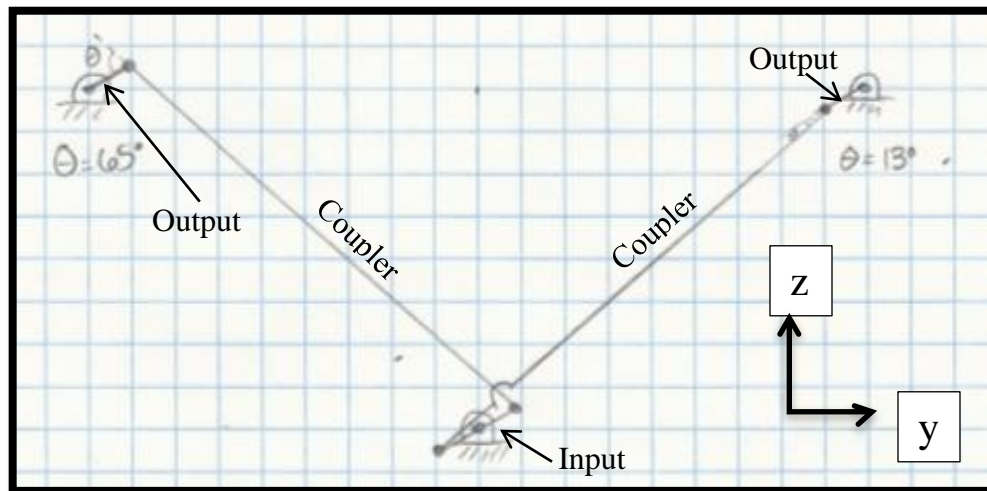


Figure 62: Cross Linkage Turned Position (revised)

## 6.5.2 Long John Style Steering System

The Long John Style Steering System uses two parallelogram linkage systems using the output of one system as the input to the other as seen in Figure 63. The same device assumptions as used in the previous two systems were used for this system. The following values were calculated with these assumptions:

Transmission Angle =  $90^\circ$  (neutral) and  $45^\circ$  (turned)

Coupler Link Length = 18 inches

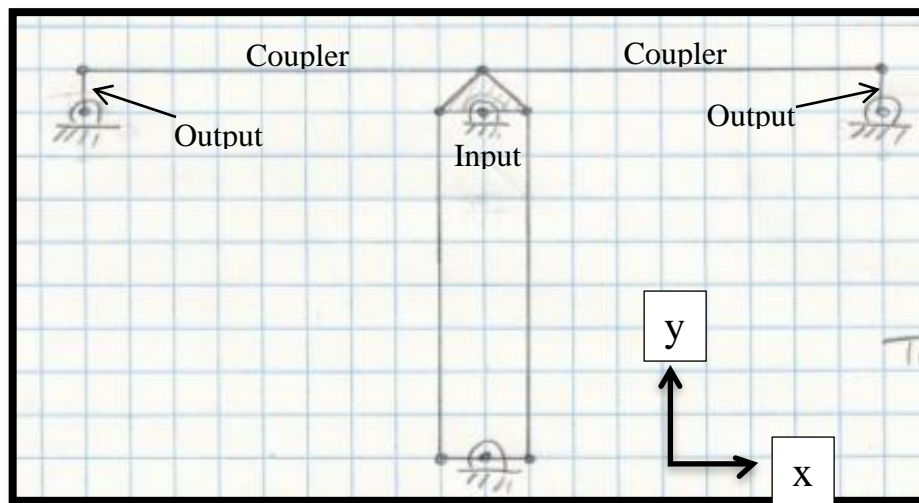


Figure 63: Long John Style Neutral Position

The Long John Style steering system would be capable of reaching our expectation of  $45^\circ$  steering angle without reaching any toggle positions as seen in Figure 64.

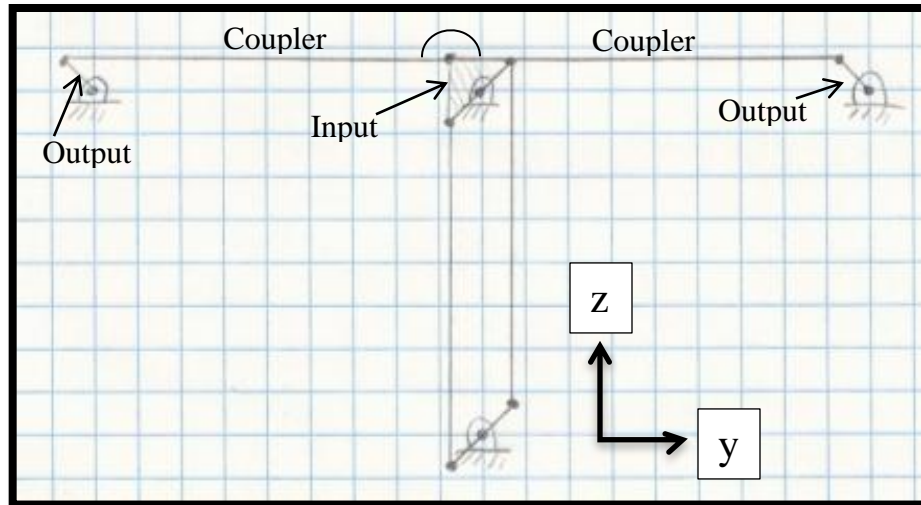


Figure 64: Long John Style Turned Position

## 6.6 Computer Aided Kinematic Analysis

The next step in analyzing these two steering system was to use the Design of Machinery program Four Bar for the kinematic analysis.

### 6.6.1 Cross Linkage Steering System

The first illustration, seen in Figure 65, is the screenshot for the FourBar model created for the Cross Linkage steering system. The model was constructed using anticipated dimensions for the device frame and wheel placement. When initially modeled, the system was unable to reach the  $45^\circ$  steering angle without reaching a toggle position. The steering angle was reduced until the system did not reach the toggle position which was found to be  $24^\circ$ . This value is  $6^\circ$  less than the steering angle found during graphical analysis. This steering angle is approximately half the design specification of a  $45^\circ$  steering angle. This model provides sufficient proof that the Cross Linkage steering system will not be suitable for this application.

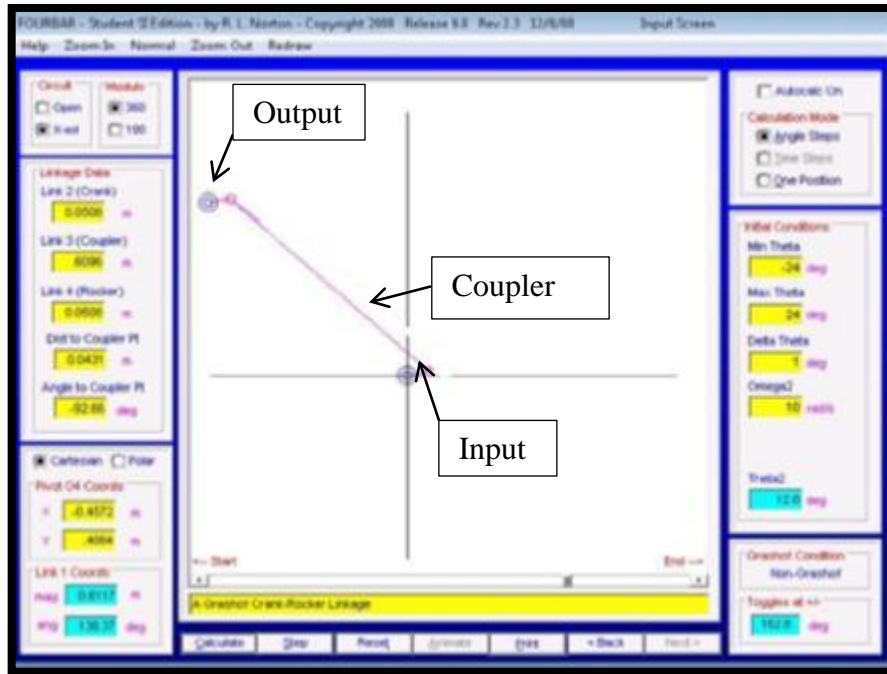


Figure 65: Cross Linkage Four Bar Model

## 6.6.2 Long John Style Steering System

The Long John Style steering system was then modeled in Four Bar using the same device dimensions and anticipated link lengths for the device. The Four Bar model screenshot can be seen in Figure 66.

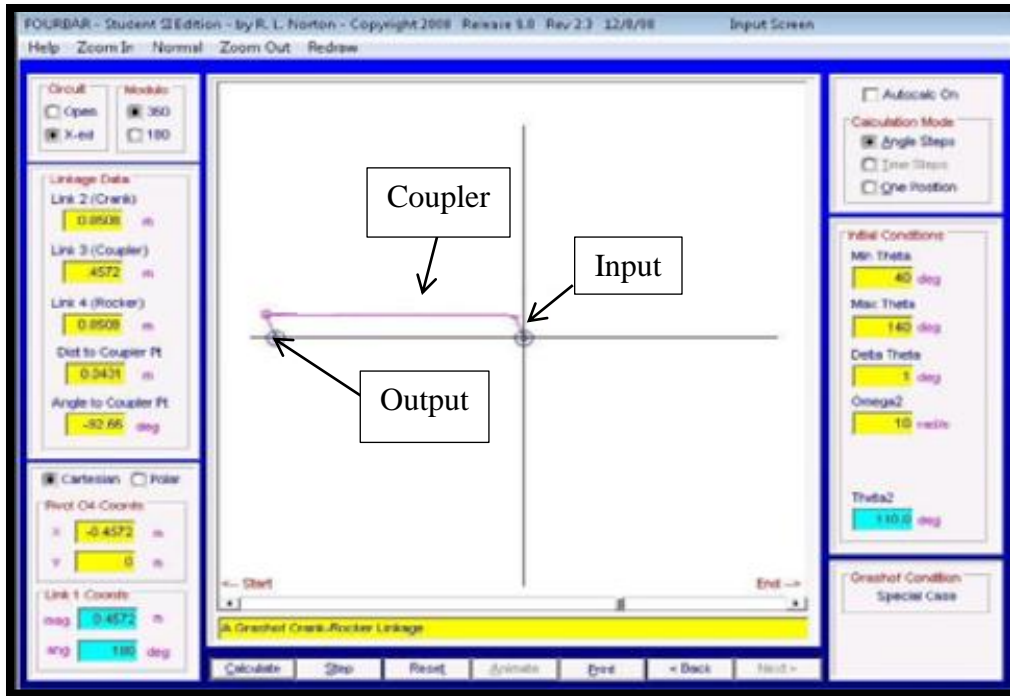


Figure 66: Long John Style Four Bar Model

Using the plotting tool within the Four Bar program, the theta values (angles between adjacent links) and the transmission angle (angle between the coupler and output links) were graphed during the motion of the mechanism between  $-45^\circ$  and  $+45^\circ$ . The graphs in Four Bar can be seen in Figure 67. The key graph for this analysis is the bottom graph showing the transmission angles shown in a red circle in the figure. This analysis shows that the transmission angle for this mechanism begins at  $90^\circ$  in the neutral position and falls to  $40^\circ$  in the fully turned position in either direction.

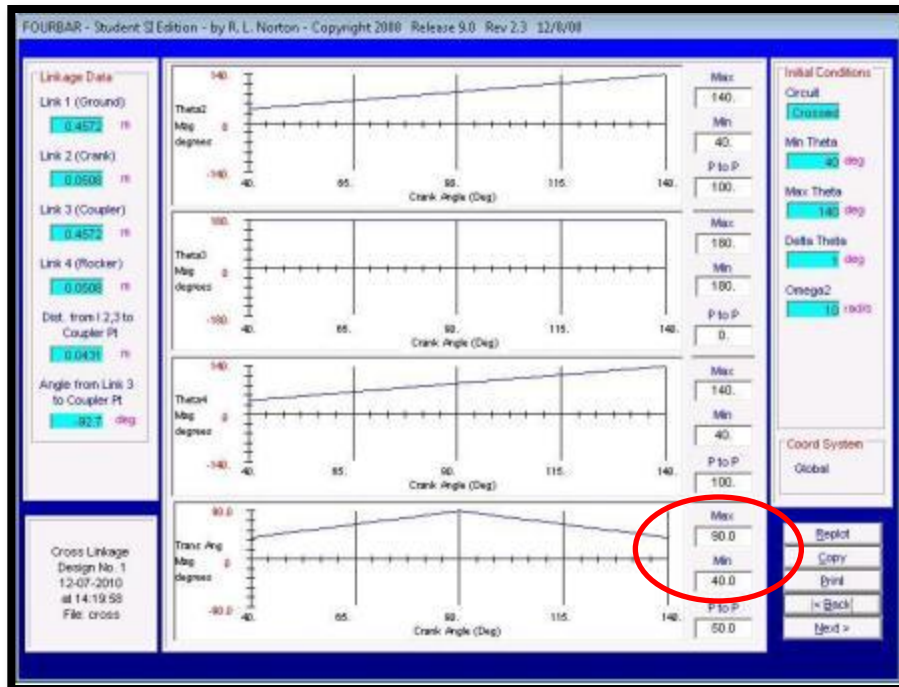


Figure 67: Long John Style Four Bar Model Theta Values and Transmission Angle

### 6.6.3 Steering System Re-Design

As structural analysis of the device frame was performed, an excessive moment centered at the attachment mechanism was found. This load was too large for the attachment mechanism to maintain under static conditions, so the device was altered to include the front bicycle wheel. This extra support at the front of the bicycle would drastically lower the forces and moments on the attachment system and device. The Long John Style steering system was chosen as the final steering system for this design, and was altered to eliminate the input parallelogram linkage because the device steering wheels were moved back and along the same axis as the existing bicycle wheel hub. The right side of the parallelogram linkage system for the device steering can be seen in Figure 68.



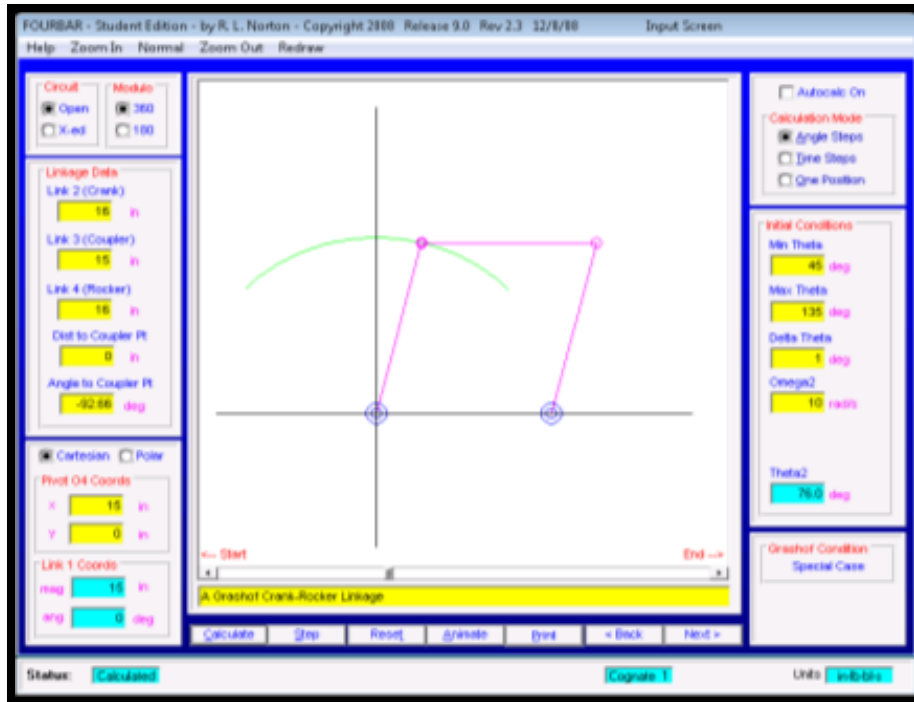


Figure 68: Device Steering Kinematics

In Figure 69, an exploded view of the steering system is shown. The green horizontal fork denotes the input link connected to the bicycle wheel. The red horizontal fork denotes the device steering wheels. The attachment points of the horizontal forks are shown with double sided black arrows, these holes are located where the wheel hubs pass through the horizontal fork arms. The coupler links are the blue flat bars in the figure with the light blue rods being the coupler rods.

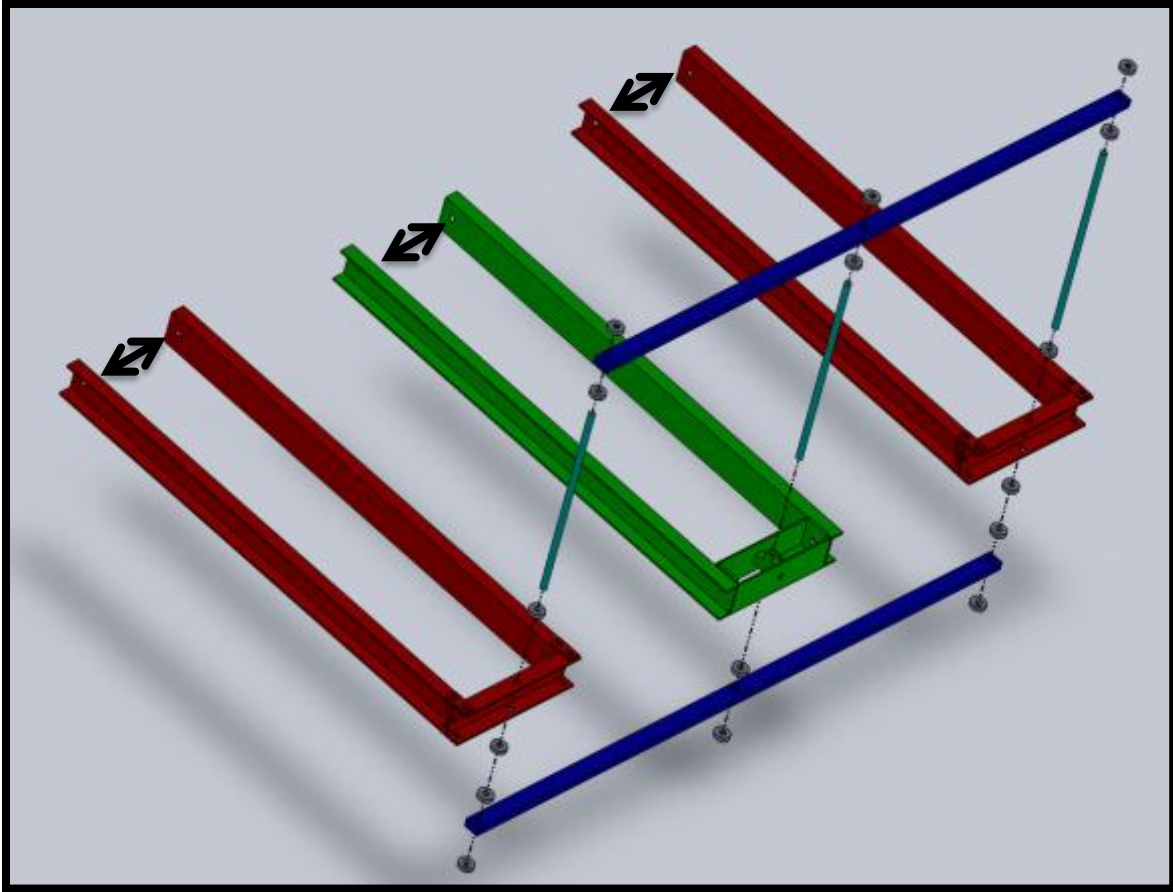


Figure 69: Detailed CAD Illustration of Steering System

## 6.7 Steering Analysis

To determine the input forces acting on the steering system, the following test was performed to provide input data for the analyses. Using a mountain bike with 22" diameter wheels (26" diameter including the tire), the team measured the input moment applied to the horizontal forks by the driver via rotation of the handlebars. The driver of the bicycle first remained stationary while on a carpeted surface and rotated the handlebars and front bicycle wheel. Next, a manual force gauge was attached to one fork arm and the driver rotated the handlebars while the bicycle was on a smooth, tile floor. The driver rotated the handlebars until the resistance provided by the force gauge made rotation difficult. Using the force reading and the measured moment arm between the pivot point of the bicycle fork and the attachment point

of the force gauge, the team estimated the input moment provided by the driver for one wheel contacting the ground will be 15 lbf\*ft. The couple force to this input moment will provide a 45 lbf axial force along each arm of the input (middle) horizontal fork. Given that this device will require three turning wheels in contact with the ground, a reasonable assumption was made that the driver will input 45 lbf\*ft. to the steering system.

In Figure 70, a side view of the horizontal fork is shown is the forces acting on the body.

A description of these forces are given below:

Normal Force A: Vertical Force supplied by the rigid connection between the horizontal fork and the device wheel hub.

Normal Force B: Vertical Force supplied by the rigid vertical connection between the horizontal fork and the coupler link of the steering system.

Weight Force: Gravitational Force acting on the center of gravity of the horizontal fork.

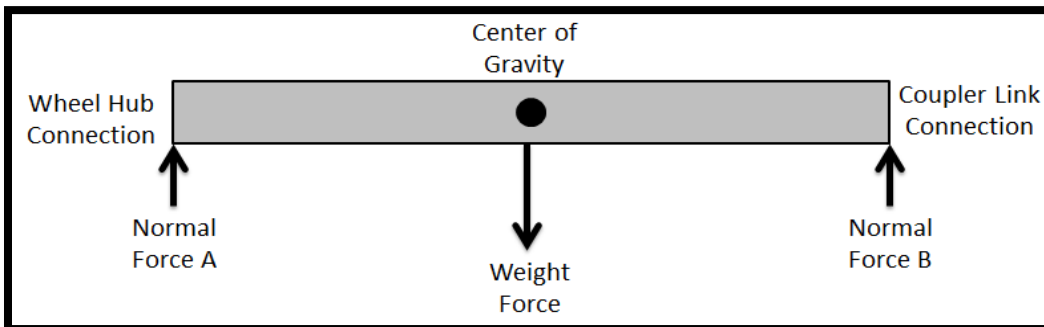


Figure 70: Horizontal Fork Side View Free Body Diagram

In Figure 71, the horizontal fork arm free body diagram is labeled with all forces acting upon it. Descriptions of the forces and their origin can be seen below:

$F_{ex}$  – Input Moment decomposed to Couple Forces acting on each Fork Arm supplied by the driver of the bicycle through rotation of the handlebars.

$F_{bolt}$  – Compressive Force supplied by tightening the bicycle wheel hub causing contact between the Horizontal Fork Arm and the Vertical Fork of the bicycle wheel.

$N_{bolt}$  – Normal Force opposing the compressive force  $F_{bolt}$  caused by the structural rigidity of the Vertical Fork of the bicycle wheel.

$N_{support}$  – Shear and Axial Forces (acting along the horizontal fork arm) provided by the support components connecting the Fork Arm Connection member to the Fork Arms.

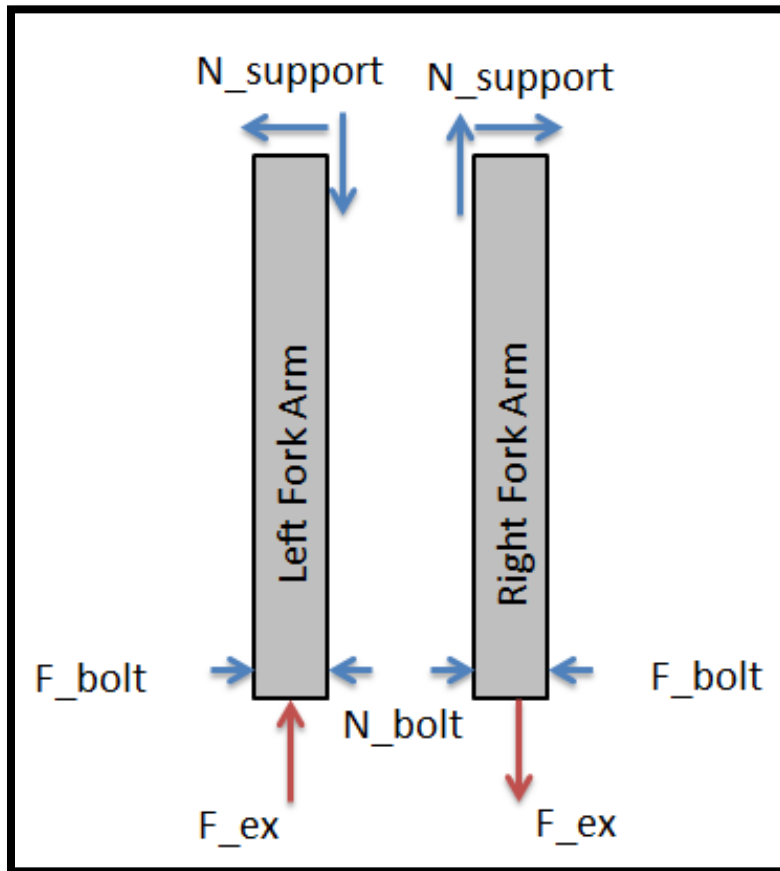


Figure 71: Fork Arm Free Body Diagram

In Figure 71, the horizontal fork arm free body diagram is labeled with all forces acting upon it. Descriptions of the forces and their origin can be seen below:

$F_{ex}$  – Input Moment decomposed to Couple Forces acting on each Fork Arm supplied by the driver of the bicycle through rotation of the handlebars.

$N_{support}$  – Normal Forces supplied by the support components connecting the Fork Arm Connection and the Fork Arms.

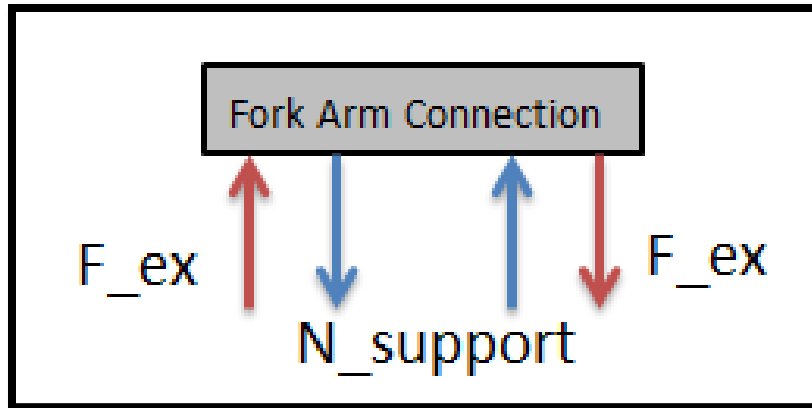


Figure 72: Fork Arm Connection Free Body Diagram

The sum of these forces acting on the horizontal fork under dynamic loading as illustrated in the above two figures results in rotation of the horizontal fork about the vertical fork axis.

## 6.8 Stress Analysis

Using the Solid Works 2010 software, a von Misses stress analysis and displacement analysis was produced using accurate, simple geometry for each component and approximate locations of forces acting upon the component.

### 6.8.1 Horizontal Fork Analysis

The horizontal forks are identical in dimensions and profile to each other, however the loading conditions for the input and output horizontal forks are significantly different.

The approximate moment being applied to each horizontal fork by the driver is about 15 lbf\*ft. The couple force of 45 lbf per arm of the fork is the value used to perform the displacement and stress analyses on the forks.

The displacement and stress analysis illustrations of a simple geometry model of the horizontal fork are shown in Figure 73 and Figure 74 respectively. A 45 lbf force (shown in purple) was applied on each arm of the horizontal fork in opposite directions and the coupler connection hole was the fixture point (shown by green markers). This analysis was performed to determine the maximum displacement of the horizontal fork under loading conditions. The

displacement is a primary concern because the clearance around the tires and wheels is small and contact between the tire and horizontal fork will be a major safety hazard for the passenger and driver. The blue color in **Figure 73** represents lower displacement and red represents areas of higher displacement. In this analysis, the highest amount of displacement experienced by the horizontal fork laterally is 0.13 mm. This deflection will not cause any interference between the bicycle wheel and the horizontal fork.

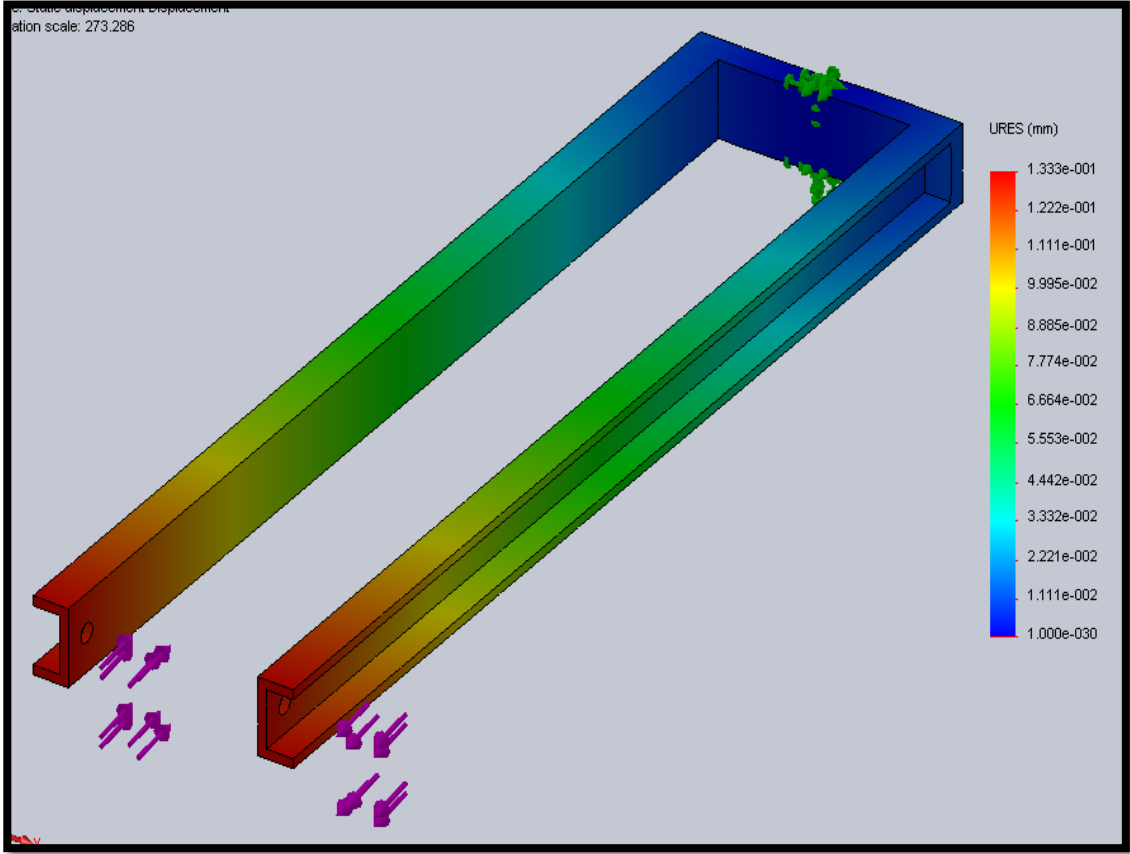


Figure 73: Input Horizontal Fork Displacement

In Figure 74, the areas of highest stress are illustrated in red or yellow and areas of lower stress are in blue. The areas of highest stress for the input horizontal fork is are the fork arm and cross member joints and at the coupler point of the cross member. The maximum stress

experienced is far less than the yield strength of the Aluminum 6061 used to construct the arms even with a safety factor of 3.

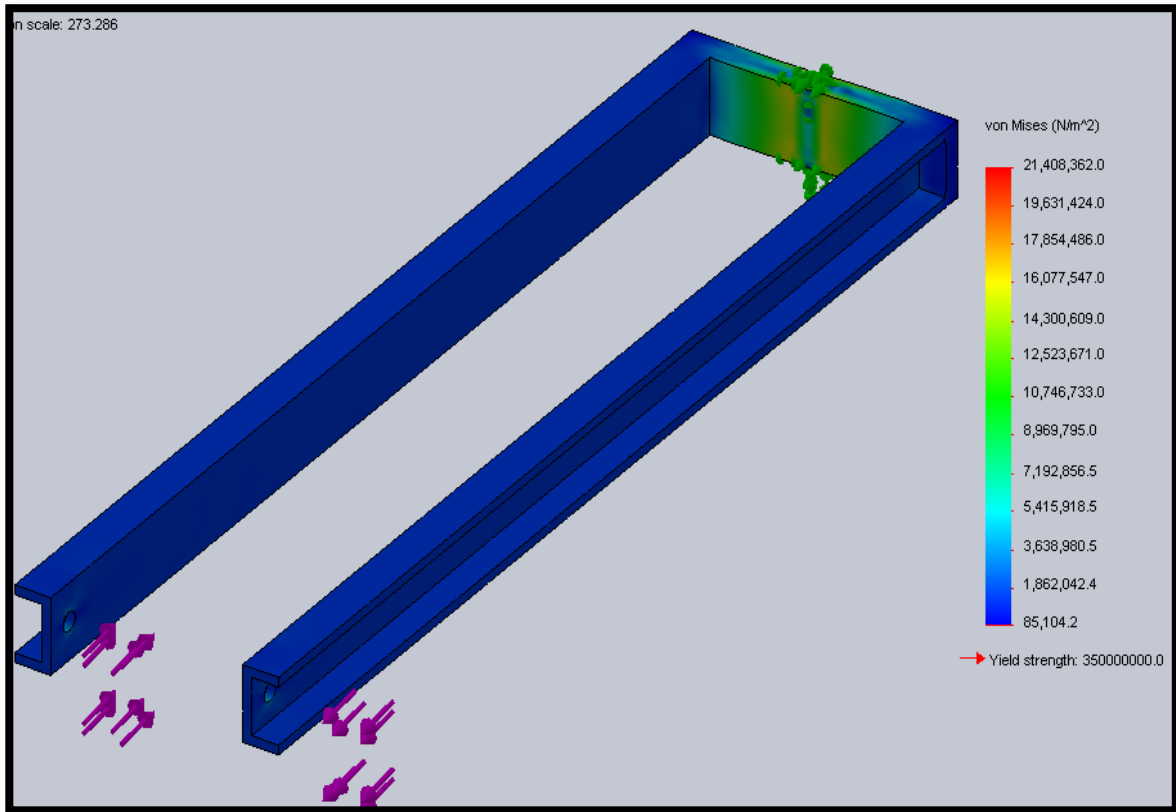


Figure 74: Input Horizontal Fork Stress Analysis

The displacement and stress analysis illustrations shown in Figure 75 and Figure 76 respectively are for the right output horizontal fork. The actual loading force supplied by the coupler link is estimated at 15 lbf, for this analysis an exaggerated load of 25 lbf force was applied to the coupler connection hole axially along the cross member between the fork arms, shown as purple arrows in the figures. The hub connection holes in each fork arm were used as the fixture points, shown by green markers, for this analysis. The displacements of the left and right horizontal forks are of particular concern because these two components are loaded with a lateral force from the coupler acting perpendicular to the fork arms (in the neutral position). The lengths of the fork arms make these parts most susceptible to bending under this loading

condition. The displacement analysis illustrates areas of higher displacement in red and lower displacement in blue. This analysis shows that when the coupler link supplies a 30 lbf to the horizontal fork, the fork has a maximum displacement of 1.3 mm in the direction of the coupler force. This small displacement will not cause any clearance issues with our device or its surroundings.

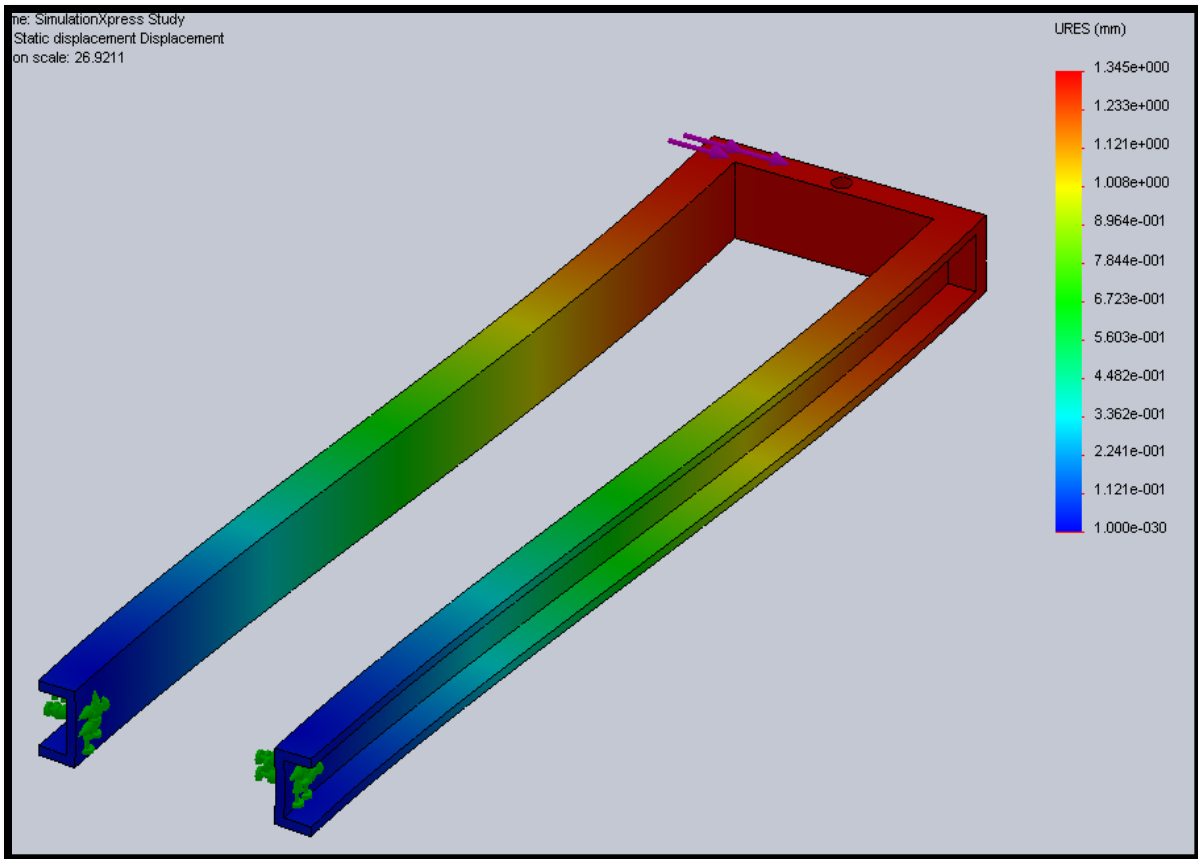


Figure 75: Right Output Horizontal Fork Displacement

In Figure 76, the stress analysis of the right horizontal fork is shown. Areas of high stresses are illustrated in red or yellow and areas of lower stress are in green or blue. The areas of highest stress are located along the walls of the C-channel of the fork arms and at the connection point of the device wheel hub and the horizontal fork. Again, the maximum stresses



experienced by the Aluminum 6061 horizontal fork is far less than its yield strength even when a safety factor of 3 is applied.

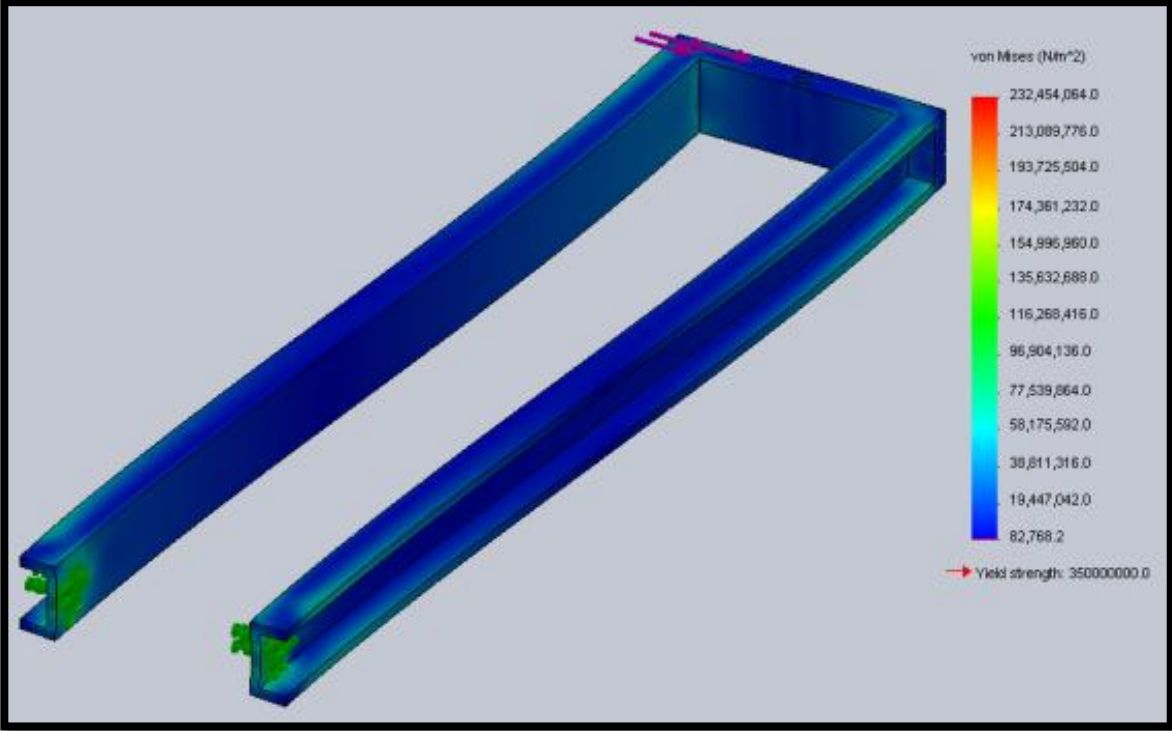


Figure 76: Right Output Horizontal Fork Stress Analysis

## **CHAPTER 7: ATTACHMENT**

The final part of the design consists of the attachment mechanism. This is critical to the product because it is necessary in order for the design to be a universal device. As part of the team's design specifications the attachment mechanism is required to work with all bicycles regardless of their head tube design or size. The attachment mechanism is also an essential device since it could have an impact on the steering of the device.

The possible locations for attachment observed by the team were few and all were incapable of securing a rigid attachment. The small number of mounting locations were caused by the design specification that the existing bicycle frame should require minimal to no modifications, interference with the brake cables, and the desire for the attachment design to be adaptable for most bikes. The three points on the frame for attachment as initially determined by the team were the head tube, the front fork, and the front hub. The preliminary designs are described below.

### **7.1 Head Tube**

One attachment concept involves removing both the front bicycle wheel as well as the front fork. The fork is then replaced with a tube which is extended up into the head tube and fixed to a bar that extends out laterally so that it can be attached to two new bicycle forks and wheels.

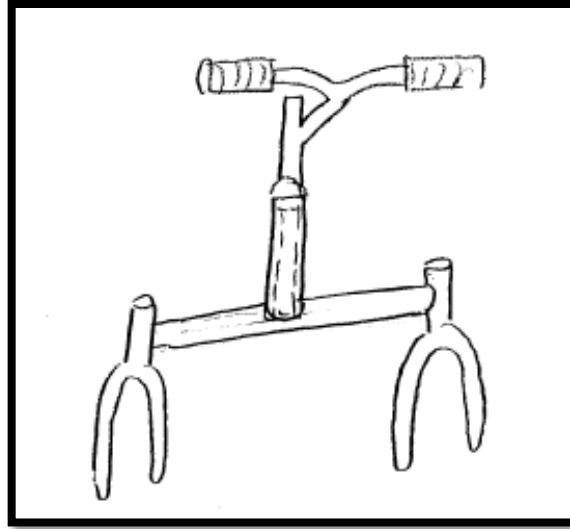


Figure 77: Head Tube Attachment

## 7.2 Front Hub

Another attachment point on a bicycle is the front hub. Designs featuring this type of attachment involve a smaller, supportive wheel connected to the hub. This wheel would be able to pivot to allow this supportive wheel to move independently of the bicycle fork. In this design, the steering linkages would be connected to the front fork of the bicycle and the frame can be connected to the wheel support. Attaching to the front hub would allow the device to be attached or detached from the bicycle very quickly and require very little bicycle knowledge from the user.

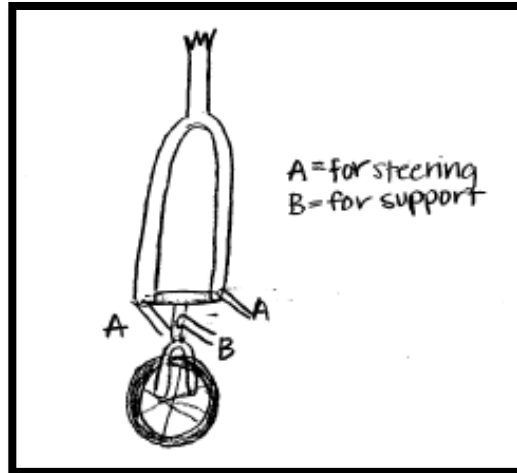


Figure 78: Front Hub Attachment

### 7.3 Direct Fork Connection to Device

The last attachment point on the bicycle is the front fork. Designs featuring this connection have a rigid attachment directly from the front fork to the device so that the bicycle steering is directly related to steering of the overall system. In this design, the front fork sits in two tubes that are connected both to the support wheel as well as the frame of the device.

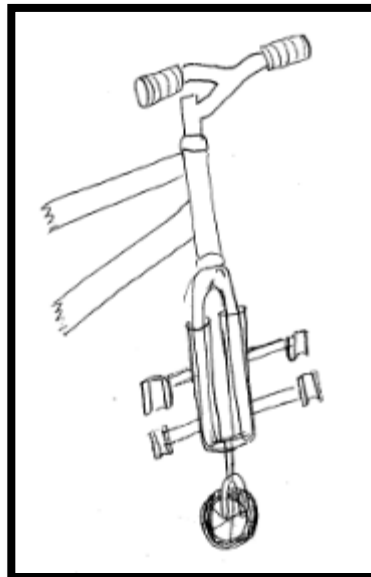


Figure 79: Direct Fork Connection

## 7.4 Attachment Decision

In order to determine which design was best, the team determined that the following features were important to an attachment design.

*Ease of Attachment* – How easy it is to connect the device to any bicycle. Items considered include time it takes to attach the device and how many tools are needed.

*Necessary Knowledge of Bicycles*– How much the consumer needs to know about bicycles in order to complete the attachment. A device that only requires a simple manual to understand is much better than one that requires the cyclist to understand the mechanisms behind their bicycle, how it works, and how to take it apart and put it back together.

*Safety* – How securely the device is attached to the bicycle.

Each of the above areas was rated on importance and then the different designs were rated on how well they met the criteria.

First, the head tube design was discarded because it became evident that it did not meet a number of the standards required for the attachment mechanism. The primary item violated was the design specification of requiring little to no modification to the bicycle; once the team took apart a bicycle it became evident that removing the front fork, including the part that extends up the head tube, is a large, time-consuming task. It would be difficult to complete this task without harming the bicycle, and, even if the bicycle wasn't harmed, this particular design is much worse in "Ease of Attachment" than originally rated. Because of these reasons this design was removed from consideration.

The second two designs were also discarded because of how they were attached to the front fork. An article was found online that rated other bike systems, like the Nihola, that carried passengers in the front and it indicated that designs that had the support system separate from the

steering system were ideal. It claimed any product that pushed the weight through the steering system was incredibly difficult to steer (Nihola). Due to this discovery, the team decided to discard any designs that connected the front fork to the frame of the device.

The team analyzed the bicycle and discovered another point to be used for attachment; the space between the head tube and down tube of the bicycle. The team determined that this area could be used, in addition to the outside of the head tube, to clamp the attachment to the bicycle. This way the head tube attachment point could be utilized without removing the front fork. The team used this new design concept to create a new design; the composite attachment.

This design features a pulley-shaped member, which is slid into the space in between the top tube and down tube of the bicycle. Another block is placed on the outside of the head tube with a C shaped channel so the head tube sits securely against it. A threaded rod is used to pull the two pieces snugly together but allows for the distance in between them to be adjusted for different bicycle frames. For attachment purposes, each piece also has a rod running through it that is connected to an L-bracket on both sides. The L brackets are used to connect the two pieces to the threaded rod, as seen in Figure 80 and Figure 81.

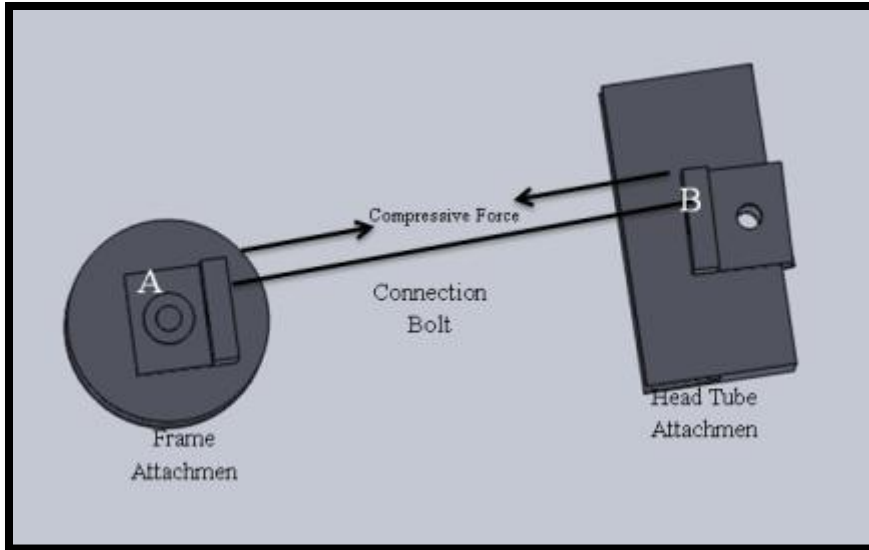


Figure 80: C Attachment Side View

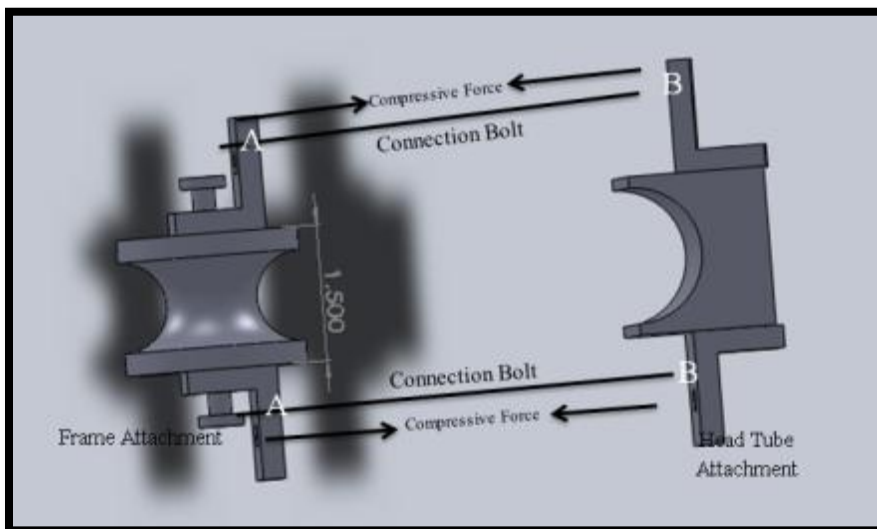


Figure 81: C Attachment Top View

The complication of this design was attaching the block, or head tube attachment, to the frame of the device. Originally the team discussed using a piece of tubing that ran horizontally from the head tube to the device frame. However, as analysis was completed of the frame, it became obvious that the chosen design was not adequate. The forces and moments carried by the attachment and connecting tubing were excessive. Changes to the attachment mechanism were

made so that the connecting tubing was slanted downwards towards the device in hopes that such a change would reduce the forces and moments.

However, while the forces were reduced, the reduction wasn't sufficient, and, with this change, the attachment now partially relied on friction which was determined to be unreliable. It was decided that the only way to make a significant reduction in these forces and moments was to change the design to include the front bicycle wheel. While this change did cause some issues in other parts of the design, like steering, it did greatly reduce the forces.

Due to the addition of the front bicycle wheel, components of the attachment changed. The size of the wheel forced the device to be moved further away from the bicycle, causing the attachment tubing to be extended. And although the two objects – the bicycle and device – were further apart, the forces in the attachment tubing were not greatly affected because the bicycle was now self-supporting. Because this tubing didn't need to hold as much weight, the attachment mechanism acted only as a pushing mechanism and no longer also needed to be a structural support.

While making these changes, the team decided to add an aspect of flexibility to the attachment mechanism. Two items were changed to achieve this; first, a ball joint was added to the middle of the attachment's tubing, and, second, the fitting that connected the attachment tubing to the device tubing was milled out so that it could rotate freely about the device allowing the attachment tubing to be positioned at a range of angles from horizontal to almost vertical. The purpose of these two pivot points was to make the attachment adjustable for bikes of any height and any head tube angle.



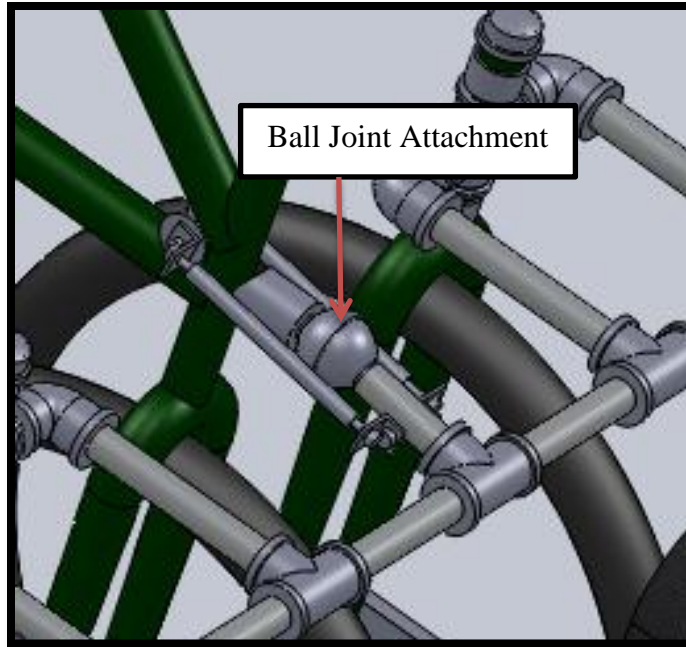


Figure 82: Elbow Joint Attachment

However, this was still not the final design of the attachment mechanism. It was decided that although the ball joint provided the desired flexibility, the fact that it could not lock into place was undesirable for its function. Instead of relying on two rotating joints, the mechanism was changed to include two new features. The first feature allows the attachment mechanism to be adjusted vertically. A box was built into the back of the device frame with a vertical piece of tubing running up the middle. This tubing featured a series of holes that allowed the attachment system to be positioned at a variety of heights. The second feature allows for rotational adjustment. There are two pieces of tubing with two bolts running through them. One bolt acts as a pivot joint and the second bolt can be placed in a series of holes along a curved path that allow the attachment to be fixed at different angles. The attachment system is able to rotate 20 degrees on either side of horizontal.

## CHAPTER 8: FINAL DESIGN

Since the attachment, steering and frame preliminary designs were nearly interchangeable to form a device, the best suited of each respective system were chosen to form the final design, which can be seen below.

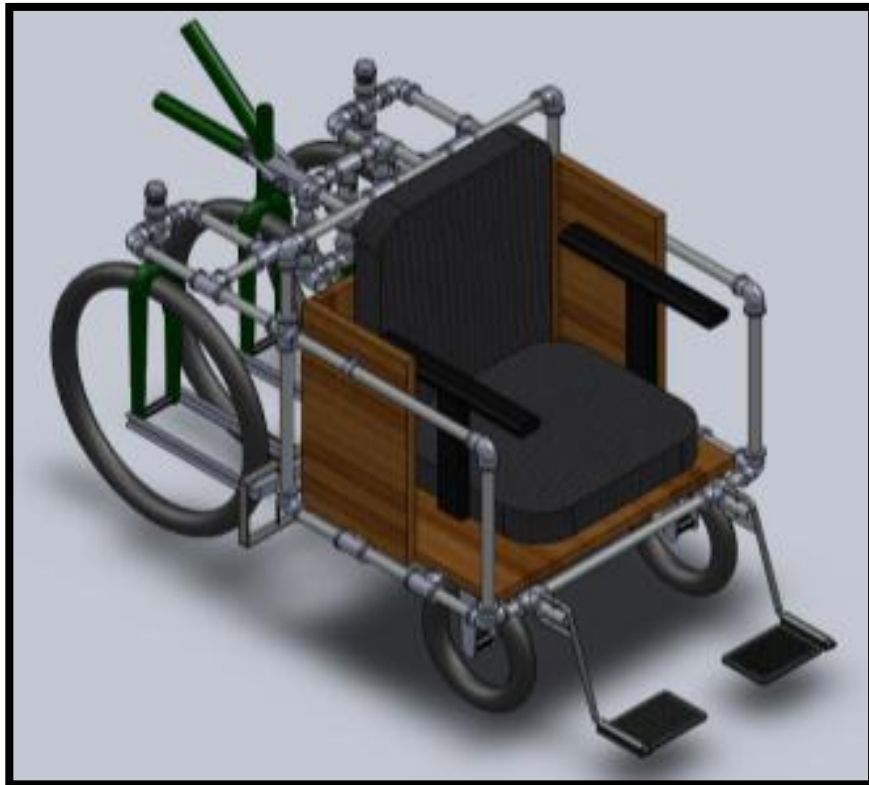


Figure 83: Final Design

### 8.1 Attachment

One freedom of adjustability required is the vertical adjustment to allow for bicycles with varying frame geometries and wheel diameters to be attached. To form this adjustment, a box was built into the back of the device frame with a vertical piece of tubing running up the middle. A CAD model of this design can be seen in Figure 84.

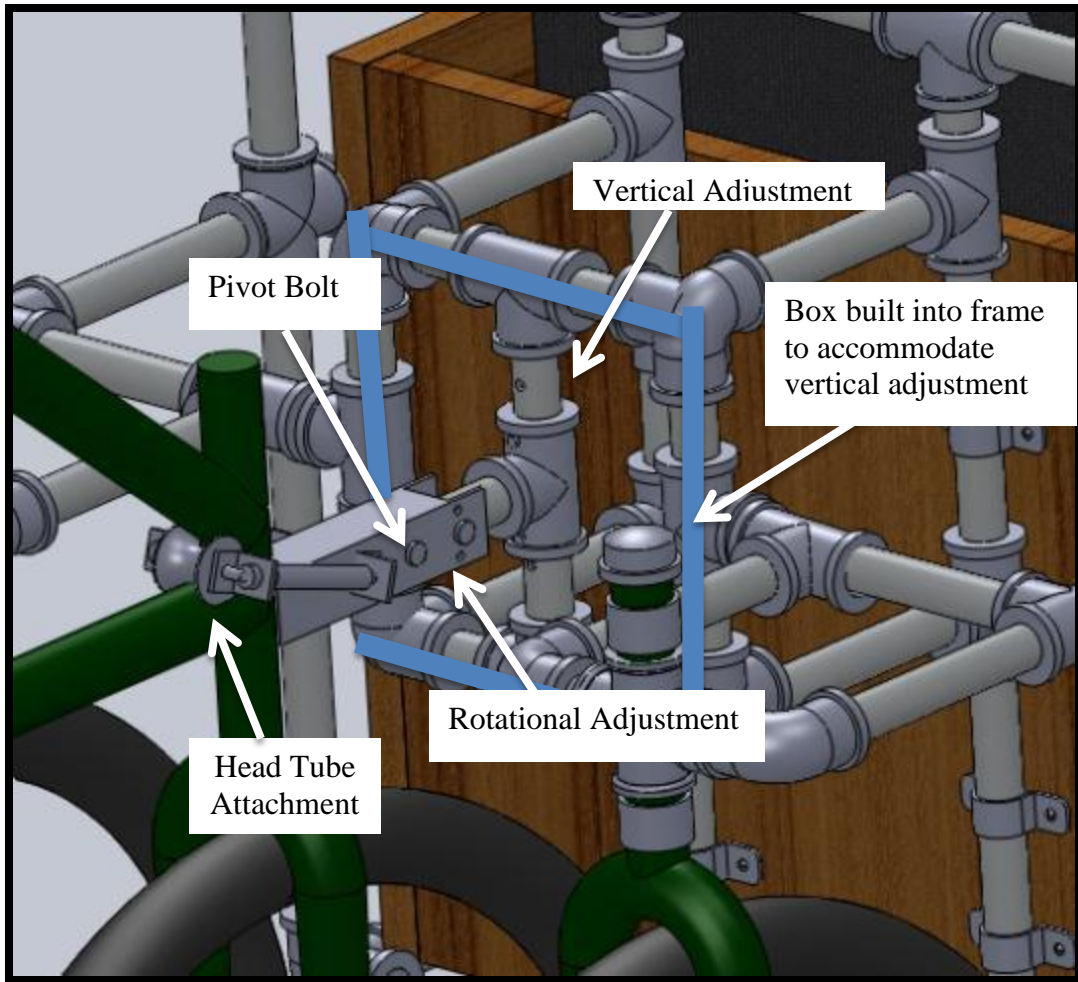


Figure 84: Vertical Adjustment of Attachment Mechanism

A milled out T fitting can slide up and down along this vertical tubing. The tubing has a series of holes that line up with holes in the fitting so that the fitting could be bolted securely at a number of different heights. This milled T fitting can be seen in Figure 85.

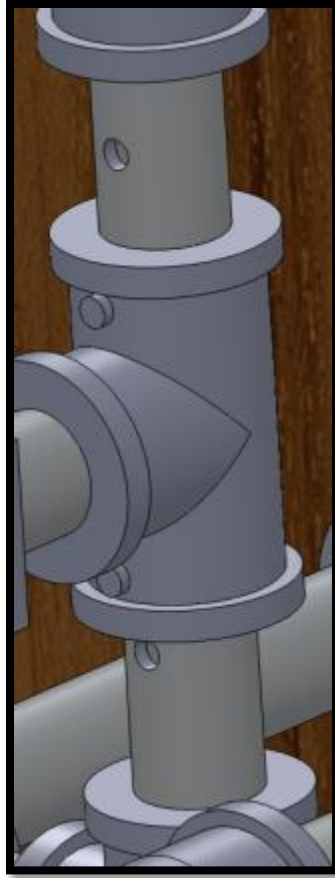


Figure 85: Vertical Adjustment T Fitting

A second feature allows for angular adjustment. The tubing that extended horizontally from the vertical fitting slides inside a piece of 1.5" square aluminum tubing. The two pieces are connected through a stationary bolt running through the middle of both pieces which acts as a rotation point. The square tubing contains a series of bolt holes located on a curve that allows the square tubing to be rotated up or down up to 20 degrees in either direction and then bolted into place. The series of holes allows the square tubing to be connected at a number of different angles. The top and bottom of the square tubing are removed up to 1" from the edge on the side connected to the 1" tubing so that it can rotate without interference. The side view of this angular adjustment can be seen in Figure 86.

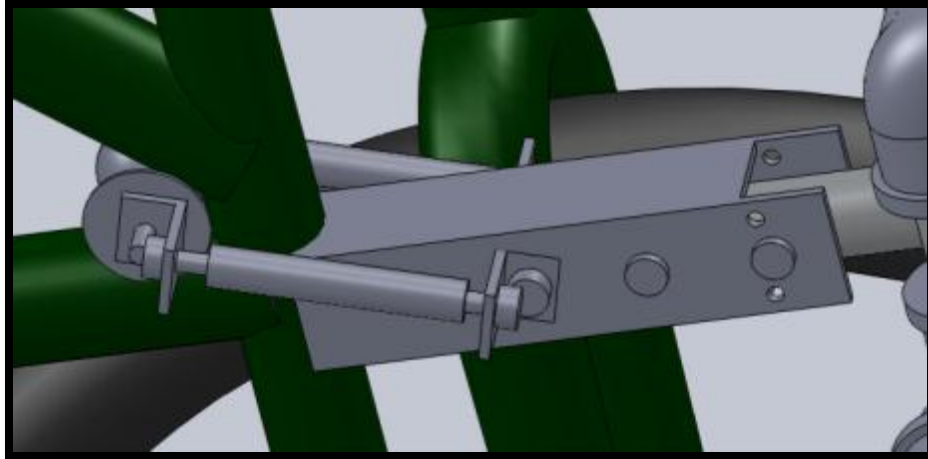


Figure 86: Angular Adjustment of Attachment Mechanism

Once this design was finalized it was necessary to analyze the rotating joint which allows the attachment mechanism to adjust its angle. This connection was analyzed in order to ensure that it will not fail under significant loads. Through an experimental procedure which involved pushing one of the design team members while measuring the force with a force meter, it was determined that the necessary pushing force would be 35 lbf. Although the force was tested to be 35lbf, the principal and Von Misses stresses in the attachment mechanism were calculated using forces of 35lbf and 100 lbf. When analyzed with a load of 100 lbf the Von Misses stress was calculated to be 984 psi. The yield strength of aluminum is 45 kpsi which is far greater than the calculated stress so the attachment mechanism will not fail. This analysis can be found in Appendix B.

## 8.2 Steering

An illustration of the three dimensional steering system can be seen in Figure 87. The extended coupling pins between the horizontal forks (input and output links to four bar mechanism) and coupler link is used to allow varying bicycle wheel hub heights to be used with the steering system.

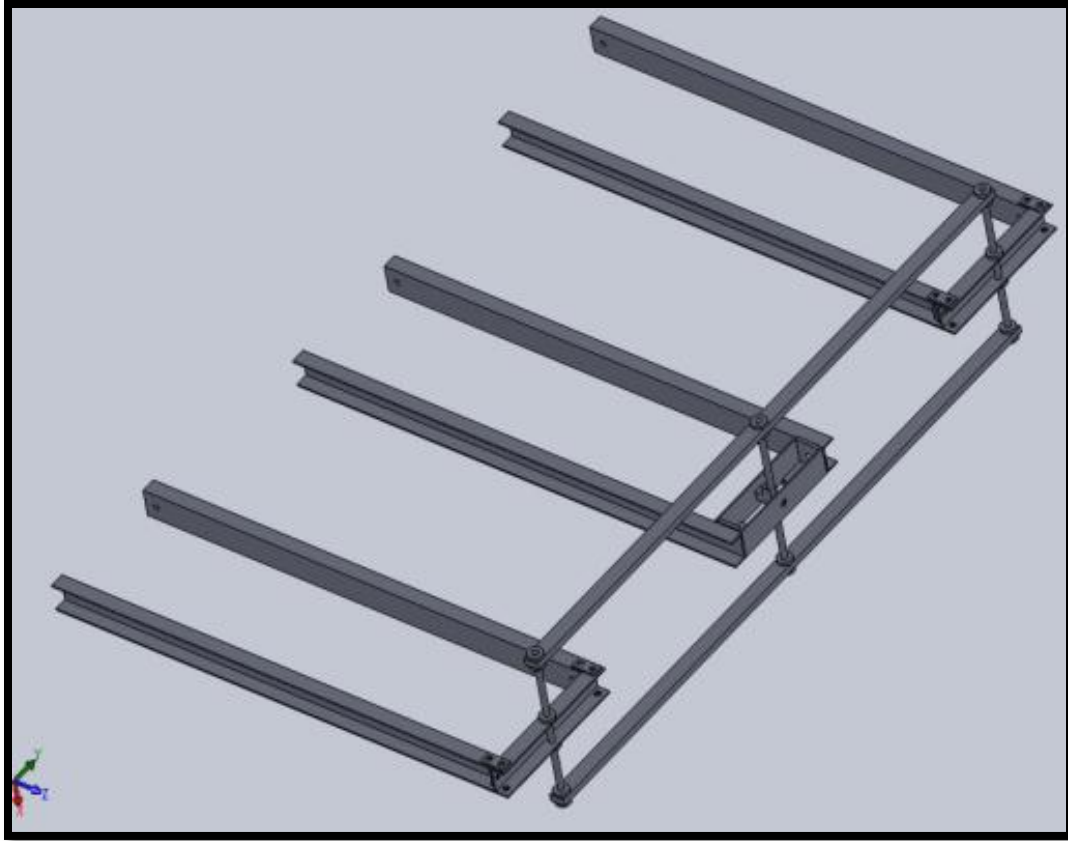


Figure 87: CAD Illustration of Steering System

The free vertical movement of the middle horizontal fork between the two coupler links relieves the load bearing characteristics and improves the steering capabilities of the device. If left rigid (without the vertical degree of freedom), any deflection of the device or existing bicycle wheels will exert a load on the coupler link. The coupler link of this system is designed to transfer an input moment axially from the middle horizontal fork to the left and right horizontal fork, not to bear a vertical bending load. Since the existing bicycle wheel can move independently of the device wheels in the vertical direction, the bending load on the coupler is reduced and the device wheels acting as “training wheels” for the entire device is prevented. The horizontal forks of the device wheels are set at a constant height because these wheels will remain at a constant height.

The middle horizontal fork is also capable of adjusting to different bicycle head tube angles by rotating towards the left and right using a pivot joint on the coupler rod. The close up illustration of the middle horizontal fork and this pivot joint can be seen in Figure 88. The two degrees of freedom of the middle horizontal fork (vertical displacement denoted by red arrows in Figure 88 and angular adjustment denoted by a blue arrow in the figure) allow the steering system to adapt to a wider range of wheel diameters and head tube angles. The device wheels are connected to the chassis with vertically mounted forks. Any existing bicycle has a fork set at an angle (head tube angle), so the angular adjustability is necessary to compensate for these differences in axes of rotation between the device wheels and an existing bicycle wheel. The angular adjustment will allow an input moment to transmit axially along the coupler link via a couple forces along the middle horizontal fork arms.

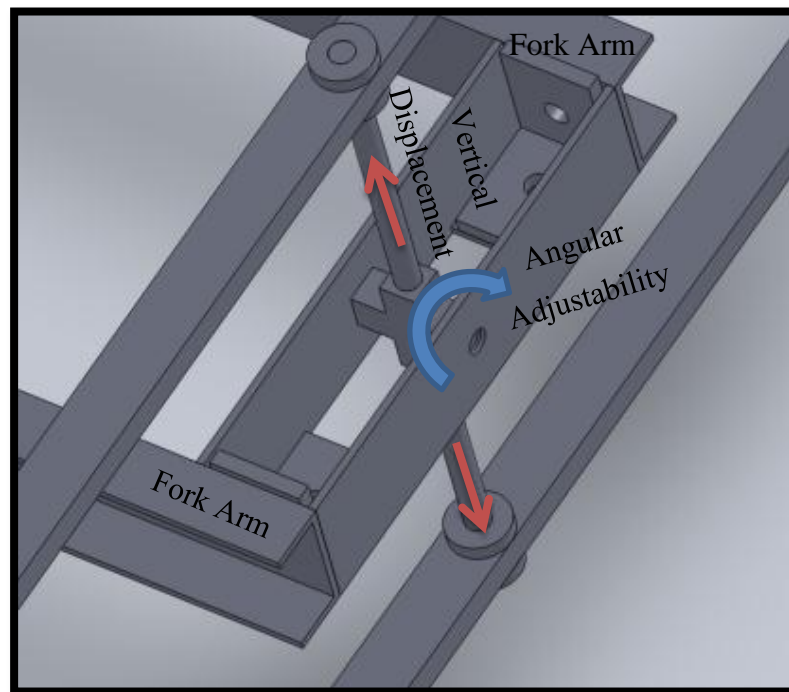


Figure 88: Middle Horizontal Fork Angle Adjustability

### 8.3 Device Frame

This frame design was analyzed and was determined capable of meeting the design specifications. However, the originally chosen steering system and attachment mechanism both proved to be inefficient and the new changes required modifications to be made to the frame. In order to accommodate these new changes, the wheels of the frame had to be pushed back so that they are parallel to the wheel of the attached bicycle. Since the device wheels were pushed back, two load bearing caster wheels were added underneath the front of the frame.



Figure 89: Design with New Wheel Placement

The device steering wheels on the rear of the device are mounted using two cross fittings with the threads milled out down the center. The device wheel forks are taken from donor bicycles and the steerer tube, the vertical column protruding upwards from the front fork, passes



through the milled sections of the cross fittings. A shaft collar is placed on the exposed section of the steerer tube to hold the forks onto the device frame and to improve safety by reducing sharp edges at the end of the steerer tube.

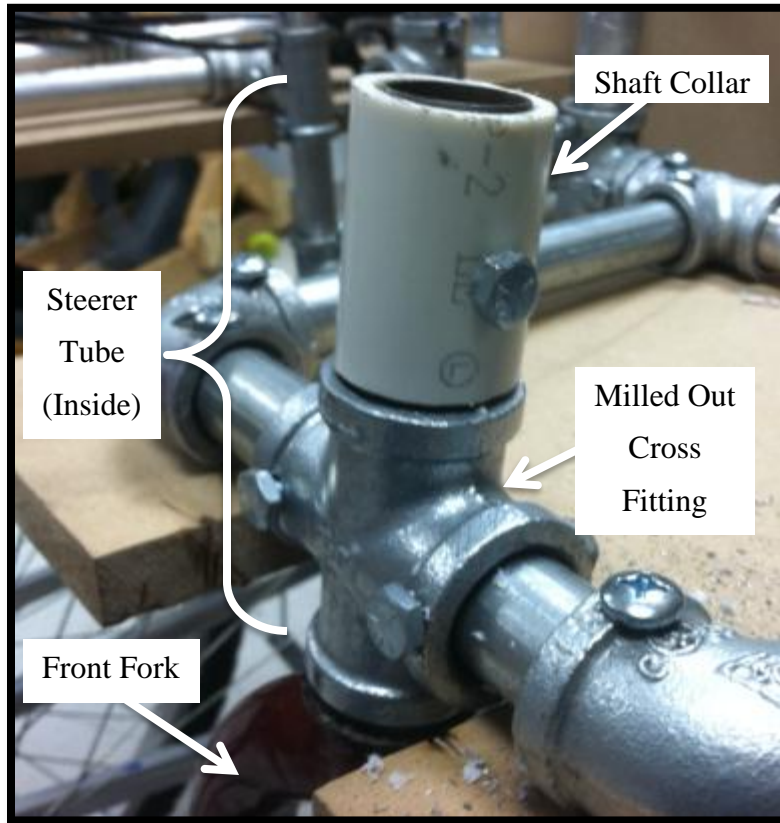


Figure 90: Device Wheel Attachment

To increase safety for the passenger, footrests and a seatbelt were added to hold the passenger in the seat. The mounting locations of the anchors for the seatbelt are bolted directly to the back portion of the passenger seat. The footrests are mounted to two T fittings protruding out of the forward frame cross member.

## 8.4 Safety Details

Additional items were added for passenger safety. A two point, automotive grade seat belt was installed and, to assist with loading and unloading of passenger, a parking brake was

added to the device steering wheels to lock these wheels and keep the device stationary. To prevent the passenger from injuring their legs while riding, footrests were added to keep their feet off the ground.

## CHAPTER 9: MANUFACTURING

The device is assembled from a variety of parts that were bought, reused, or manufactured. Described in detailed below is the origin of all of the parts and how they were assembled to create the bicycle attachment.

### 9.1 Purchased Parts

Many of the parts of this design were purchased. The frame of the device is made out of 1" 6061 aluminum tubing of 1/8" thickness that was ordered from Peterson Steel. The tubing was then cut into the desired lengths and the ends were altered as needed for the frame assembly. The ends were either threaded or turned down depending on whether the tube was going to be screwed into a fitting or bolted to it.



Figure 91: Piece of tubing that will be bolted on the left and threaded on the right

The figure above (Figure 91) shows how the tubing was prepared for the two different types of connections. To make the threaded fitting, a die was used to create threads on the end of the tube. For a bolted fitting, the tube was first turned down to about .95" for a distance of 3/4" on a lathe. A 1/4" hole was also drilled through the turned down tubing at the center of the

machined section. The assembly of the device will be explained in a later section. Twenty-four feet of tubing was ordered for \$95.

The 3/4" galvanized steel fittings used to connect the tubing were also bought online, from Aubuchon Hardware, but altered in order to accommodate the areas where the fitting needed to be bolted to the tubing. These bolted connections will be referred to as "slip fits" in this report. In order to accommodate this particular attachment, the surface of the fitting was faced to produce a smooth surface; the removal of the lip on the end of the fitting allowed for a bolt to sit flush against the material. Bolt holes were also added to accommodate 1/4" bolts. Below a T fitting is shown that has all three ends machined to be slip fits. The team purchased 8 elbows, 23 T's, 8 side outputs, and 4 crosses.



Figure 92: T fitting with three bolt fits

All of the parts of the steering system were also purchased. The metal surrounding the wheels, referred to as horizontal forks, is made out of C channel aluminum with dimensions 1/16" thickness x 3/4" wall height x 1" width. The vertical members are 1/4-20 threaded rods, and the bars connecting all three horizontal forks are 1/8" thickness x 1" width steel flat bar.

The steering system is composed of three horizontal forks (two for the device wheels and one for the bicycle wheel), two coupler links, and three coupler rods. The horizontal forks are constructed of 1/16" thickness x 1" width x 3/4" height aluminum 6061 C-channel. The device

wheel horizontal forks use 15" fork arms and a 4 3/4" fork arm connection piece. The fork arms and fork arm connection part are connected with two L-brackets and a straight connection piece seen in Figure 93. The hardware used for these connections are #8-32 1/2" length cap screws with #8-32 machine nuts. A 1/4" hole is drilled in the center of the fork arm connection piece to pass the coupler rod through.

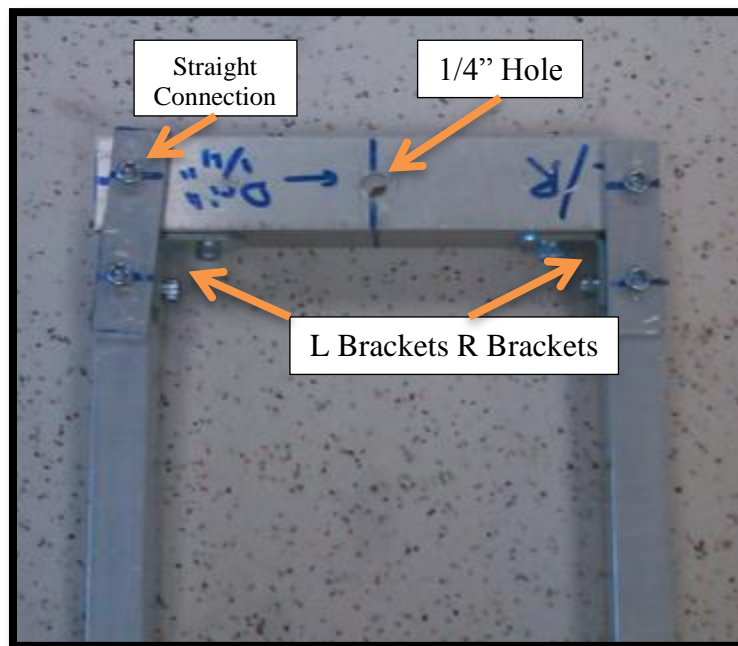


Figure 93: Horizontal Fork Prototype

The coupler link is 1/8" thickness x 1" width x 36" length steel flat bar with three 1/4" holes drilled in it through which the coupler rod passes. Six 1/4"-20 nuts are used to locate the device wheel horizontal forks and four are used on the bicycle wheel horizontal fork only to locate the coupler links vertically.

The entire first order prototype for the steering system can be seen in Figure 94.

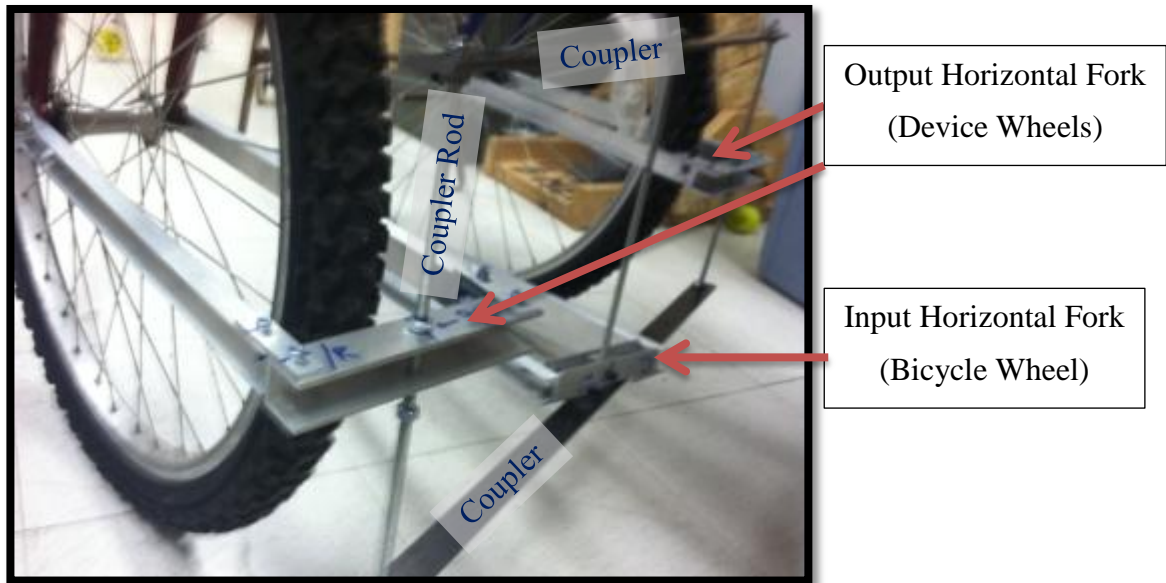


Figure 94: Steering System

Some items in the attachment system were also purchased. The part that fits in between the top tube and down tube of the bicycle frame is a polyethylene pulley purchased from McMaster-Carr. This particular pulley is 5" in diameter and was purchased because of its 1 – ¼" width and semicircular cut out which is ideal for bike frames. This item cost \$35.

The seat was also purchased online for a discount rate of \$20 from a local individual, and the seatbelt was bought from McMaster-Carr for \$24. The wood was purchased from Home Depot; it is ¾" MDF that cost \$30.

The two 10" caster wheels that support the front of the device were purchased from Harbor Freight Tools for \$15 each.

Additionally, all screws, bolts, nuts and other fixture pieces were purchased. These items had a combined cost of about \$20.

## 9.2 Reused Parts

The larger device wheels that are used for steering are reused parts. Bicycles were donated to the project from family, friends, and neighbors for free. The bikes were disassembled and the front wheel and front fork were removed in order to be added to the device.

Other reused parts were the footrests and the 2" square tubing used for the attachment system. The footrests were taken from the Rehab Lab at WPI and the square tubing was found in the machine shop. Steel tubing with a diameter of  $\frac{3}{4}$ " was also acquired from the machine shop; the use of this tubing will be described in assembly.

A small block of Nylon (1"x 2" x3") was donated by another MQP team and was used for the attachment. An arc was cut into the plastic that removed material up to  $\frac{1}{2}$ " into the block to create a channel down the long side of the block so that it would be able to sit flush against most bicycle head tubes (Figure 95).



Figure 95: Head Tube Attachment

### 9.3 Budget

Item	Size	Individual Price	Amount	Overall Price (Rounded)	Location	Notes
<b>Frame</b>						
Aluminum Tubes	1" Tubing with 3/8" thickness	\$80/24ft	24	\$120	Peterson Steel	6061
90° Steel Elbows	3/4" Steel Tubing Connection	\$3.74/ea	8	28	Aubuchon Hardware	Part# 243089
Tee's	3/4" Steel Tubing Connection	\$5.38	23	124	Aubuchon Hardware	Part# 243881
90° Corner Side Output	3/4"	\$4.29	8	34	Aubuchon Hardware	Part# 12507
Wheel Castors	10"	\$13/ea	2	26	Harbor Freight Tools	Part# 38944
Bike Parts		Free	2	0	Donor Bikes	Wheels and Forks
				\$332		
<b>Steering</b>						
Horizontal Forks	1" dia, 2" dia, 1/16" Square Tube	21.64	1	22	Home Depot	Part# 368210
Bar	1" dia 6" dia, 1/4" Steel Flat Bar	7.27	2	15	Home Depot	Part# 380686
Coupler Rod	5/16" dia 2" Threaded Rod	\$1.17/ea	2	3	Home Depot	Part# 1671002
Smaller Bolts	5/16" dia 8 Hex Nut	\$2.46/bag	3	3	Home Depot	Part# 328639
				\$43		
<b>Bicycle/Device Connection</b>						
Pulley	5" dia, 1/4" width	\$30	1	\$30	McMaster Carr	Part# 5284K21
Bracket	1"	\$2	4	\$8	Home Depot	
1/4" Bolt		\$15	100	\$15	Home Depot	Part# 504548
Threaded Rod	1/4"	\$3	2	\$6		
1/4" Nut		\$6/package	4	\$6	Home Depot	Part# 254231
				\$65		
<b>Seat</b>						
Chair	Office Chair	\$20	1	20	Craigslist	
Flange		\$7	8	40	Aubuchon Hardware	Part# 243220
Seatbelt	Car Seatbelt	\$24	1	24	McMaster Carr	Part# 88875K581
Foot Rest	Wheelchair Footrests	Free	1	0	Donor Wheelchair	
Corner Bracket	2.5"	3.68/ea	2	7	Home Depot	Part# 030699153190
Brackets	2.5"	3.57/ea	3	10	Home Depot	Part# 030699150519
Wood Panels	MDF	30	1	30	Home Depot	
				\$131		
<b>Shipping</b>						
Fixtures	Misc			20		
				\$20		

**Total \$591**

### 9.4 Assembly

As mentioned before, the frame is made up of 1" 60601 aluminum tubing and 3/4" galvanized steel fittings. Because the frame is made up of a series of closed structural loops, the parts couldn't have been simply screwed together. To address this concern, slip fits were added in the necessary locations so that the frame could be assembled. The team tried to assign the slip fits to areas that may not carry as much load or that may not be as essential to the overall frame lengths. Below are a series of images that show which joints were screwed and which were slip fits. Places where the tube was screwed into the tubing are colored red and the bolted fittings are yellow. This color scheme is used throughout the rest of the report.

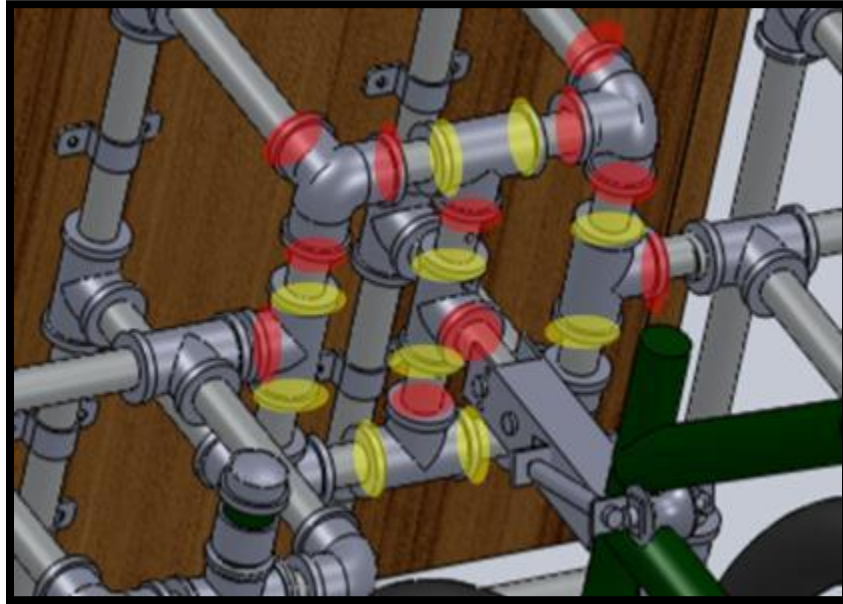


Figure 96: Slip vs. Screw of Attachment

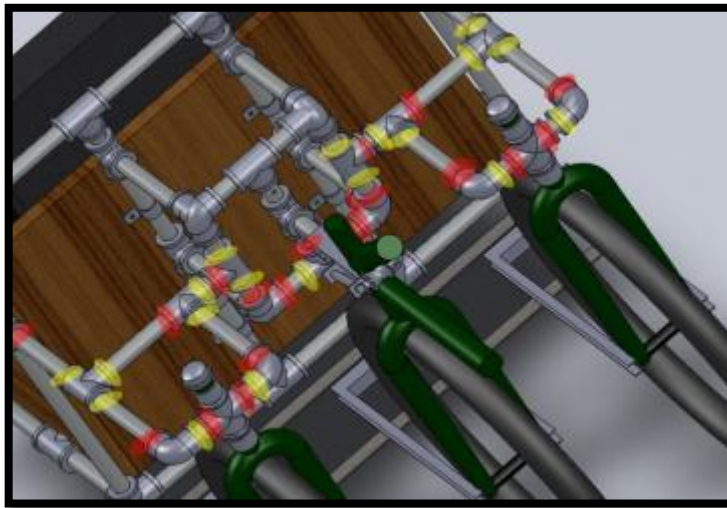


Figure 97: Slip vs. Screw for Bicycle Connection



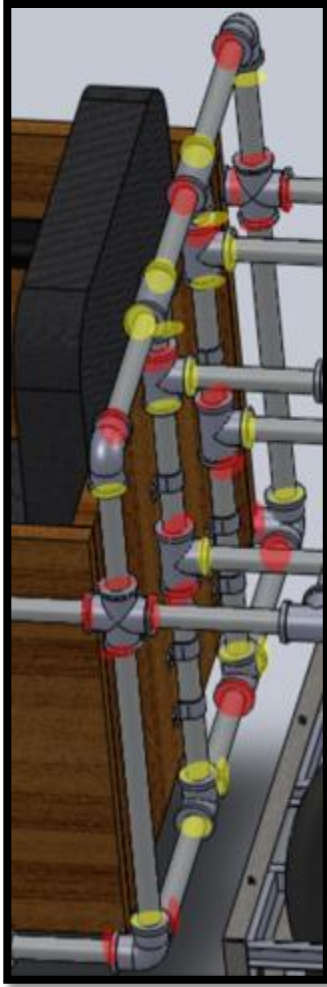


Figure 98: Slip vs. Screw for Back of Device

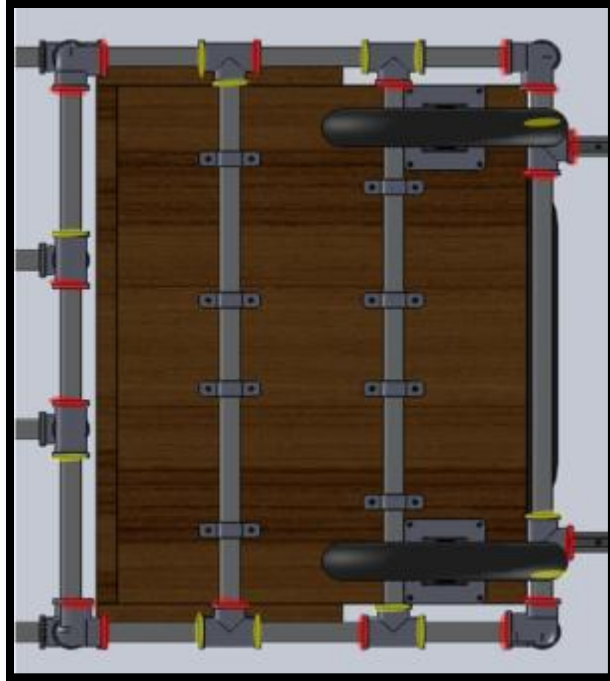


Figure 99: Slip vs. Screw for Bottom of Device

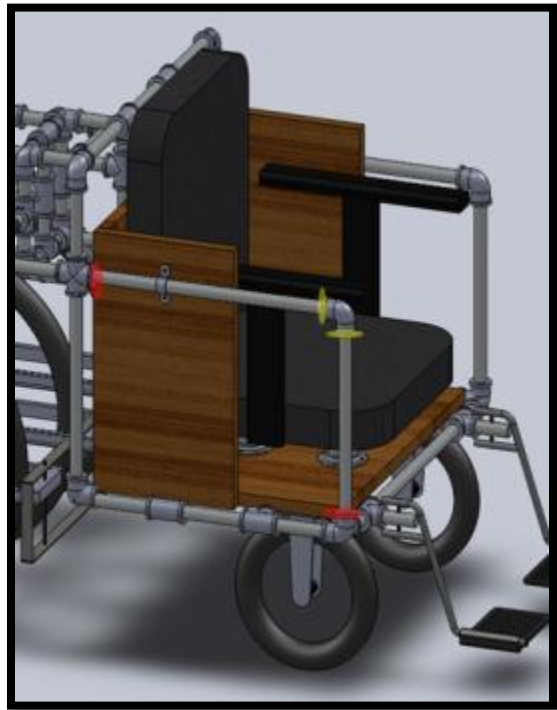
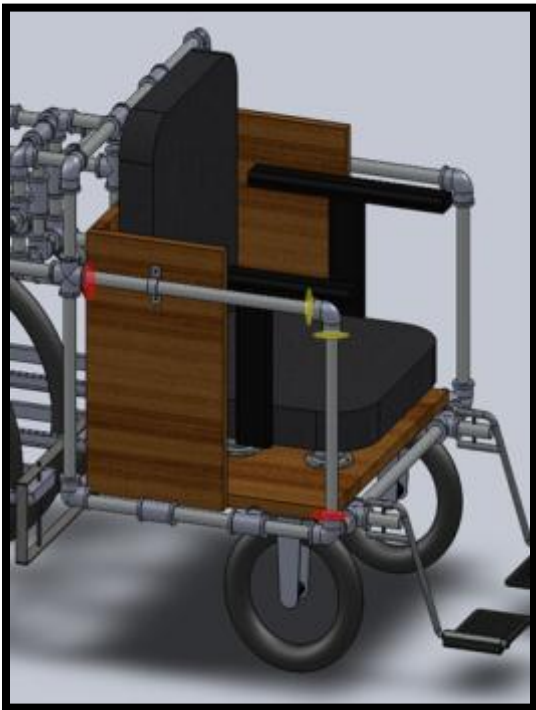


Figure 100: Screw vs. Slip for Arms of Device

For ease of assembly, all of the fittings and pieces of tubing were numbered. Below are tables that show details about each piece of tubing and all of the fittings. The first table lists the lengths of the 61 pieces of tubing and which ends needed to be made into a slip fit, which ones needed to be made into a screw fit, and which ones needed no alteration.

All of the fittings are organized by type, either elbow, side output, T, or cross, each of the pieces are numbered and the ends are either marked as slip fit or screw fit. For the T's and crosses where it was essential which end was slip fit vs. screw fit, a diagram was provided next to the table to ensure the right ends would be machined. Typically the side outputs would also have to be labeled, but for our case, only one end need to be slip fit, so it didn't matter which end was machined. All of this documentation of the fittings can be found in Appendix E.

For the seat area,  $\frac{3}{4}$ " MDF was purchased from Home Depot and cut into four pieces; two larger pieces used for the back and base and smaller triangles used at the corners to ensure stability. The purpose of this wood is to both hold the seat and act as a connection point for the rest of the frame. The wood is placed in a way that it encloses the passenger from the rest of the device, but is open enough so that the person doesn't feel too confined and uncomfortable. The MDF pieces were connected to each other through metal L brackets and corner brackets.



Figure 101: Wood Frame

The casters are an easy attachment; the metal plate that is attached to the castors has 4 bolt holes that can be used to screw the wheel directly into the bottom of the wood. However, an additional piece of MDR was added in between the bottom of the device and caster wheels to add additional height in the front of the device.

The larger wheels were much more difficult to attach. To include each wheel and fork, a section of the tubing was extended backwards 18” (Figure **102**) so that once a bicycle is attached to the device the axes of both the device wheels and bicycle wheel would be collinear. This extension was also necessary to ensure that the wheels and steering system did not hit the back of the seating area. A cross fitting was included in the center of this extended frame member. The cross was tightened securely to the tubing that extends horizontally, but the hole that runs top to bottom was milled out so that the front fork of the device wheel would be able to easily rotate within the fitting. A piece of PVC is placed on the fork above the fitting and bolted to the steering tube so that it could act as a shaft collar and ensure that the device wheel wasn’t able to slide out of the fitting. By attaching the wheel in this manner it will still be able to act as a

support while rotating freely within the cross, allowing it to be turned by the steering system and help turn the device.

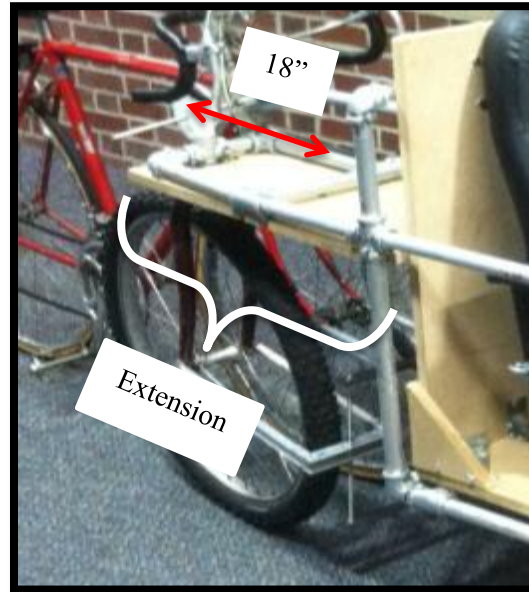


Figure 102: Extension for Back Wheel Attachment



Figure 103: Large Device Wheel

As seen in Figure 103, a few adjustments needed to be made during manufacturing. Due to the Manufacturing Lab unexpectedly closing on the scheduled day of manufacturing, some of

the smaller pieces of aluminum tubing did not get machined to accommodate slip fits. To address this issue, the team replaced these pieces with  $\frac{3}{4}$ " steel tubing which was able to slide into the fittings without any changes. However, because the  $\frac{3}{4}$ " tubing has a slightly smaller diameter than the turned down aluminum tubing, the connection between the tubing and fittings was not as tight; the connection was secure, but the tubing was able to wiggle slightly within the fittings. Because of this unplanned for movement, the team felt that the back of the device was not as secure as it needed to be and effects could be seen on the device wheels. To address this, the team added in additional pieces of MDF underneath the tubing, as seen above. By connecting these new pieces of MDF to both the tubing in the back and the MDF surrounding the seating, the team was able to make sure the device remained rigid. The back of the device with the added MDF can be seen in the below figure.

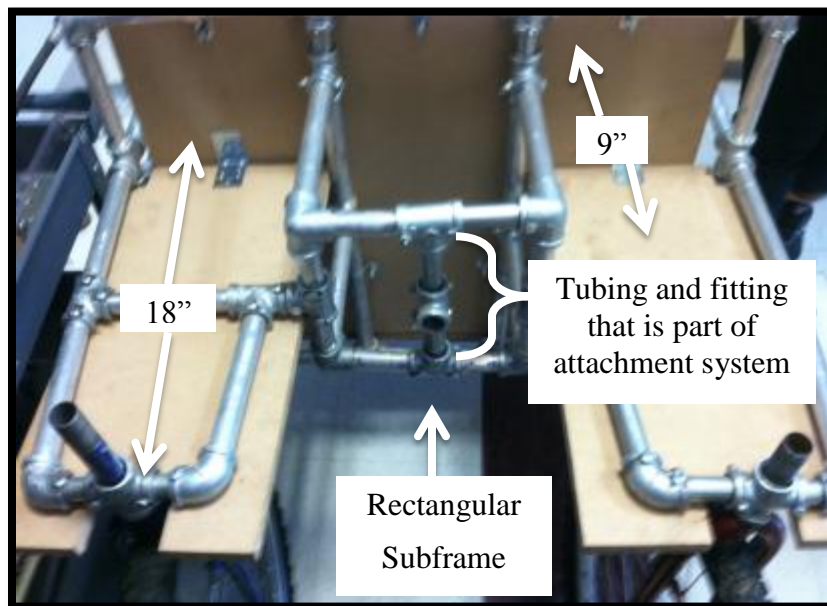


Figure 104: Back View of the Device Showing Wheel Attachments

Also seen in Figure **104**, a rectangular sub frame was constructed 9" off the back of the device, half way in between the back of the seating area and device wheel connection. This feature was added so that a piece of vertical tubing could be added in the middle of the frame.

This tubing, shown above with a T fitting on it, is part of the attachment system. This fitting has two bolt holes and the tubing has a series of holes placed 1” apart along the length of the tubing. This allows the fitting to be secured at different heights along the tube in order to adapt to bicycles of different sizes.



Figure 105: Vertical Adjustment of Attachment System

A piece of tubing that was screwed into this T fitting was then extended outward and bolted in a piece of 2” square tubing which is then attached to a pulley shaped member, as seen in Figure **106**.

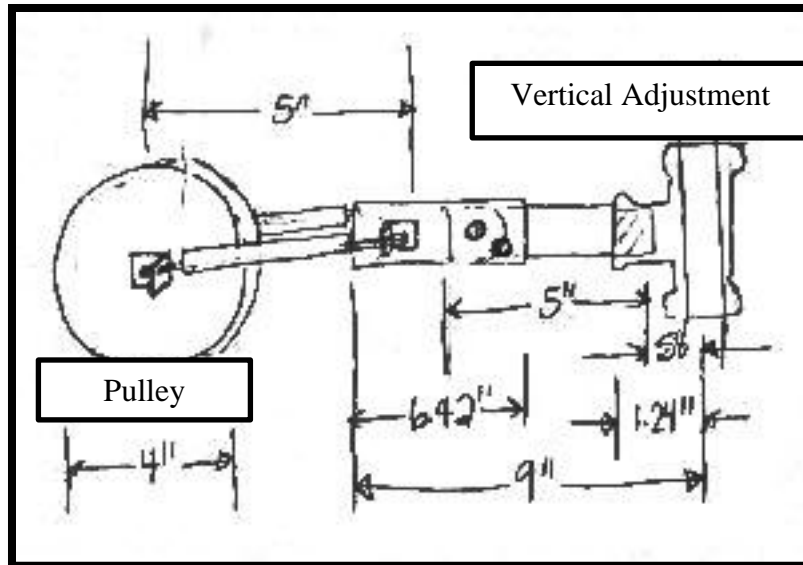


Figure 106: Side View of the Attachment System

Shown in both Figure **105** and Figure **106** there are two bolts running through both the square tubing and the circular tubing inside of it. The bolt further away from the device is stationary and acts as a pivot for the square tubing. The bolt closer to the device is adjustable; on the square tubing there is a series of three bolt holes located along an arc at a distance of 1.25” away from the stationary bolt. The adjustable bolt can be tightened in any of the three holes; the middle hole allows the attachment to remain horizontal and the other two bolt holes allow the square tubing to be fixed at angles of either 20° above vertical or 20 ° below vertical. The attachment system has this rotational adjustment so that it will be easy to attach to bikes of different head tube angles.

The square tubing is connected to a Nylon block through small L brackets. A curved channel was created down the length of the plastic block to allow the attachment to fit securely against a bicycle head tube. A piece of foam was glued to the plastic to protect the bicycle.



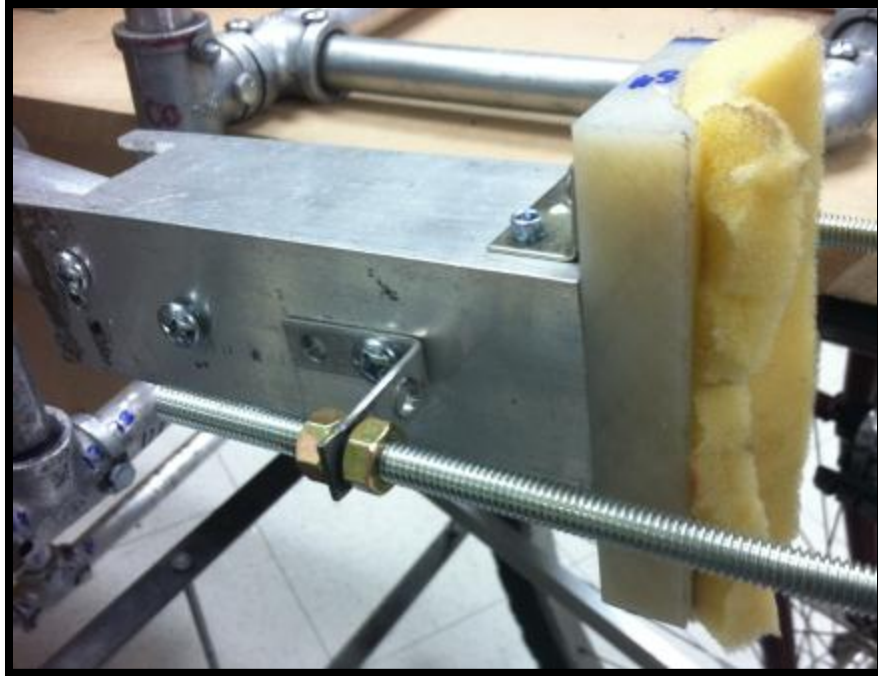


Figure 107: Square Tubing and Head Tube Connection

Also connected to the square tubing are threaded rods that run parallel to the tubing on either side. These rods are attached through L brackets and secured into place with nuts. These rods are also attached to a pulley shaped piece that is slid into the space between the top tube and the down tube of the bicycle. The nuts on the pulley side of the attachment are tightened until the attachment system is compressed securely against the bicycle head tube. The rods were left long so that the pulley could be adjusted at different locations depending on the style of the bike frame; some bicycle frame styles have top tubes and down tubes that are very close together so the pulley would only be able to fit further down the opening. The attachment system, connected to a bicycle, is shown in Figure **108**. For this bike, a reflective attachment had to be moved to the side in order to make room for the attachment.



Figure 108: Attachment System

The seat was added to the bike through tubing and flanges. The legs of the chair were removed so that the seat could be placed at an appropriate height. It was essential that the seat was high enough so that it would be easy for a person with limited mobility to enter and exit the chair, while being low enough for the cyclist to see over the passenger. The tubing was cut and threaded, and then flanges were screwed on either end, one to be screwed into the bottom of the chair, and one to be screwed into the MDF. This assembly acted as the new leg of the chair and the attachment between the chair and the device. The seat and legs were positioned underneath the device and spots were marked on the device where the bolt holes needed to be added in the MDF. The legs were then removed and the holes were drilled. The flanges were then screwed into the bottom of the chair and then repositioned on the device. Bolts were slid through the flanges and into the predrilled holes in the device and tightened underneath.

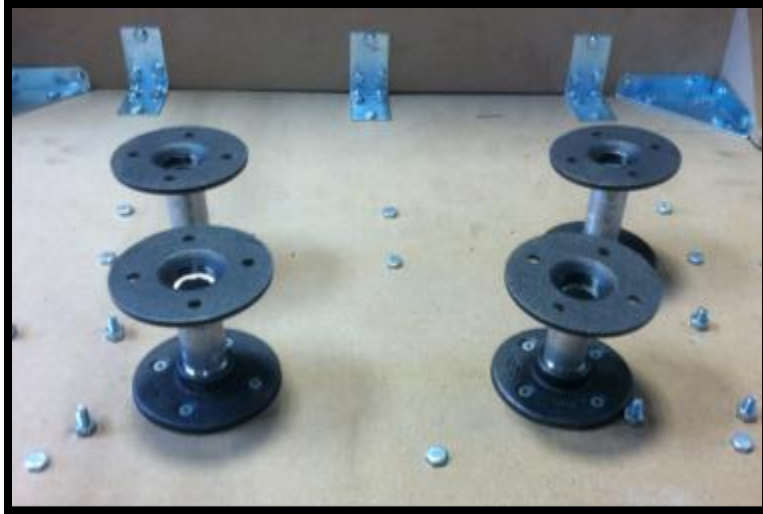


Figure 109: Seat Attachment

To increase the safety for the passenger, an automotive grade seatbelt was added to our device, seen in Figure **110**. An eye-hook was screwed into the side of the chair through the plastic underneath the armrest, seen in Figure **111**.



Figure 110: Device Seatbelt



Figure 111: Seatbelt Attachment

In addition to the seatbelt, footrests were added for passenger safety and comfort. Two T fittings had been incorporated into the tubing underneath the device that extended outward on the front of the device. The footrest was cut so that the only tubing left on the footrest was the vertical piece and one horizontal piece extending a few inches back. The horizontal piece was placed within the empty side of the T fitting and bolted into place.



Figure 112: Footrest

To keep the device stationary during loading and unloading as well as when the device is parked on an inclined surface, a parking brake was added to one of the device wheels to prevent the wheel from rotating. The control for this brake was a shifter removed from one of the donor bicycles seen in Figure 113



Figure 113: Parking Brake Control

The brake used is a standard V-brake removed from a donor bicycle seen in Figure **114**. The shifter was connected via brake cable to the V-brake. The shifter remains in one position via locking gears until the cyclist rotates it. This characteristic is ideal because it allows the cyclist to engage the parking brake and the brake will remain engaged until the cyclist disengages it.



Figure 114: Parking V-Brake on Device Wheel

## **CHAPTER 10: TESTING**

The procedures used for testing of this device were researched and altered using pre-existing bicycle, wheelchair and PediCab testing methods. These procedures will be used to ensure that the design specifications are met, and determine if the device is structurally sound. The analysis based on the wheelchair test will be based on the ISO International Standards for Wheelchairs, ISO/FDIS 7176-8. The wheelchair standards will be used due to the similarities between the device and a wheelchair.

The testing procedures are divided into three areas: device frame/braking, steering system and dynamic functionality. Any testing requiring a passenger weight placed inside the device, sandbags are used to simulate the passenger weight.

### **10.1 Device Frame Testing**

The following testing procedures were performed under static conditions both with and without a maximum weight passenger (250 lbs) in the device seat.

#### **10.1.1 Device Weight Test**

To improve the portability and performance of the device, aluminum was selected as the material for a large portion of the device components. The task specification of a net device weight of 100 lbs was produced to create a measurable target value for the specification. The Device Weight Test is performed by placing the device frame with no attached bicycle on a flat surface with the parking brake on. Four calibrated scales were placed under the two trailing caster wheels and the two device steering wheels. The sum of these four measurements is added to yield the total device weight. This procedure is performed once. This test passes if the device weight is equal to or less than the task specification of the maximum device weight of 100 lbs.

## **10.2 Steering Testing**

The steering has two main areas requiring testing: force transmission and maximum steering angle. The following testing procedures were performed under static conditions both with and without a maximum weight passenger (250 lbs) in the device seat.

### **10.2.1 Force Transmission Test**

For force transmission, the testing procedure used will include the three members of the design team. The varying skill levels and strength will provide varying results to simulate a wide range of potential users.

The device and attached bicycle were placed on a smooth, flat tiled surface (low friction) with one testing subject seated on the bicycle seat. A manual force gauge is connected to the input horizontal fork coupler rod. The subject then rotates the bicycle handlebars in small rotational intervals describing at what angles the external force created by the force gauge causes the steering to be easy, neutral, difficult, and very difficult, where neutral is the force required to steering a normal bicycle. The same procedure is repeated with a maximum weight passenger (250 lbs) in the passenger seat. Three iterations of the test are performed with cyclists of low, medium and high strength to obtain data based upon varying strength levels.

The second part of this test is identical to the first with the removal of the manual force gauge from the steering system. Using the defined steering resistance recorded from the first part of testing, the cyclist rotates the steering system on a smooth, flat carpeted surface and asked to describe the resistance on the scale easy, neutral, difficult, and very difficult corresponding to their descriptions from part one of the testing. This test passes if all three test subjects define the steering system as easy, neutral, or difficult to steer because these ratings are closest to an existing bicycle. If the steering is described as very difficult, a redesign of the steering system



will be required to improve this rating. One possible option of redesign is replacing the device steering tires with lower static friction coefficients (e.g. smoother road tires)

### **10.2.2 Steering Angle Test**

The maximum steering angle for the parallelogram four-bar linkage system as defined by the task specifications is 45°. To measure the maximum steering angle, a protractor is mounted at the coupler point on the left horizontal fork with the 90° marking perpendicular to the fork arm cross member. The handlebars are rotated to the right until the assembly will not physically move further and the angle between the coupler link and horizontal fork arm cross member is the maximum steering angle. The same procedure is repeated for a full left turn. As this test is dependent on the mechanical characteristics of the steering system, a single iteration of the test will suffice. The Steering Angle test passes if the steering angle measured is equal to or greater than the 45° steering angle defined in the task specifications and fails if less than 45°.

### **10.3 Parking Brake Test**

The parking brake of the device utilizes one bicycle V-brake mounted to one of the device steering wheels and a shifter removed from a donor bicycle. The shifter is connected to the bicycle V-brake to create a variable tension parking brake. The shifter was used because it locks in position after movement of the shifting lever. This characteristic is desirable so the parking brake can be engaged without an external lever locking mechanism.

To test the parking brake, the device is attached to a bicycle and then parked on a hill. The parking brake is engaged and the entire assembly is rocked forward and back to check for slipping or undesired motions. If slipping of the brake pads on the device wheel rim occurs, the parking brake cable may be tightened to ensure full brake pad pressure on the device wheels. This test is performed three times to ensure components do not loosen or fail and continue to

function properly. This test passes if all components remain secured and function, it fails if the parking brake is unable to keep the device stationary.

## **10.4 Dynamic Testing**

The dynamic portion of testing was not performed due to the first order prototype not functioning properly. The remainder of this section will detail dynamic tests capable of measuring the performance of the device.

These tests are performed first with no passenger then with a maximum weight passenger (250 lbs). Velocities of the device and attached bicycle are measured using a specialized cycling computer connected to the front wheel of the bicycle. All dynamic tests are performed outdoors in a flat, smooth, dry asphalt surface with no obstacles within the testing area.

### **10.4.1 Braking Test**

The device and attached bicycle are brought to a constant velocity of 10 mph on a smooth, flat asphalt surface; the cyclist then depresses the brakes aggressively without causing the bicycle wheels to lock. The distance between 10 mph to a full stop will be measured. The same procedure is used while the cyclist is only using the bicycle to allow comparison between the stopping capabilities of the existing bicycle to when it is attached to the device.

### **10.4.2 Steering Test**

The dynamic steering test used will generate data pertaining to the turning radius of the device as well as the steering performance of the device. The device is first brought to a flat, smooth open asphalt area with no obstacles within the testing area. The cyclist turns the bicycle handlebars to the maximum steering angle to the left. The cyclist begins to propel the device forward while keeping the handlebars at the maximum steering angle. A chalk line is drawn where the rear bicycle tire contacts the asphalt until a full circle is completed. Using a tape

measure, the diameter of the drawn circle is measured and divided by two to determine the turning radius. The Steering Test is performed three times and an average of the three values is used as the device turning radius. Three more iterations are performed turning the device to the right to ensure symmetry in the steering system. A similar procedure is used to determine the turning radius of the bicycle only (without the device) to allow a comparison to be formed. Creating a ratio between the turning radiuses of the device compared to the turning radius of the existing bicycle will define the amount which the bicycle steering is degraded with the device attached. The most desirable outcome to this test is a ratio of 1 representing steering identical to that of the bicycle. Higher ratios are more likely because of the reduced maximum steering angle. This test can be used to re-design the device to lower this ratio and improve steering performance.

## CHAPTER 11: RESULTS

Once the device was constructed it was necessary to test based on the design specifications. Although not all of the tests were able to be performed, all possible tests were done to evaluate the device.

There are five general design specifications for the device. The first is that the device must be able to attach to an existing bicycle. This design specification was met through the use of the attachment mechanism (Figure 115) and horizontal bicycle forks (Figure 116) used on the steering system. Related to this specification is the next design specification stating that the attachment device must be capable of accommodating bicycles of different heights and frame styles. The attachment mechanism can be adjusted both vertically and rotationally for the head tube connection. The combination of these two adjustments will allow this mechanism to be used on most bicycles. The vertical adjustment of the horizontal fork attachment also meets the second design specification. This attachment allows bicycles of any wheel diameter to be used with the device.



Figure 115: Head Tube Attachment Mechanism



Figure 116: Horizontal Fork Attachment

The third design specification is related to the device's seating conditions. It states that the device's seating must be accessible by an adult casual ambulant or an adult of limited mobility. The frame has been design with a seat placed 18 inches above the ground. Due to this placement, the passenger is able to walk up to the device and seat as easily as sitting in a regular chair. The device also contains two armrests, which the passenger can use for support.

The fourth device specification states that adults capable of riding a bicycle should be capable to operate the device. The device has been designed with a one to one steering system. In theory this will allow a person capable of riding a bicycle to ride the device with no learning curve. Unfortunately it wasn't possible to perform dynamic testing on this device due to dysfunctional caster wheels. For this reason this design specification cannot be qualified as met.

The steering and braking design specifications could not be evaluated. This was also caused by the unanticipated behaviors of the front caster wheels. The only manner of remedying this issue is a redesign of the steering system and remanufacturing the frame with tighter tolerances. For these reasons the steering and braking design specifications have not been

evaluated. One specification that has been met is the addition of a parking brake to a device steering wheel.

The safety specifications for this device can be evaluated. The safety specifications require the device to have a set off footrests, a seat belt and armrests. The device will require all moving parts to be away from the passenger's reach. It will also contain armrests and all sharp edges to be removed. The safety specifications are met for this device. The device includes a pair of footrests in the front of the frame. The device also contains a seatbelt and two pairs of armrests. The first armrests are those attached to the chair, the second set are those created by the frame of the device. The moving parts for this device are behind the passenger; therefore they will not pose a risk. Due to the device being built with tubing sharp edges will not pose a problem.

The design specifications state that maintenance of the device should only require the driver to have common knowledge of bicycles. In the same manner assembly will also require the use of common tools such as a wrench set, screwdriver, and set of pliers. These design specifications have also been met. After the manufacturing of the parts, assembly of the device required a hex screwdriver and wrench. Once the device has been assembled the attachment mechanism can be mounted in 10 minutes, this meets the assembly specification. The time will vary depending on the length of the rods which tighten the attachment mechanism to the head tube.

## **CHAPTER 12: RECOMMENDATIONS**

To improve on the final design, the following areas were identified during the design and manufacturing of the prototype.

### **12.1 Device Frame**

The use of galvanized steel fittings drastically increased weight of the device and resulted in the first order prototype exceeding the task specification for a maximum device weight of 100 lbs. Although some strength will be sacrificed, the weight of the device can be greatly reduced by using lighter fittings such as stainless steel or aluminum. The weight could also be reduced by removing the fittings and welding the joints of the frame. Given the time constraint of this project and the lack of experience with aluminum welding, welding the frame was not an option for our design team.

The inconsistency in the dimensions of the threaded pipe fittings, although small, caused an even greater inconsistency in the length that the tubing was able to thread into the fittings. The resulting inaccuracy in tubing lengths made it difficult to obtain the assembly dimensions as defined in the CAD. To address this issue, either Slip Fits can be used for the entire frame because they are more predictable, or, the fittings can be removed altogether and the frame can be welded.

It was found that the device's footrests were not located in comfortable position for taller occupants. For ease of manufacturing, two wheelchair footrests were used even though their dimensions were not ideal for this application. This custom fitment of wheelchair footrests created the uncomfortable position for the passenger. The use of specially designed mounting hardware or using a different mount technique to connect the footrests to the device will improve the positioning. This will require use of anthropometric data to define the desired footrest location.

In our prototype, trailing caster wheels influence the direction of the device more than the steering wheels. To increase contact area of the steering wheels, the use of oversized tires on the current 22" diameter device steering wheels or increasing wheel diameter/width to 26" with increased width tires (e.g. 26 x 2.1 tires). To reduce ground contact area of the caster wheels, different caster wheels, similar to those on a wheelchair, with a smooth tread and narrow width should be used.

## **12.2 Attachment**

The head tube attachment was not capable of reaching the head tube of the driving bicycle because the bicycle fork was pitched back in an unanticipated manner. The attachment mechanism was extended using a longer piece of tubing between the head tube attachment and the milled T fitting for the vertical adjustment. In the future, the attachment should be adjusted to also include a horizontal adjustment. This way, the attachment would be able to reach the bicycle no matter where the head tube is located in relation to the bike wheel.

The material selection for the L-brackets was found to not provide the strength required for the attachment system. The compressive force used for the attachment system caused the L-brackets to plastically deform. Further stress analysis and free body analysis of the attachment system could provide more information for material selection for the components.

## **12.3 Steering**

Currently, the steering system is allowed to rotate until the bicycle wheel contacts one of the device steering wheels which is approximately at 60°. To limit the steering system to the 45° steering angle defined in the design specifications, the use of a physical stop on the device frame which could prevent the rotation of the device steering wheels beyond this -45°/+45° steering angle. The steering angle of 45° was chosen to increase safety of the passenger and driver while



riding. This angle should provide enough maneuverability for typical bicycle paths and rail trails, while maintaining safety for the occupants.

## **CHAPTER 13: CONCLUSION**

The goal of this project was to design and build a prototype for a front mounting bike attachment that is adaptable to different bike styles and sizes and is accessible for adults, including those with limited mobility. The design was broken into three areas of focus: frame, steering and attachment.

Through much iteration, the team designed a device meeting the required accessibility and adaptability. By researching anthropometric data, the team defined the seat location was at a comfortable height for someone with limited mobility to get into and out of. Unlike benchmarks on the market requiring the passenger to climb up into a compartment, this device allows the passenger to simply turn around and sit down, just as they would for a chair. The device successfully attaches to bicycles with a variety of frame styles and sizes. The attachment mechanism was designed with two areas of adjustability: vertical and rotational. This ensures that with a range in the height of the wheel or in the angle of the head tube, the attachment will be adequate. With further engineering, the attachment could attach to all bikes, but the current design will attach to most common models.

The main issue that caused the prototype to be inoperable was the device steering. The steering system itself seems to turn the device wheels smoothly and maintains the required 1:1 steering ratio to maintain driver intuition. However, the steering does not work overall because of unpredictable caster wheels. Instead of rotating freely as trailing casters are intended, the purchased casters are instead contributing to the steering of the device. To remedy this problem, the trailing casters could serve as steering wheels or the device wheels could be relocated to remove the caster wheels completely.

Many of the design specifications were met but there were some flaws in the device. With the recommendations provided, a successful second generation prototype could be built improving upon the first order prototype.

## WORKS CITED

Active transportation making the link from transportation to physical activity and obesity. (2009,

Summer). *Active Living Research*

Bella Bike. 24 Sep 2010. <<http://bellabike.dk/>>.

Bicycle Compliance Test Manual. (1976). *Bureau of engineering sciences*. Washington DC:

Consumer Product Safety Commission.

Consumer Product Safety Commission, (2010). Federal Code of Regulation, Chapter 2,

Washington DC: Consumer Product Safety Commission.

CDC Childhood overweight and obesity. <<http://www.cdc.gov/obesity/childhood/index.html> >.

"Christiania Bikes." 24 Sep 2010. <[http://www.christianiabikes.com/english/uk\\_main.htm](http://www.christianiabikes.com/english/uk_main.htm)>.

"Disc Brakes or Rim Brakes" All Content. 8 Oct 2010. <<http://www.all-content.info/mountain-bike-disc-brakes-or-rim-brakes-20100816-151>>.

Dozier, Emily. (2009). Health benefits of "active transportation". *Plan On I*

"Feetz." 24 Sep 2010. <<http://www.feetz.nl/>>.

Lightfoot Cycles. 8 Oct 2010. <<http://lightfootcycles.com/>>.

"Main Street Pedicab." 19 Sep 2010. <<http://www.pedicab.com/pedicabs.html>>.

"Main Street Pedicab Manual." 19 Sep 2010. <<http://www.pedicab.com/documents/msp-pedicab-manual-2008.pdf>>.

"Nihola." Web. 24 Sep 2010. <<http://www.nihola.info/>>.

"Our Christiana Trike" Velocouture 15 August 2010.

<<http://velocouture.wordpress.com/2010/08/05/our-christiania-trike>>.

"Pedillac Pedicab." 19 Sep 2010. <<http://www.pedillac.com/Pictures.html>>.

"Premier Pedicab." 19 Sep 2010.

<<http://www.premierpedicabs.com/specifications%20%28dist%29.htm>>.

"Quick Release Front Hub" Shimano. 8 Oct 2010.

<[http://bike.shimano.com/publish/content/global\\_cycle/en/us/index/products/mountain/Alivio/product.-code-HB-MC12-P.-type-hb\\_mountain.html](http://bike.shimano.com/publish/content/global_cycle/en/us/index/products/mountain/Alivio/product.-code-HB-MC12-P.-type-hb_mountain.html)>

"The Science of Differentials and Rear-End Gears" Stock Car Science.

<<http://www.stockcarscience.com/blog/index.php/2008/04/01/differentials>>.

"Side-Kick" American Speedster. 8 Oct 2010. <<http://www.americanspeedster.com/side-kick.htm>>.

"Taga." 24 Sep 2010. <<http://www.tagabikes.com/>>.

"Trio Bike.". 24 Sep 2010. <<http://www.triobike.co.uk/>>.

Ulrich, Karl. (2006). The environmental paradox of bicycling. *Department of Operations and Information Management, The Wharton School*

"Zigo." 24 Sep 2010. <<http://www.myzigo.com/>>.

# APPENDIX A: BICYCLE REGULATIONS

## Consumer Product Safety Commission Code of Federal Regulations for Bicycles

### § 1512.5

may be, exposed to hands or legs; sheared metal edges that are not rolled shall be finished so as to remove any feathering of edges, or any burrs of spurs caused during the shearing process.

(c) *Integrity.* There shall be no visible fracture of the frame or of any steering, wheel, pedal, crank, or brake system component resulting from testing in accordance with: The handbrake loading and performance test, §1512.18(d); the foot brake force and performance test, §1512.18(e); and the road test, §1512.18(p) (or the sidewalk bicycle proof test, §1512.18(q)).

(d) *Attachment hardware.* All screws, bolts, or nuts used to attach or secure components shall not fracture, loosen, or otherwise fail their intended function during the tests required in this part. All threaded hardware shall be of sufficient quality to allow adjustments and maintenance. Recommended quality thread form is specified in Handbook H28, "Screw Thread Standards for Federal Service,"<sup>1</sup> issued by the National Bureau of Standards, Department of Commerce; recommended mechanical properties are specified in ISO Recommendation R898, "Mechanical Properties of Fasteners," and in ISO Recommendations 68, 262, and 263, "General Purpose Screw Threads."<sup>2</sup>

(e)-(f) [Reserved]

(g) *Excluded area.* There shall be no protrusions located within the area bounded by (1) a line 89 mm (3½ in) to the rear of and parallel to the handlebar stem; (2) a line tangent to the front tip of the seat and intersecting the seat mast at the top rear stay; (3) the top surface of the top tube; and (4) a line connecting the front of the seat (when adjusted to its highest position) to the junction where the handlebar is attached to the handlebar stem. The top tube on a female bicycle model shall be the seat mast and the down tube or tubes that are nearest the rider in the normal riding position. Control cables no greater than 6.4 mm (¼ in) in diameter and cable clamps made from

<sup>1</sup>Copies may be obtained from: Superintendent of Documents, U.S. Government Printing Office, Washington, D.C. 20402.

<sup>2</sup>Copies may be obtained from: American National Standards Institute, 1430 Broadway, New York, New York 10018.

### 16 CFR Ch. II (1-1-10 Edition)

material not thicker than 4.8 mm (¾ in) may be attached to the top tube.

(h) [Reserved]

(i) *Control cable ends.* Ends of all control cables shall be provided with protective caps or otherwise treated to prevent unraveling. Protective caps shall be tested in accordance with the protective cap and end-mounted devices test, §1512.18(c), and shall withstand a pull of 8.9 N (2.0 lbf).

(j) *Control cable abrasion.* Control cables shall not abrade over fixed parts and shall enter and exit cable sheaths in a direction in line with the sheath entrance and exit so as to prevent abrading.

### § 1512.5 Requirements for braking system.

(a) *Braking system.* Bicycles shall be equipped with front- and rear-wheel brakes or rear-wheel brakes only.

(b) *Handbrakes.* Handbrakes shall be tested at least ten times by applying a force sufficient to cause the handlebar to contact the handlebar, or a maximum of 445 N (100 lbf), in accordance with the loading test, §1512.18(d)(2), and shall be rocked back and forth with the weight of a 68.1 kg (150 lb) rider on the seat with the same handbrake force applied in accordance with the rocking test, §1512.18(d)(2)(iii); there shall be no visible fractures, failures, movement of clamps, or misalignment of brake components.

(1) *Stopping distance.* A bicycle equipped with only handbrakes shall be tested for stopping distance by a rider of at least 68.1 kg (150 lb) weight in accordance with the performance test, §1512.18(d)(2)(v) and (vi), and shall have a stopping distance of no greater than 4.57 m (15 ft) from the actual test speed as determined by the equivalent ground speed specified in §1512.18(d)(2)(vi).

(2) *Hand lever access.* Hand lever mechanisms shall be located on the handlebars in a position that is readily accessible to the rider when in a normal riding position.

(3) *Grip dimension.* The grip dimension (maximum outside dimension between the brake hand lever and the handlebars in the plane containing the centerlines of the handgrip and the hand brake lever) shall not exceed 89

times onto a paved surface with weights attached in accordance with the sidewalk bicycle proof test, § 1512.18(g). There shall be no fracture of wheels, frame, seat, handlebars, or fork during or resulting from this test.

(c) *Ground clearance.* With the pedal horizontal and the pedal crank in its lowest position and any training wheels removed, it shall be possible to tilt the bicycle at least 25° from the vertical without the pedal or any other part (other than tires) contacting the ground plane.

(d) *Toe clearance.* Bicycles not equipped with positive foot-retaining devices (such as toe clips) shall have at least 89 mm (3½ in) clearance between the pedal and the front tire or fender (when turned to any position). The clearance shall be measured forward and parallel to the longitudinal axis of the bicycle from the center of either pedal to the arc swept by the tire or fender, whichever results in the least clearance. (See figure 6 of this part 1512.)

#### § 1512.18 Tests and test procedures.

(a) *Sharp edge test.* [Reserved]

(b) [Reserved]

(c) *Protective cap and end-mounted devices test.* (Ref. § 1512.4(i), § 1512.6(d).) Any device suitable for exerting a removal force of at least 67 N (15 lbf) for protective caps and 8.9 N (2.0 lbf) for end caps at any point and in any direction may be used. All protective caps and end-mounted handlebar devices shall be tested to determine that they cannot be removed by application of the specified forces.

(d) *Handbrake loading and performance test.* (Ref. § 1512.5(b)).

(1) *Apparatus.* A spring scale or other suitable device for measuring the specified forces on the handbrake levers and a dry, clean, level, paved surface of adequate length.

(2) *Procedure.* The loading test, § 1512.18(d)(2)(i), and the rocking test, § 1512.18(d)(2)(iii), shall be performed before the performance test, § 1512.18(d)(2)(v), is performed and no adjustments shall be made between these tests.

(i) *Loading test procedure.* The hand levers shall be actuated with a force applied at a point no more than 25 mm

(1.0 in) from the open end of the lever. If the hand lever contacts the handlebar (bottoms) before a force of 445 N (100 lbf) is reached, the loading may be stopped at that point, otherwise the loading shall be increased to at least 445 N (100 lbf).<sup>4</sup> Application of the loading force shall be repeated for a total of 10 times and all brake components shall be inspected.

(ii) *Loading test criteria.* There shall be no visible fractures, failures, misalignments, and clearances not in compliance with applicable parts of § 1512.5.

(iii) *Rocking test procedure.* A weight of at least 68.1 kg (150 lb) shall be placed on the seat; the force required for the hand levers to contact the handlebars or 445 N (100 lbf), as determined in § 1512.18(d)(2), shall be applied to the hand levers;<sup>4</sup> and the bicycle shall be rocked forward and backward over a dry, clean, level, paved surface at least six times and for a distance of at least 76 mm (3 in) in each direction.

(iv) *Rocking test criteria.* There shall be no loosening of the brake pads, pad holders, or cable and hand-lever securing devices or any other functional brake component.

(v) *Performance test procedure.* The following test conditions, unless otherwise specified in this part 1512, shall be followed:

(A) The bicycle shall be ridden over a dry, clean, smooth paved test course free from protruding aggregate. The test course shall provide a coefficient of friction of less than 1.0 and shall have a slope of less than 1 percent.

(B) The wind velocity shall be less than 11 km/h (7 mph).

(C) Only the brake system under test shall be actuated.

(D) The bicycle shall attain the specified ground speed while the rider is in the normal riding position.

(E) The rider shall remain in the normal riding position throughout the test.

(F) The bicycle must be moving in a straight line at the start of brake application.

<sup>4</sup>For hand lever extensions, the loading shall be continued until a force of 445 N (100 lbf) is reached or the hand lever extension is in the same plane as the upper surface of the handlebars or the extension lever contacts the handlebars.



(G) Corrections for velocity at the initiation of braking may be made. The corrected braking distance shall be computed as follows:

$$S_c = (V_s / V_m)^2 S_m$$

where:

- $S_c$  = Corrected braking distance.
- $V_s$  = Specified test velocity.
- $V_m$  = Measured test velocity.
- $S_m$  = Measured braking distance.

The test run is invalid if at the commencement of the test, the measured test speed of the bicycle is not less than nor greater than the test speed required by this part 1512 by 1.5 km/h (0.9 mph).

(H) Four test runs are required. The stopping distance shall be determined by averaging the results of the four test runs.

(I) The stopping distances specified are based on a rider weight of at least 68.1 kg (150 lb) and a maximum rider and weight combination of 91 kg (200 lb). Greater stopping distances are allowable for heavier riders and test equipment weights at the rate of 0.30 m per 4.5 kg (1.0 ft per 10 lb).

(J) A test run is invalid if front-wheel lockup occurs.

(vi) *Performance test criteria.* The stopping force applied to the hand lever at a point no closer than 25 mm (1.0 in) from the open end shall not exceed 178 N (40 lbf). Bicycles with an equivalent ground speed in excess of 24 km/h (15 mph) (in its highest gear ratio at a pedal crank rate of 60 revolutions per minute)<sup>3</sup> shall stop from an actual test speed of 24 km/h (15 mph) or greater within a distance of 4.57 m (15 ft); when the equivalent ground speed is less than 24 km/h (15 mph) under the same conditions, the bicycle shall stop from an actual test speed of 16 km/h (10 mph) or greater within a distance of 4.57 m (15 ft).

(e) *Footbrake force and performance test.* (Ref. § 1512.5(c) (1) and (2)):

(1) *Apparatus.* Suitable devices for exerting and measuring the required forces and a dry, clean, level, paved surface of adequate length.

(2) *Force test.* The braking force shall be measured as the wheel is rotated in a direction of forward motion, and the

braking force is measured in a direction tangential to the tire during a steady pull after the wheel completes one-half revolution but before the wheel completes one revolution. The brake shall be capable of producing a linearly proportional brake force for a gradually applied pedal force from 89 N to 310 N (20 to 70 lbf) and shall not be less than 178 N (40 lbf) for an applied pedal force of 310 N (70 lbf). All data points must fall within plus or minus 20 percent of the brake force, based on the measured brake load using the least square method of obtaining the best straight line curve.

(3) *Performance test.* The procedure of § 1512.18(d)(2)(v) shall be followed to test the footbrake performance. The stopping distance shall be less than 4.57 m (15 ft) from an actual test speed of 16 km/h (10 mph). In addition, if the equivalent ground speed of the bicycle is in excess of 24 km/h (15 mph) (in its highest gear ratio at a pedal crank rate of 60 revolutions per minute),<sup>3</sup> the stopping distance shall be 4.57 m (15 ft) from an actual test speed of 24 km/h (15 mph) or greater.

*NOTE:* No allowance shall be made for rider weight. See § 1512.5(d) for additional requirements for bicycles with both handbrakes and footbrakes.

(f) *Sidewalk bicycle footbrake force test.* For sidewalk bicycles, the footbrake force test is the same as for bicycles except; the brake force transmitted to the rear wheel shall continually increase as the pedal force is increased from 44.5 N to 225 N (10 to 50 lbf). The ratio of applied pedal force to braking force shall not be greater than two-to-one.

(g) *Handlebar stem test.* (Ref. § 1512.6(b)):

(1) *Procedure.* The handlebar stem shall be tested for strength by applying a force of 2000 N (450 lbf), in a forward direction, for bicycles, or 1000 N (225 lbf) for sidewalk bicycles, at a point in line with the handlebar attachment point and at an angle of 45° from the stem centerline (See fig. 2).

(2) *Criteria.* No visible fractures shall result from this test.

(h) *Handlebar test.* (Ref. § 1512.6(e)):

(1) *Stem-to-fork clamp test—(i) Procedure.* The handlebar and handlebar stem shall be assembled to the bicycle

<sup>3</sup>See footnote 3 to § 1512.5.

in accordance with the manufacturer's instructions. The handlebar-fork assembly shall be subjected to a torque applied about the axis of the stem, and shall then be disassembled and examined for signs of structural damage including cracking, splitting, stripping of threads, bearing damage, and bulging of the stem and fork structures. The handlebar and handlebar stem components shall be inspected for visible signs of galling, gouging, and scoring not due to normal assembly and disassembly operations.

(ii) *Criteria.* There shall be no visible movement between the stem and fork when a torque of  $47+3, -0$  N-m ( $35+2, -0$  ft=lb) for bicycles and  $20+3, -0$  N-m ( $15+2, -0$  ft=lb) for sidewalk bicycles is applied to the handlebar about the stem-to-fork axis. There shall be no visible signs of damage to the stem-to-fork assembly or any component part thereof.

(2) *Handlebar strength and clamp test—*  
(i) *Procedure.* The stem shall be in place on the bicycle or in an equivalent test fixture and secured according to manufacturer's instructions. A load shall be applied equally to each handlebar end in a direction to cause the greatest torque about the handlebar-to-stem clamp; deflection shall be measured along the line of applied force.

(ii) *Criteria.* The handlebars shall support a force of no less than 445 N (100 lbf) or absorb no less than 22.6 J (200 in-lb) of energy through a maximum deflection of no more than 76 mm (3.0 in.); the handlebar clamp shall prevent rotational movement of the handlebars relative to the clamp, and there shall be no visible fractures.

(i) *Pedal slip test.* [Reserved]

(j) *Rim test.* (Ref. §§1512.10 and 1512.11(c)):

(1) *Procedure.* Only one wheel need be tested if the front and rear wheel are of identical construction. The wheel to be tested shall be removed from the bicycle and be supported circumferentially around the tire sidewall. A load of 2000 N (450 lbf) shall be applied to the axle and normal to the plane of the wheel for at least 30 seconds. If the wheel hub is offset, the load shall be applied in the direction of the offset.

(2) *Criteria.* The wheel and tire assembly shall be inspected for compliance

with the requirements of §1512.11(a) and shall be remounted on the bicycle according to the manufacturer's instructions and shall turn freely without roughness and shall comply with the requirement of §1512.11(b).

(3) *Front hub retention test.* (Ref. §1512.12(c)).

(i) *Procedures.* Front hub locking devices shall be released. When threaded nuts and axles are used, the nuts shall be open at least 360° from a finger tight condition. A separation force of at least 111 N (25 lb) shall be applied to the hub on a line along the slots in the fork ends.

(ii) *Criteria.* The front hub shall not separate from the fork; fenders, mudguards, struts, and brakes shall not be allowed to restrain the separation.

(k) *Fork and frame test.* (Ref. §§1512.13 and 1512.14):

(1) *Fork test—(i) Procedure.* With the fork stem supported in a 76 mm (3.0 in) vee block and secured by the method illustrated in figure 1 of this part 1512, a load shall be applied at the axle attachment in a direction perpendicular to the centerline of the stem and against the direction of the rake. Load and deflection readings shall be recorded and plotted at the point of loading. The load shall be increased until a deflection of 64 mm (2½ in) is reached.

(ii) *Criteria.* Energy of at least 39.5 J (350 in-lb) shall be absorbed with a deflection in the direction of the force of no more than 64 mm (2½ in.).

(2) *Fork and frame assembly test—(i) Procedure.* The fork, or one identical to that tested in accordance with the fork test, §1512.18(k)(1), shall be replaced on the bicycle in accordance with the manufacturer's instructions; and a load of 890 N (200 lbf), or an energy of at least 39.5 J (350 in-lb), whichever results in the greater force, shall be applied to the fork at the axle attachment point against the direction of the rake in line with the rear wheel axle. The test load shall be counteracted by a force applied at the location of the rear axle during this test.

(ii) *Criteria.* There shall be no visible evidence of fracture and no deformation of frame that significantly limits the steering angle over which the front wheel can be turned.

## APPENDIX B: FRAME ANALYSIS

**This analysis is to determine the Von Mises Stress in the Frame. If the Von Mises Stress is larger than the Yield Strength of the hosen material the frame will fail.**

Known Values

Youngs Modulus of Aluminum

$$\text{Mpsi} := 10^6 \text{ psi} \quad \text{kpsi} := 10^3 \text{ psi}$$

$$E_{al} := 9.86 \cdot 10^6 \text{ psi}$$

Yield Strength Aluminum

$$S_{yal} := 45 \text{ kpsi}$$

Tube Diameters

Aluminum tube Schedule 40 1 inch nomila diameter

$$\text{OD} := 1.315 \text{ in} \quad \text{ID} := 1.049 \text{ in}$$

$$R_w := \frac{\text{OD}}{2}$$

I.s is the moment of inertia

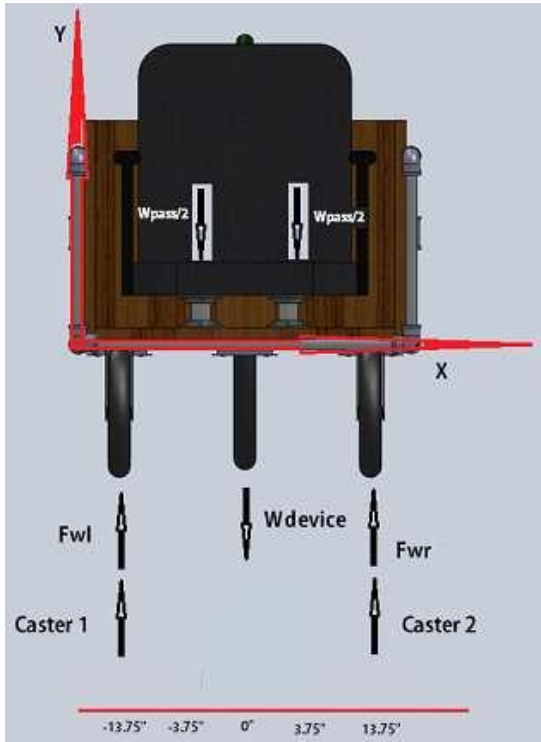
$$I := \frac{\pi}{64} \cdot (\text{OD}^4 - \text{ID}^4)$$

Forces Acting on the Frame

$$W_{\text{Passweight}} := 250 \text{ lbf}$$

$$W_{\text{device}} := 100 \text{ lbf}$$

Free Body Diagram of the Front View of the Device



Dimensions

$$c := 0 \text{ in} \quad a := -13.75 \text{ in} \quad b := -3.75 \text{ in} \quad d := 3.75 \text{ in} \quad e := 13.75 \text{ in}$$

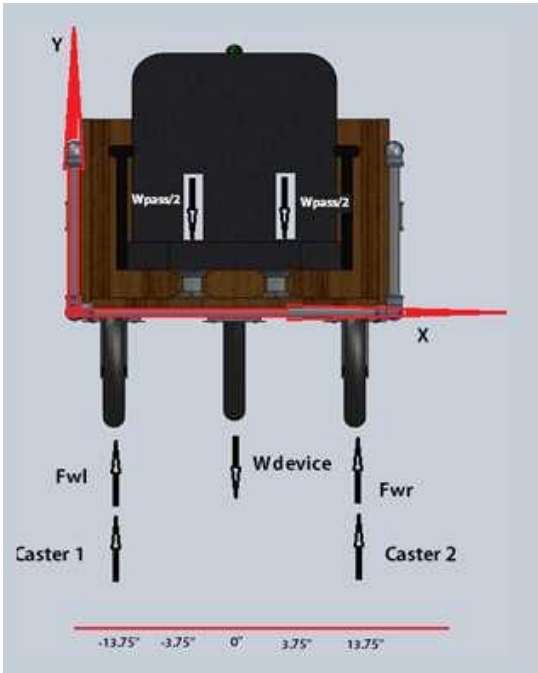
Static  
Analysis

$$\sum F(y) = F_{wr} + F_{wl} - W_{device} - W_{Passweight} + Caster1 + Caster2 = 0$$

$$F_{wl} = -F_{wr} + W_{device} - Caster1 - Caster2 + \frac{W_{Passweight}}{2} + \frac{W_{Passweight}}{2}$$

$$\sum M(a) = \frac{-W_{Passweight}}{2} \cdot (b - a) - (c - a) - \frac{W_{Passweight}}{2} \cdot (d - a) - (W_{device}(c - a) + F_{wl}) \cdot (e - a) + Caster2 \cdot (e - a) = 0$$

Free Body Diagram of the Side View of the Device



Dimensions

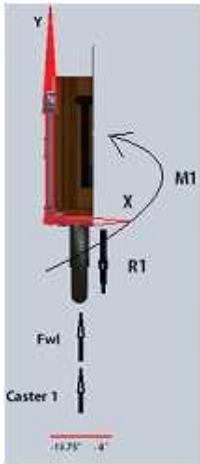
$$f := -22\text{in} \quad g := 0\text{in} \quad h := 10\text{in}$$

$$\sum F(y) = F_{wr} + F_{wl} - W_{\text{device}} + \text{Caster1} + \text{Caster2} - W_{\text{Passweight}} = 0$$

$$\sum M(f) = -W_{\text{device}} \cdot (g - f) - W_{\text{Passweight}} \cdot (g - f) + \text{Caster1}(h - f) + \text{Caster2}(h - f)$$

$$\text{Caster1} = -\text{Caster2} + \frac{W_{\text{device}} \cdot (g - f) + W_{\text{Passweight}} \cdot (g - f)}{h - f}$$

Free Body Diagram of Section A

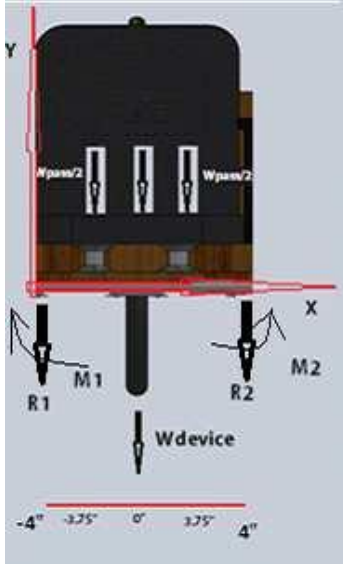


$$j := -4\text{in}$$

$$\sum F(y) = \text{Caster1} + F_{wl} - R_1 = 0$$

$$\sum M(a) = M_1 - R_1(j) = 0$$

Free Body Diagram of Section B



$$i := 4\text{in}$$

$$\sum F(y) = \frac{-W_{\text{Passweight}}}{2} - \frac{W_{\text{Passweight}}}{2} - W_{\text{device}} - R_1 - R_2$$

$$\sum M(f) = \frac{-W_{\text{Passweight}}}{2}(b-j) - \frac{W_{\text{Passweight}}}{2}(d-j) - W_{\text{device}}(c-j) \dots$$

$$+ M_1 - M_2 - R_2 \cdot (i-j)$$

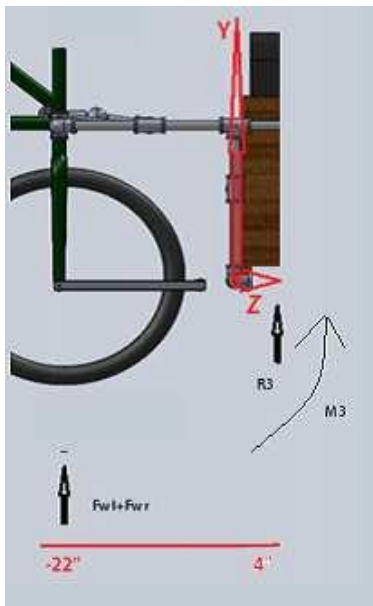
Free Body Diagram of Section C



$$\sum F(y) = -R_2 + F_{wr} + Caster2 = 0$$

$$\sum M(e) = R_2 \cdot (e - i) - M_2 = 0$$

Free Body Diagram of Side View Section .

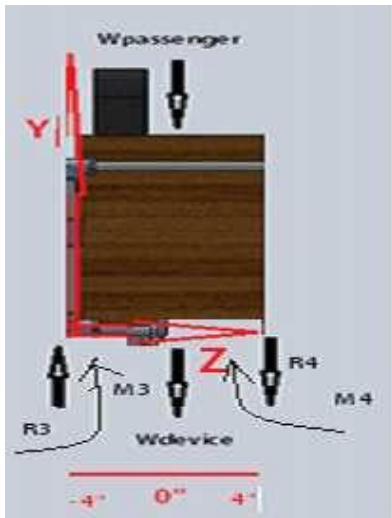


$$\sum F(y) = F_{wr} + F_{wl} + R_3 = 0$$

$$\sum M(f) = R_3 \cdot (g - j) + M_3 = 0$$

$$\sum M(j) = -F_{wl} \cdot (j - f) - F_{wr} \cdot (j - f) - \cdot (j - f) + \cdot (j - f) + M_3 = 0$$

Free Body Diagram of Side View Section B

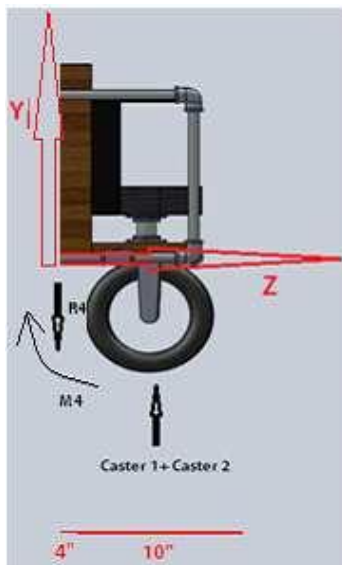


$$k := 4 \text{ in}$$

$$\sum F(y) = R_3 - W_{\text{Passweight}} - W_{\text{device}} - R_4 = 0$$

$$\sum M(j) = M_3 + W_{\text{device}}(g - j) + W_{\text{Passweight}}(g - j) - R_4(k - j) + M_4 = 0$$

Free Body Diagram of Side View Section C



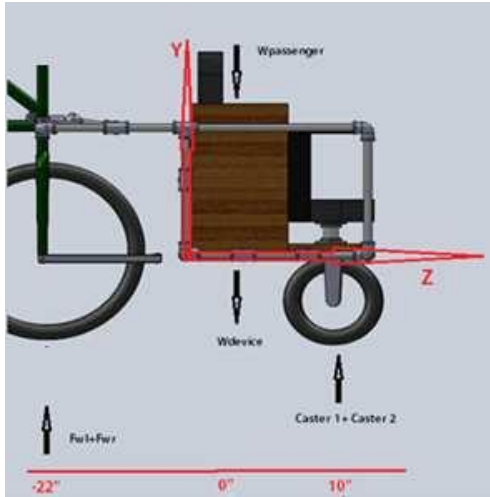
$$\sum F(y) = -R_4 + \text{Caster1} + \text{Caster2} = 0$$

$$\sum M(h) = R_4 \cdot k - M_4 = 0$$

$$\sum M(k) = \text{Caster1} \cdot (e - k) + \text{Caster2} \cdot (e - k) - M_4 = 0$$



If the frame is dcut in half and analysed through a side view we can get the following



$$\sum F(y) = F_{wr} - \frac{W_{device}}{2} - \frac{W_{Passenger}}{2} + Caster2$$

$$\sum M(f) = \frac{-W_{device} \cdot (g - f)}{2} - \frac{W_{Passweight} \cdot (g - f)}{2} + Caster2(h - f)$$

$$Caster2 := \frac{W_{device} \cdot (g - f)}{2(h - f)} + \frac{W_{Passweight} \cdot (g - f)}{2(h - f)}$$

The calculated equations can be combined to obtain teh forces acting on the frameCombining Equations

$$\sum M(f) = -W_{device} \cdot (g - f) - W_{Passweight} \cdot (g - f) + Caster1(h - f) + Caster2(h - f)$$

$$Caster1 := \left[ -Caster2 + \frac{W_{device} \cdot (g - f) + W_{Passweight} \cdot (g - f)}{h - f} \right]$$

From

$$Caster2 = R_4 - Caster1$$

$$Caster1 = -Caster2 + \frac{W_{device} \cdot (g - f) + W_{Passweight} \cdot (g - f)}{h - f}$$

$$R_4 := \frac{W_{device} \cdot (g - f) + W_{Passweight} \cdot (g - f)}{h - f}$$

**From**

$$\sum M(k) = \text{Caster1} \cdot (e - k) + \text{Caster2} \cdot (e - k) - M_4 = 0$$

$$M_4 := \text{Caster1} \cdot (e - k) + \text{Caster2} \cdot (e - k)$$

**From**

$$\sum F(y) = R_3 - W_{\text{Passweight}} - W_{\text{device}} - R_4 = 0$$

$$\sum M(j) = M_3 + W_{\text{device}}(g - j) + W_{\text{Passweight}}(g - j) - R_4(k - j) + M_4 = 0$$

$$R_3 := W_{\text{Passweight}} + W_{\text{device}} + R_4$$

$$M_3 := -W_{\text{device}} \cdot (g - j) - W_{\text{Passweight}} \cdot (g - j) + R_4 \cdot (k - j) + M_4$$

$$R_3 = 2.627 \times 10^3 \text{ N} \quad M_3 = 72.926 \text{ m lbf} \quad R_4 = 1.07 \times 10^3 \text{ N} \quad M_4 = 59.591 \text{ m lbf}$$

**From**

$$\sum F(y) = F_{\text{wr}} + F_{\text{wl}} + R_3 = 0$$

$$\sum M(j) = -F_{\text{wl}} \cdot (j - f) - F_{\text{wr}} \cdot (j - f) + M_3 = 0$$

$$F_{\text{wr}} = -F_{\text{wl}} + R_3$$

**From**

$$\sum M(a) = \frac{-W_{\text{Passweight}}}{2} \cdot (b - a) - \frac{W_{\text{Passweight}}}{2} \cdot (d - a) - W_{\text{device}}(c - a) \dots = 0$$
$$+ F_{\text{wl}} \cdot (e - a) + \text{Caster2} \cdot (e - a)$$

$$F_{\text{wl}} := \frac{W_{\text{Passweight}}}{2} \cdot \frac{(b - a)}{e - a} + \frac{W_{\text{Passweight}}}{2} \cdot \frac{(d - a)}{(e - a)} + \frac{W_{\text{device}} \cdot (c - a)}{e - a} - \text{Caster2}$$

$$F_{\text{wl}} = 243.262 \text{ N}$$

$$F_{\text{wr}} := -(F_{\text{wl}} - W_{\text{device}} + \text{Caster1} + \text{Caster2} - W_{\text{Passweight}})$$

The Forces were Calculated to be:

$$F_{w1} = 243.262 \text{ N}$$

$$\text{Caster2} = 535.177 \text{ N}$$

$$F_{wr} = 243.262 \text{ N}$$

$$\text{Caster1} = 535.177 \text{ N}$$

$$R_2 := F_{wr} + \text{Caster2}$$

$$M_2 := R_2 \cdot (e - i)$$

Singularity functions will be used to analyse the frame, these are based on the equations established earlier with the frame on static conditions

To determine the singularity functions for shear, moment, slope and deflection we integrate in the following manner.

$$V(x) = \int -q(x) + C_1$$

$$M(x) = \int V(x) + C_1 \cdot x + C_2$$

$$\theta(x) = \int M(x) + \frac{C_1 \cdot x^2}{2} + C_2 \cdot x + C_3$$

$$y(x) = \int \theta(x) + \frac{C_1 \cdot x^3}{6} + \frac{C_2 \cdot x^2}{2} + C_3 \cdot x + C_4$$

for these integrations the following rules apply.

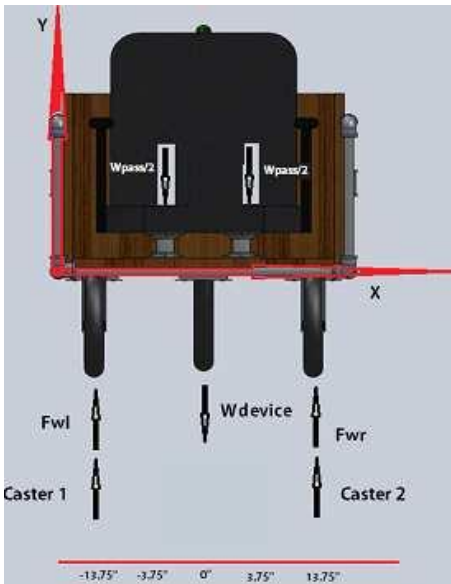
If  $n > 0$  and the expression inside the angular parenthesis is positive then  $fn(x) = (x-a)^n$  the expression is a normal algebraic formula

If  $n < 0$  then  $fn = 1$  for  $x = a$  and  $fn(x) = 0$  otherwise

If  $n = 0$  then  $fn = 1$  for  $x \geq a$  and  $fn(x) = 0$  otherwise

If  $n \geq 0$ , the integration rule is  $\int \langle x-a \rangle^n dx = \frac{\langle x-a \rangle^{n+1}}{(n+1)}$  This is the same for normal brackets

If  $n < 0$ , the integration rule is  $\int \langle x-a \rangle^n dx = \langle x-a \rangle^{n+1}$



unit step function  $S(x, z) := \text{if}(x \geq z, 1, 0)$

$c := 0\text{in}$      $a := -13.75\text{in}$      $b := -3.75\text{in}$      $d := 3.75\text{in}$      $e := 13.75\text{in}$      $C_1 := 0$      $C_2 := 0$

Range of x  $x := a, (a + 0.001\text{in})..e$

Singularity Functions

$$q_1(x) := F_{wl} \cdot S(x, a) \cdot (x - a)^{-1} + \text{Caster1} \cdot S(x, a) \cdot (x - a)^{-1} - \frac{W_{\text{Passweight}}}{2} \cdot S(x, b) \cdot (x - b)^{-1} \dots$$

$$+ \left[ -W_{\text{device}} \cdot S(x, c) \cdot (x - c)^{-1} \right] - \frac{W_{\text{Passweight}}}{2} \cdot S(x, d) \cdot (x - d)^{-1} \dots$$

$$+ F_{wr} \cdot S(x, e) \cdot (x - e)^{-1} + \text{Caster2} \cdot S(x, e) \cdot (x - e)^{-1}$$

$$V_1(x) := \left[ F_{wl} \cdot S(x, a) \cdot (x - a)^0 + \text{Caster1} \cdot S(x, a) \cdot (x - a)^0 - \frac{W_{\text{Passweight}}}{2} \cdot S(x, b) \cdot (x - b)^0 \dots \right]$$

$$+ \left[ -W_{\text{device}} \cdot S(x, c) \cdot (x - c)^0 \right] - \frac{W_{\text{Passweight}}}{2} \cdot S(x, d) \cdot (x - d)^0 \dots$$

$$+ F_{wr} \cdot S(x, e) \cdot (x - e)^0 + \text{Caster2} \cdot S(x, e) \cdot (x - e)^0 + C_1$$

$$M_1(x) := F_{wl} \cdot S(x, a) \cdot (x - a)^1 + \text{Caster1} \cdot S(x, a) \cdot (x - a)^1 - \frac{W_{\text{Passweight}}}{2} \cdot S(x, b) \cdot (x - b)^1 \dots$$

$$+ \left[ -W_{\text{device}} \cdot S(x, c) \cdot (x - c)^1 \right] - \frac{W_{\text{Passweight}}}{2} \cdot S(x, d) \cdot (x - d)^1 \dots$$

$$+ F_{wr} \cdot S(x, e) \cdot (x - e)^1 + \text{Caster2} \cdot S(x, e) \cdot (x - e)^1 + C_1 \cdot x + C_2$$

$$\theta_1(x) := \frac{1}{E_{al} \cdot I} \left[ \begin{aligned} & \frac{F_{wl} \cdot S(x, a) \cdot (x - a)^2}{2} + \frac{Caster1 \cdot S(x, a) \cdot (x - a)^2}{2} - \frac{W_{Passweight}}{4} \cdot S(x, b) \cdot (x - b)^2 \dots \\ & + \left[ \frac{-W_{device} \cdot S(x, c) \cdot (x - c)^2}{2} \right] - \frac{W_{Passweight}}{4} \cdot S(x, d) \cdot (x - d)^2 \dots \\ & + \left[ \frac{F_{wr} \cdot S(x, e) \cdot (x - e)^2}{2} + \frac{Caster2 \cdot S(x, e) \cdot (x - e)^2}{2} + \frac{C_1 \cdot x^2}{2} + C_2 \cdot x + C_3 \right] \end{aligned} \right]$$

$$y_1(x) := \frac{1}{E_{al} \cdot I} \left[ \begin{aligned} & \frac{F_{wl} \cdot S(x, a) \cdot (x - a)^3}{6} + \frac{Caster1 \cdot S(x, a) \cdot (x - a)^3}{6} - \frac{W_{Passweight}}{12} \cdot S(x, b) \cdot (x - b)^3 \dots \\ & + \left[ \frac{-W_{device} \cdot S(x, c) \cdot (x - c)^3}{6} \right] - \frac{W_{Passweight}}{12} \cdot S(x, d) \cdot (x - d)^3 \dots \\ & + \frac{F_{wr} \cdot S(x, e) \cdot (x - e)^3}{6} + \frac{Caster2 \cdot S(x, e) \cdot (x - e)^3}{6} + \frac{C_1 \cdot x^3}{6} + \frac{C_2 \cdot x^2}{2} + C_3 \cdot x + C_4 \end{aligned} \right]$$

Boundary Conditions

$$y_1(x) = 0 \quad C_4 = -C_3 \cdot a$$

When at

$$x = a \quad \text{and} \quad x = e \quad x = e$$

at

$$x = a$$

$$\begin{aligned} -C_4 &= \frac{F_{wl} \cdot (e - a)^3}{6} + \frac{Caster1 \cdot (e - a)^3}{6} - \frac{W_{Passweight}}{12} \cdot (e - b)^3 \dots \\ & + \frac{-W_{device} \cdot (e - c)^3}{6} - \frac{W_{Passweight}}{12} \cdot (e - d)^3 \dots \\ & + \frac{F_{wr} \cdot (e - e)^3}{6} + \frac{Caster2 \cdot (e - e)^3}{6} + C_3 \cdot e \end{aligned}$$

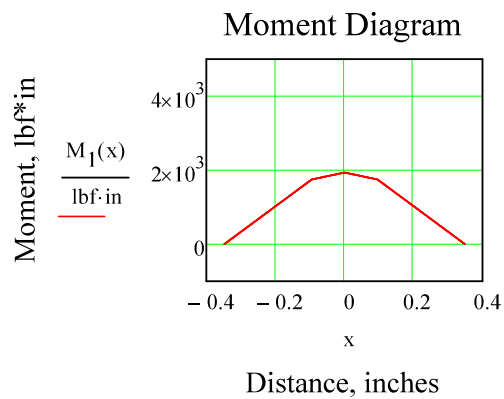
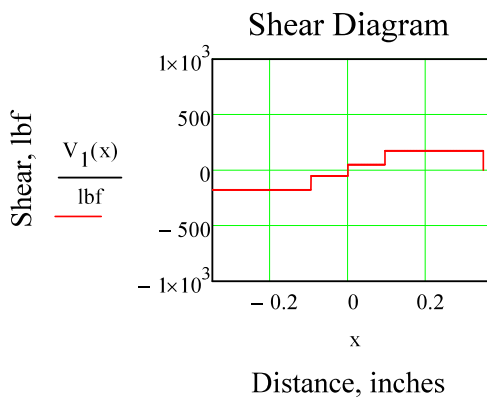
$$\begin{aligned} C_3 \cdot a &= \frac{F_{wl} \cdot (e - a)^3}{6} + \frac{Caster1 \cdot (e - a)^3}{6} - \frac{W_{Passweight}}{12} \cdot (e - b)^3 \dots \\ & + \frac{-W_{device} \cdot (e - c)^3}{6} - \frac{W_{Passweight}}{12} \cdot (e - d)^3 \dots \\ & + \frac{F_{wr} \cdot (e - e)^3}{6} + \frac{Caster2 \cdot (e - e)^3}{6} + C_3 \cdot e \end{aligned}$$

$$C_3 := \frac{\left[ \begin{aligned} &\frac{F_{wl} \cdot (e - a)^3}{6} + \frac{Caster1 \cdot (e - a)^3}{6} - \frac{W_{Passweight}}{12} \cdot (e - b)^3 \dots \\ &+ \frac{-W_{device} \cdot (e - c)^3}{6} - \frac{W_{Passweight}}{12} \cdot (e - d)^3 \dots \\ &+ \frac{F_{wr} \cdot (e - e)^3}{6} + \frac{Caster2 \cdot (e - e)^3}{6} \end{aligned} \right]}{a - e}$$

$$C_4 := -C_3 \cdot a$$

$$\theta_1(x) := \frac{1}{E_{al} \cdot I} \left[ \begin{aligned} &\frac{F_{wl} \cdot S(x, a) \cdot (x - a)^2}{2} + \frac{Caster1 \cdot S(x, a) \cdot (x - a)^2}{2} - \frac{W_{Passweight}}{4} \cdot S(x, b) \cdot (x - b)^2 \dots \\ &+ \frac{-W_{device} \cdot S(x, c) \cdot (x - c)^2}{2} - \frac{W_{Passweight}}{4} \cdot S(x, d) \cdot (x - d)^2 \dots \\ &+ \left[ \frac{F_{wr} \cdot S(x, e) \cdot (x - e)^2}{2} + \frac{Caster2 \cdot S(x, e) \cdot (x - e)^2}{2} + \frac{C_1 \cdot x^2}{2} + C_2 \cdot x + C_3 \right] \end{aligned} \right]$$

$$y_1(x) := \frac{1}{E_{al} \cdot I} \left[ \begin{aligned} &\frac{F_{wl} \cdot S(x, a) \cdot (x - a)^3}{6} + \frac{Caster1 \cdot S(x, a) \cdot (x - a)^3}{6} - \frac{W_{Passweight}}{12} \cdot S(x, b) \cdot (x - b)^3 \dots \\ &+ \frac{-W_{device} \cdot S(x, c) \cdot (x - c)^3}{6} - \frac{W_{Passweight}}{12} \cdot S(x, d) \cdot (x - d)^3 \dots \\ &+ \frac{F_{wr} \cdot S(x, e) \cdot (x - e)^3}{6} + \frac{Caster2 \cdot S(x, e) \cdot (x - e)^3}{6} + \frac{C_1 \cdot x^3}{6} + \frac{C_2 \cdot x^2}{2} + C_3 \cdot x + C_4 \end{aligned} \right]$$



### Rough Stress analysis

$$M_{a,max} := M_I(c)$$

$$V_{a,max1} := V_I(d)$$

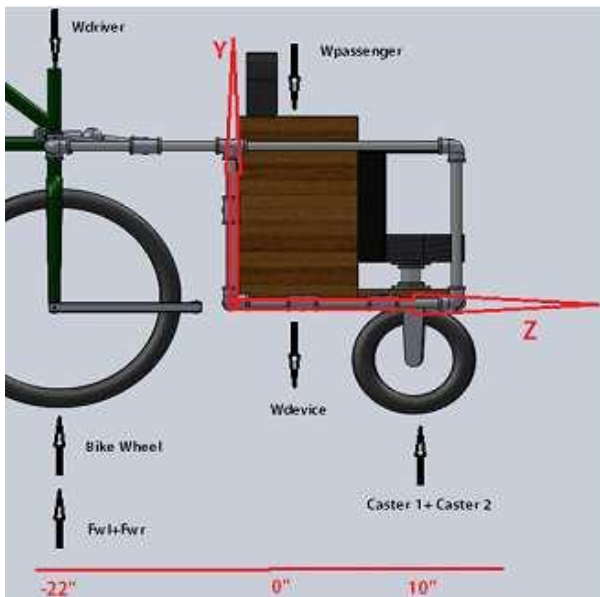
Normal bending stress

$$\sigma_x := \frac{M_{a,max} \cdot (R)}{I}$$

torsional shear stress

$$\tau_x := \frac{M_{a,max} \cdot (R)}{\frac{\pi}{32} \cdot (OD^4 - ID^4)}$$

### Free Body Diagram of Side View



$$f := -22\text{in} \quad g := 0\text{in} \quad h := 10\text{in}$$

$$\text{Range of } z \quad z := f, (f + 0.01\text{in}) .. h + .1\text{in}$$

$$q(z) := F_{wl} \cdot S(z, f) \cdot (z - f)^{-1} + \text{Caster1} \cdot S(z, h) \cdot (z - h)^{-1} - W_{\text{Passweight}} \cdot S(z, g) \cdot (z - g)^{-1} \dots \\ + - W_{\text{device}} \cdot S(z, g) \cdot (z - g)^{-1} + F_{wr} \cdot S(z, f) \cdot (z - f)^{-1} + \text{Caster2} \cdot S(z, h) \cdot (z - h)^{-1}$$

$$V(z) := \left[ \begin{array}{l} F_{wl} \cdot S(z, f) \cdot (z - f)^0 + \text{Caster1} \cdot S(z, h) \cdot (z - h)^0 - W_{\text{Passweight}} \cdot S(z, g) \cdot (z - g)^0 \dots \\ + - W_{\text{device}} \cdot S(z, g) \cdot (z - g)^0 + F_{wr} \cdot S(z, f) \cdot (z - f)^0 + \text{Caster2} \cdot S(z, h) \cdot (z - h)^0 + C_1 \end{array} \right]$$

$$M(z) := F_{wl} \cdot S(z, f) \cdot (z - f)^1 + Caster1 \cdot S(z, h) \cdot (z - h)^1 - W_{Passweight} \cdot S(z, g) \cdot (z - g)^1 \dots$$

$$+ -W_{device} \cdot S(z, g) \cdot (z - g)^1 + F_{wr} \cdot S(z, f) \cdot (z - f)^1 + Caster2 \cdot S(z, h) \cdot (z - h)^1 + C_1 \cdot z + C_2$$

$$\theta(z) := \frac{1}{E_{al} \cdot I} \left[ \begin{array}{l} \frac{F_{wl} \cdot S(z, f) \cdot (z - f)^2}{2} + \frac{Caster1 \cdot S(z, h) \cdot (z - h)^2}{2} - \frac{W_{Passweight} \cdot S(z, g) \cdot (z - g)^2}{2} \dots \\ + \frac{-W_{device} \cdot S(z, g) \cdot (z - g)^2}{2} + \frac{F_{wr} \cdot S(z, f) \cdot (z - f)^2}{2} + \frac{Caster2 \cdot S(z, h) \cdot (z - h)^2}{2} + \frac{C_1 \cdot z^2}{2} \dots \\ + C_2 \cdot x + C_5 \end{array} \right]$$

$$y(z) := \frac{1}{E_{al} \cdot I} \left[ \begin{array}{l} \frac{F_{wl} \cdot S(z, f) \cdot (z - f)^3}{6} + \frac{Caster1 \cdot S(z, h) \cdot (z - h)^3}{6} - \frac{W_{Passweight} \cdot S(z, g) \cdot (z - g)^3}{6} \dots \\ + \frac{-W_{device} \cdot S(z, g) \cdot (z - g)^3}{6} + \frac{F_{wr} \cdot S(z, f) \cdot (z - f)^3}{6} + \frac{Caster2 \cdot S(z, h) \cdot (z - h)^3}{6} + \frac{C_1 \cdot z}{6} \dots \\ + \frac{C_2 \cdot z^2}{2} + C_5 \cdot z + C_6 \end{array} \right]$$

Boundary Conditions

$$y(z) = 0 \quad C_6 = -C_5 \cdot f$$

When

$$z = f \quad \text{and} \quad z = h$$

at

$$z = f$$

at

$$z = h$$

$$-C_6 = \frac{F_{wl} \cdot (h - f)^3}{6} + \frac{Caster1 \cdot (h - h)^3}{6} - \frac{W_{Passweight} \cdot (h - g)^3}{6} \dots$$

$$+ \frac{-W_{device} \cdot (h - g)^3}{6} + \frac{F_{wr} \cdot (h - f)^3}{6} + \frac{Caster2 \cdot (h - h)^3}{6} \dots$$

$$+ C_5 \cdot h$$

$$C_5 \cdot f = \frac{F_{wl} \cdot (h - f)^3}{6} + \frac{Caster1 \cdot (h - h)^3}{6} - \frac{W_{Passweight} \cdot (h - g)^3}{6} \dots$$

$$+ \frac{-W_{device} \cdot (h - g)^3}{6} + \frac{F_{wr} \cdot (h - f)^3}{6} + \frac{Caster2 \cdot (h - h)^3}{6} \dots$$

$$+ C_5 \cdot h$$

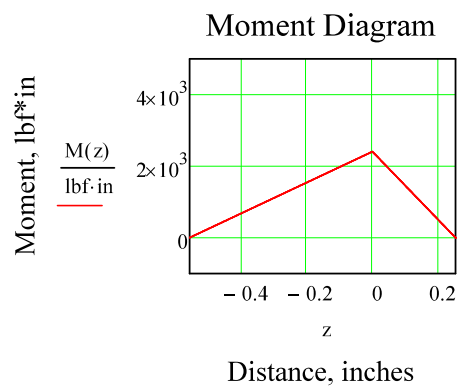
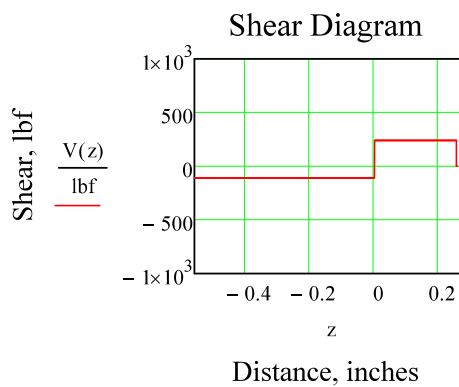


$$C_5 := \frac{\left[ \begin{array}{l} \frac{F_{wl} \cdot (h-f)^3}{6} + \frac{Caster1 \cdot (h-h)^3}{6} - \frac{W_{Passweight} \cdot (h-g)^3}{6} \dots \\ + \frac{-W_{device} \cdot (h-g)^3}{6} + \frac{F_{wr} \cdot (h-f)^3}{6} + \frac{Caster2 \cdot (h-h)^3}{6} \dots \end{array} \right]}{f-h}$$

$$C_6 := \left[ \begin{array}{l} \frac{F_{wl} \cdot (h-f)^3}{6} + \frac{Caster1 \cdot (h-h)^3}{6} - \frac{W_{Passweight} \cdot (h-g)^3}{6} \dots \\ + \frac{-W_{device} \cdot (h-g)^3}{6} + \frac{F_{wr} \cdot (h-f)^3}{6} + \frac{Caster2 \cdot (h-h)^3}{6} \dots \\ + C_5 \cdot h \end{array} \right]$$

$$\theta(z) := \frac{1}{E_{al} \cdot I} \left[ \begin{array}{l} \frac{F_{wl} \cdot S(z,f) \cdot (z-f)^2}{2} + \frac{Caster1 \cdot S(z,h) \cdot (z-h)^2}{2} - \frac{W_{Passweight} \cdot S(z,g) \cdot (z-g)^2}{2} \dots \\ + \frac{-W_{device} \cdot S(z,g) \cdot (z-g)^2}{2} + \frac{F_{wr} \cdot S(z,f) \cdot (z-f)^2}{2} + \frac{Caster2 \cdot S(z,h) \cdot (z-h)^2}{2} + \frac{C_1 \cdot z^2}{2} \dots \\ + C_2 \cdot z + C_5 \end{array} \right]$$

$$y(z) := \frac{1}{E_{al} \cdot I} \left[ \begin{array}{l} \frac{F_{wl} \cdot S(z,f) \cdot (z-f)^3}{6} + \frac{Caster1 \cdot S(z,h) \cdot (z-h)^3}{6} - \frac{W_{Passweight} \cdot S(z,g) \cdot (z-g)^3}{6} \dots \\ + \frac{-W_{device} \cdot S(z,g) \cdot (z-g)^3}{6} + \frac{F_{wr} \cdot S(z,f) \cdot (z-f)^3}{6} + \frac{Caster2 \cdot S(z,h) \cdot (z-h)^3}{6} + \frac{C_1 \cdot z}{6} \dots \\ + \frac{C_2 \cdot z^2}{2} + C_5 \cdot z + C_6 \end{array} \right]$$



$$M_{b,max} := M(g)$$

$$V_{b,max1} := V(g)$$

Normal bending stress

$$\sigma_z := \frac{M_{b,max} \cdot (R)}{I}$$

torsional shear stress

$$\tau_{z,1} := \frac{M_{b,max} \cdot (R)}{\frac{\pi}{32} \cdot (OD^4 - ID^4)}$$

### 3D Stress

$$\sigma_{.x1} := \frac{\sigma_{.x}}{\text{psi}}$$

$$\tau_{x1,1} := \frac{\tau_{x,1}}{\text{psi}}$$

$$\sigma_{z1} := \frac{\sigma_z}{\text{psi}}$$

$$\tau_{z,1} := \frac{\tau_z}{\text{psi}}$$

$$\sigma_y := 0$$

$$\tau_{zx} := 0$$

The stress cubic

$$\sigma^3 - C_c \cdot \sigma^2 - C_b \cdot \sigma - C_a = 0$$

The roots of this equation give us the principal stresses

$$C_b := \sigma_{.x1} + \sigma_{z1}$$

$$C_a := \left| \begin{pmatrix} \sigma_{.x1} & \tau_{x1,1} \\ \tau_{x1,1} & \sigma_y \end{pmatrix} \right| + \left| \begin{pmatrix} \sigma_{.x1} & \tau_{zx} \\ \tau_{zx} & \sigma_{z1} \end{pmatrix} \right| + \left| \begin{pmatrix} \sigma_{.x1} & \tau_{z,1} \\ \tau_{z,1} & \sigma_{z1} \end{pmatrix} \right|$$

$$C_c := \left| \begin{pmatrix} \sigma_{.x1} & \tau_{x1,1} & \tau_{zx} \\ \tau_{x1,1} & \sigma_y & \tau_{z,1} \\ \tau_{zx} & \tau_{z,1} & \sigma_{z1} \end{pmatrix} \right|$$

$$v := \begin{pmatrix} C_c \\ C_a \\ C_b \\ 1 \end{pmatrix}$$

$r := \text{polyroots}(v)$

$$r = \begin{pmatrix} -1.835 \times 10^4 - 1.426i \times 10^4 \\ -1.835 \times 10^4 + 1.426i \times 10^4 \\ 4 \times 10^3 \end{pmatrix}$$

$$\sigma_1 := (-3.094 \times 10^4 - 1.954i \times 10^4) \text{psi}$$

$$\sigma_2 := (-3.094 \times 10^4 + 1.954i \times 10^4) \text{psi}$$

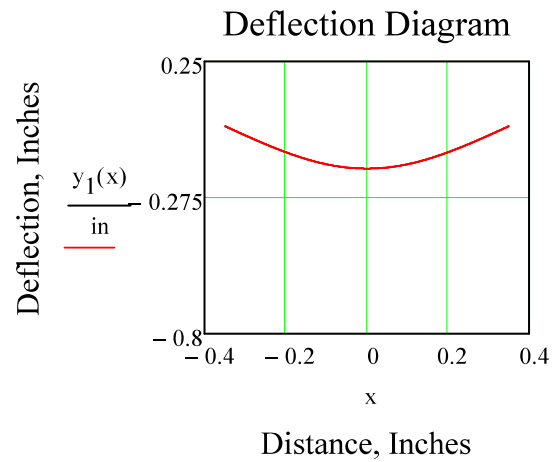
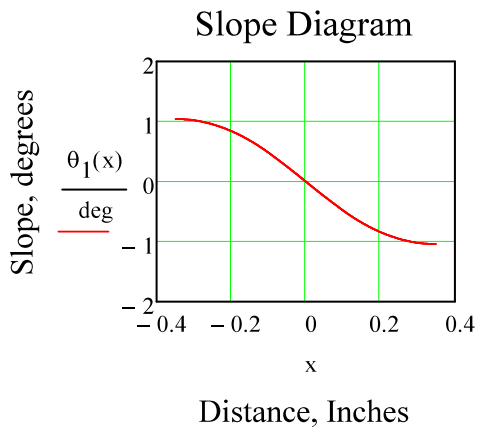
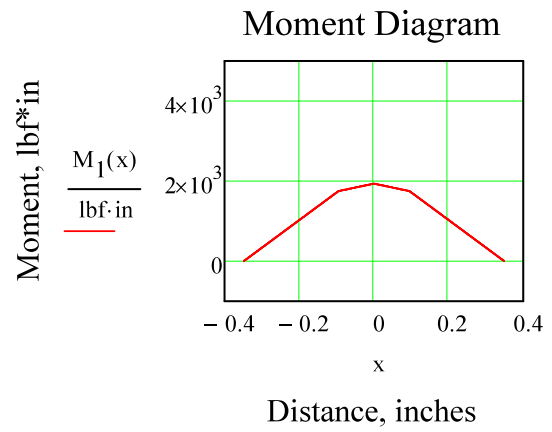
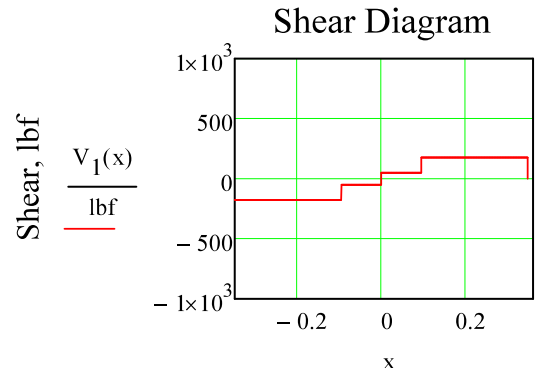
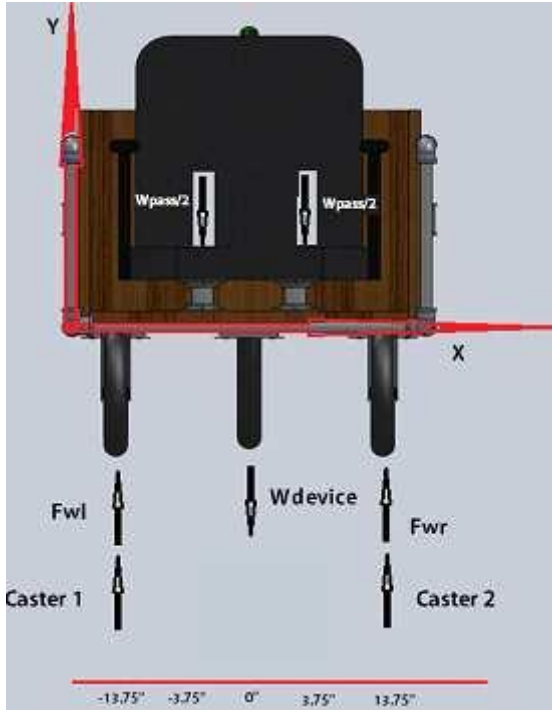
$$\sigma_3 := (6.864 \times 10^3) \text{psi}$$

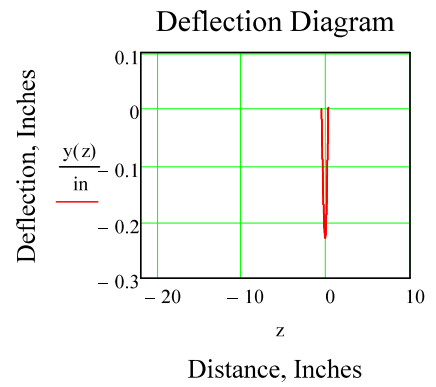
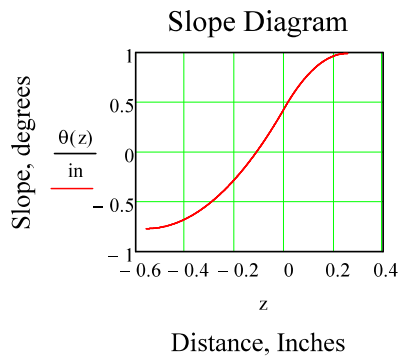
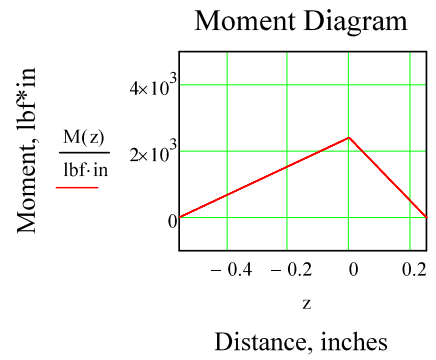
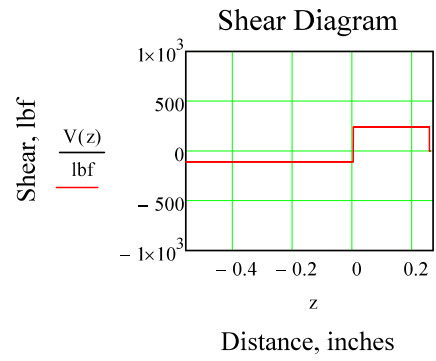
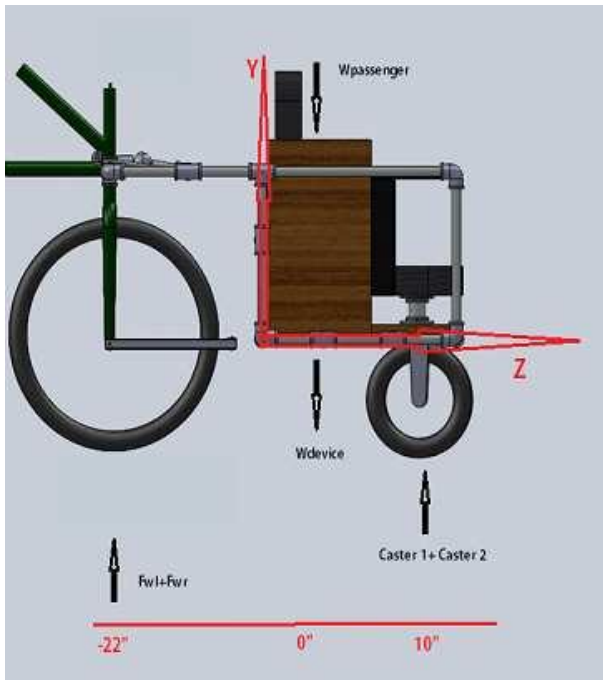
$$\sigma_v := \sqrt{\sigma_1^2 + \sigma_2^2 + \sigma_3^2 - \sigma_1 \cdot \sigma_2 - \sigma_2 \cdot \sigma_3 - \sigma_1 \cdot \sigma_3} = 16.844 \text{ kpsi}$$

$$\frac{\sigma_1 - \sigma_2}{2} = -19.54i \text{ kpsi}$$

Safety Factor under static loading

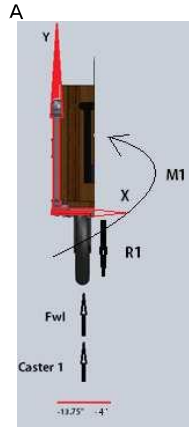
$$N := \frac{S_{yal}}{\sigma_v} = 2.672$$





Section Analysis of Each Component

Front View Section



$$n := -4\text{in}$$

$$\sum F(y) = \text{Caster1} + F_{wl} - R_1 = 0$$

$$\sum M(a) = M_1 - R_1(l) = 0$$

$$R_1 := \text{Caster1} + F_{wl}$$

$$M_1 := R_1 \cdot \text{in}$$

unit step function  $S(x, z) := \text{if}(x \geq z, 1, 0)$

Range of x  $x := a, (a + 0.001\text{in}) .. n$

$$q_A(x) := F_{wl} \cdot S(x, a) \cdot (x - a)^{-1} + \text{Caster1} \cdot S(x, a) \cdot (x - a)^{-1} - R_1 \cdot S(x, n) \cdot (x - n)^{-1}$$

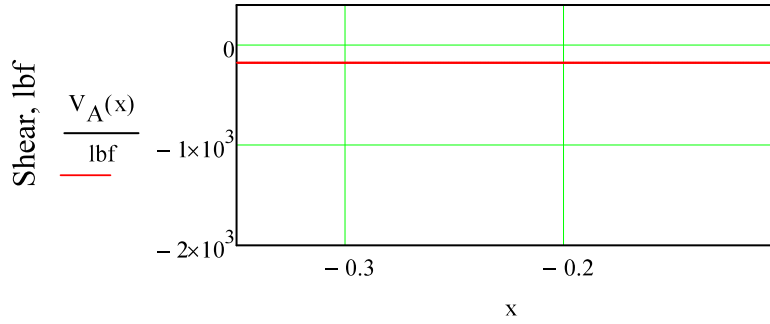
$$V_A(x) := -\left[ F_{wl} \cdot S(x, a) \cdot (x - a)^0 + \text{Caster1} \cdot S(x, a) \cdot (x - a)^0 - R_1 \cdot S(x, n) \cdot (x - n)^0 + C_1 \right]$$

$$M_A(x) := F_{wl} \cdot S(x, a) \cdot (x - a)^1 + \text{Caster1} \cdot S(x, a) \cdot (x - a)^1 - R_1 \cdot S(x, n) \cdot (x - n)^1 + M_1 \cdot S(x, n) \cdot (x - n)^0 + C_1 \cdot x + C_2$$

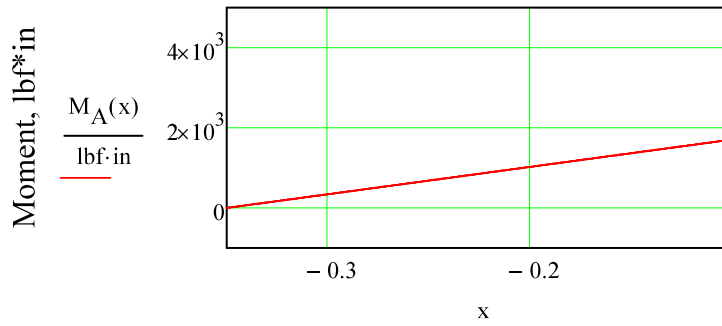
$$\theta_A(x) := \frac{1}{E_{al} I} \left[ \frac{F_{wl} \cdot S(x, a) \cdot (x - a)^2}{2} + \frac{\text{Caster1} \cdot S(x, a) \cdot (x - a)^2}{2} - \frac{R_1 \cdot S(x, n) \cdot (x - n)^2}{2} + M_1 \cdot S(x, n) \cdot (x - n)^1 + C_1 \cdot \frac{x^2}{2} + C_2 \cdot x + C_3 \right]$$

$$y_A(x) := \frac{1}{E_{al} I} \left[ \frac{F_{wl} \cdot S(x, a) \cdot (x - a)^3}{6} + \frac{\text{Caster1} \cdot S(x, a) \cdot (x - a)^3}{6} - \frac{R_1 \cdot S(x, n) \cdot (x - n)^3}{6} + \frac{M_1 \cdot S(x, n) \cdot (x - n)^2}{2} + C_1 \cdot \frac{x^3}{6} + \frac{C_2 \cdot x^2}{2} \dots \right]$$

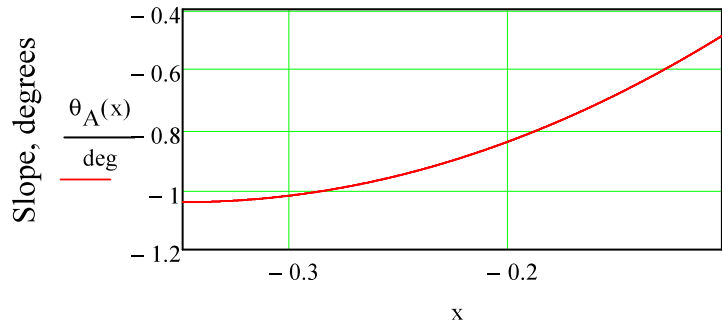
Shear Diagram Front View A



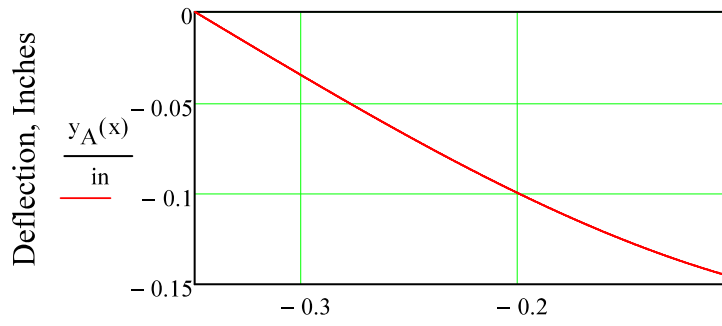
Moment Diagram Front View A



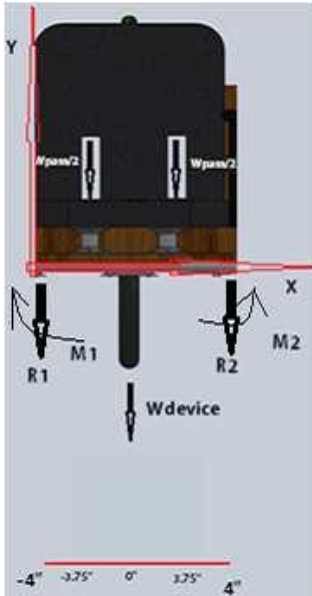
Slope Diagram Front View A



Deflection Diagram Front View A



front View Section B



Von Mises  
Analysis page 22

$$\sum F(y) = \frac{-W_{\text{Passweight}}}{2} - \frac{W_{\text{Passweight}}}{2} - W_{\text{device}} + -R_1 - R_2$$

$$\sum M(f) = \frac{-W_{\text{Passweight}}}{2}(b-f) - \frac{W_{\text{Passweight}}}{2}(b-f) - \frac{W_{\text{Passweight}}}{2} \cdot (d-n) - W_{\text{device}} \cdot (c-n) \dots$$

$$+ M_1 - M_2 - R_2 \cdot (i-n)$$

$$x := n, (n + 0.001 \text{in}) \dots i$$

$$q_B(x) := -R_1 \cdot S(x, n) \cdot (x-n)^{-1} - \frac{W_{\text{Passweight}}}{2} S(x, b) \cdot (x-b)^{-1} - W_{\text{device}} S(x, c) \cdot (x-c)^{-1} \dots$$

$$+ \frac{-W_{\text{Passweight}}}{2} S(x, d) \cdot (x-d)^{-1} - R_2 \cdot S(x, i) \cdot (x-i)^{-1}$$

$$V_B(x) := \left[ \begin{array}{l} -R_1 \cdot S(x, n) \cdot (x-n)^0 - \frac{W_{\text{Passweight}}}{2} S(x, b) \cdot (x-b)^0 - W_{\text{device}} S(x, c) \cdot (x-c)^0 \dots \\ + \frac{-W_{\text{Passweight}}}{2} S(x, d) \cdot (x-d)^0 - R_2 \cdot S(x, i) \cdot (x-i)^0 + C_1 \end{array} \right]$$

$$M_B(x) := -R_1 \cdot S(x, n) \cdot (x-n)^1 - \frac{W_{\text{Passweight}}}{2} S(x, b) \cdot (x-b)^1 - W_{\text{device}} S(x, c) \cdot (x-c)^1 \dots$$

$$+ \frac{-W_{\text{Passweight}}}{2} S(x, d) \cdot (x-d)^1 - R_2 \cdot S(x, i) \cdot (x-i)^1 \dots$$

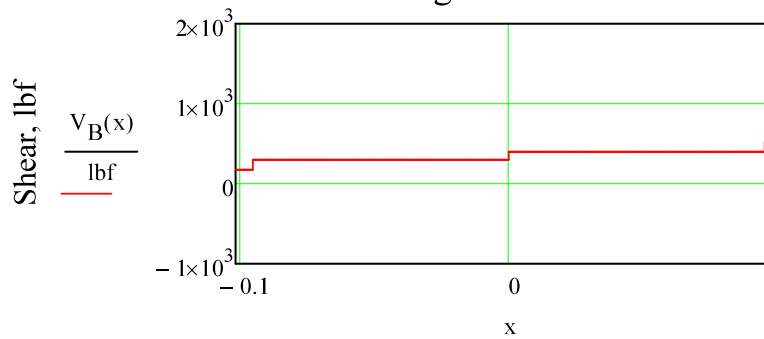
$$+ M_2 \cdot S(x, i) \cdot (x-i)^0 - M_1 S(x, n) \cdot (x-n)^0 + C_1 \cdot x + C_2$$



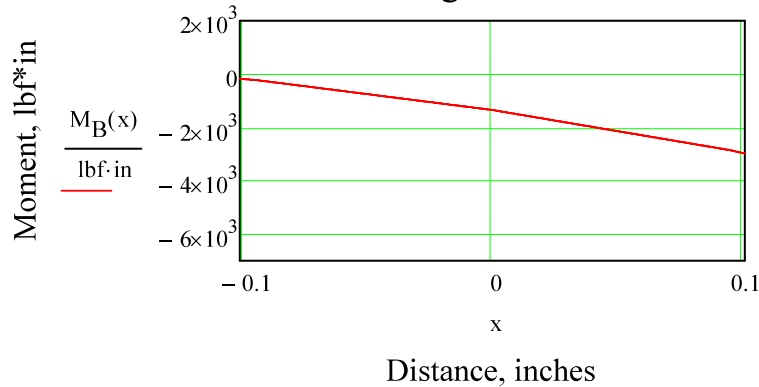
$$\theta_B(x) := \frac{1}{E_{al} I} \left[ \begin{aligned} & \frac{-R_1 \cdot S(x, n) \cdot (x - n)^2}{2} - \frac{W_{Passweight}}{4} S(x, b) \cdot (x - b)^2 - \frac{W_{device} S(x, c) \cdot (x - c)^2}{2} \dots \\ & + \frac{-W_{Passweight}}{4} S(x, d) \cdot (x - d)^2 - \frac{R_2 \cdot S(x, i) \cdot (x - i)^2}{2} \dots \\ & + M_2 \cdot S(x, i) \cdot (x - i)^1 - M_1 S(x, n) \cdot (x - n)^1 + \frac{C_1 \cdot x^2}{2} + C_2 \cdot x + C_3 \end{aligned} \right]$$

$$y_B(x) := \frac{1}{E_{al} I} \left[ \begin{aligned} & \frac{-R_1 \cdot S(x, n) \cdot (x - n)^3}{6} - \frac{W_{Passweight}}{12} S(x, b) \cdot (x - b)^3 - \frac{W_{device} S(x, c) \cdot (x - c)^3}{6} \dots \\ & + \frac{-W_{Passweight}}{12} S(x, d) \cdot (x - d)^3 - \frac{R_2 \cdot S(x, i) \cdot (x - i)^3}{6} \dots \\ & + \frac{M_2 \cdot S(x, i) \cdot (x - i)^2}{2} - \frac{M_1 S(x, n) \cdot (x - n)^2}{2} + \frac{C_1 \cdot x^3}{6} + \frac{C_2 \cdot x^2}{2} + C_3 \cdot x + C_4 \end{aligned} \right]$$

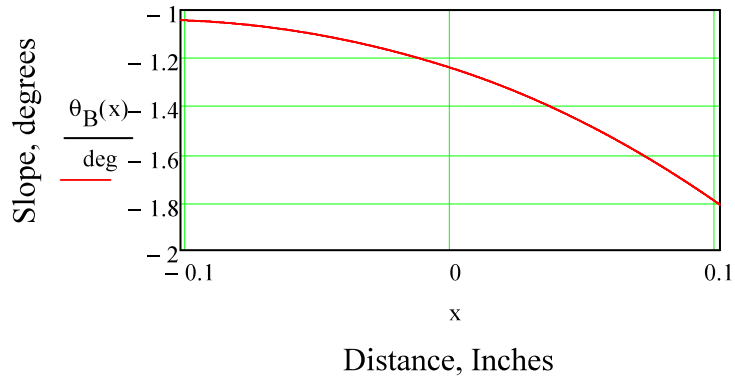
Shear Diagram Front View B



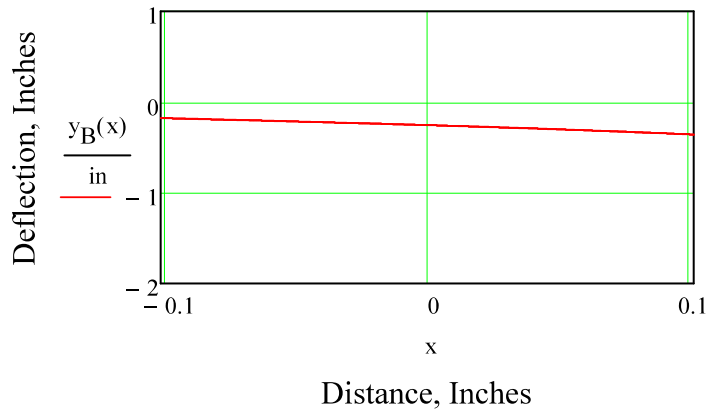
Moment Diagram Front View B



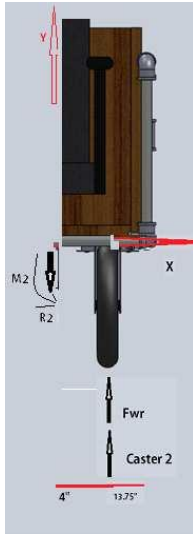
Slope Diagram Front View B



Deflection Diagram Front View B



Section C



$$\sum F(y) = -R_2 + F_{wr} + \text{Caster2} = 0$$

$$\sum M(e) = R_2 \cdot (e - i) - M_2 = 0$$

unit step function  $S(x, z) := \text{if}(x \geq z, 1, 0)$

Range of x  $x := i, (i + 0.001 \text{in}) .. e + .1 \text{in}$

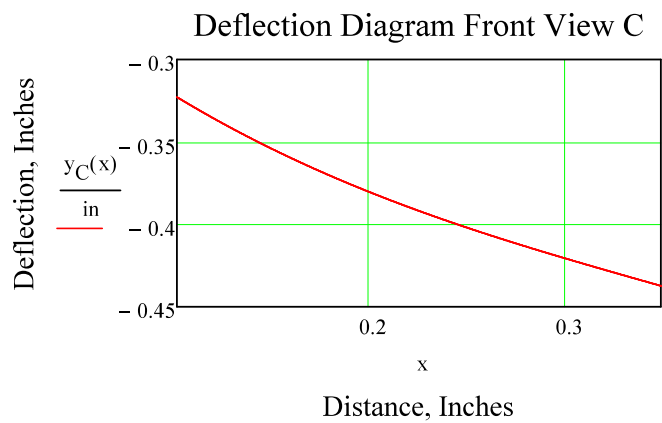
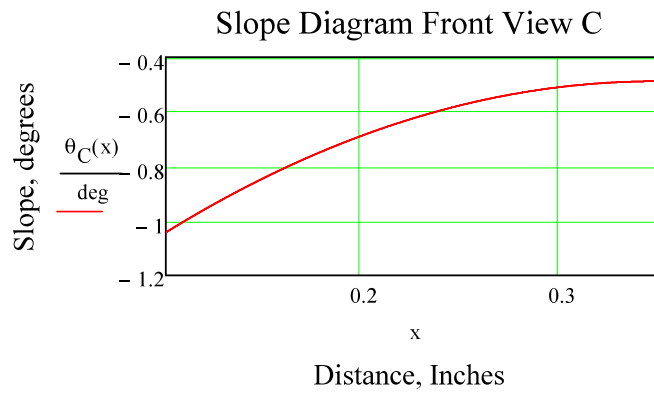
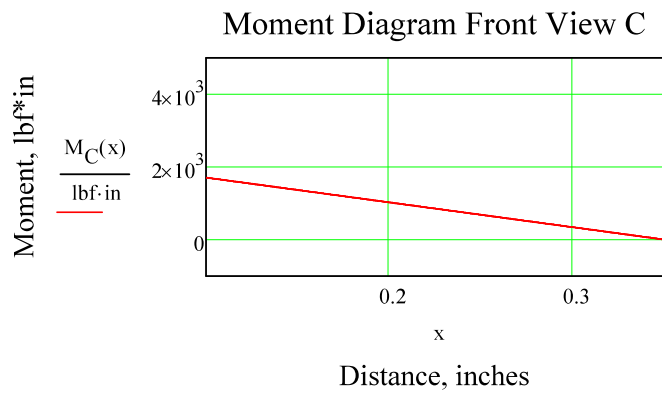
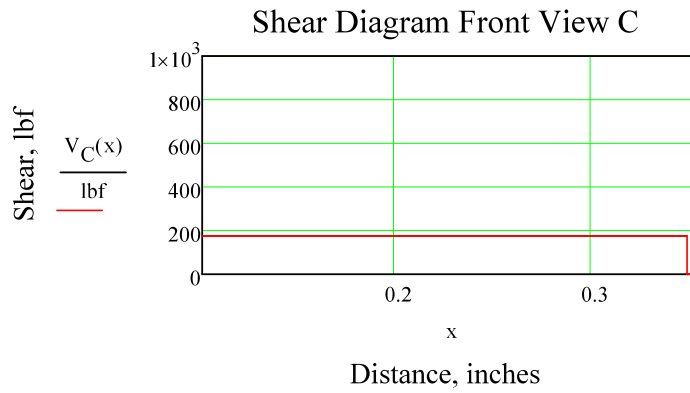
$$q_C(x) := F_{wr} \cdot S(x, e) \cdot (x - e)^{-1} + \text{Caster2} \cdot S(x, e) \cdot (x - e)^{-1} - R_2 \cdot S(x, i) \cdot (x - i)^{-1}$$

$$V_C(x) := - \left[ F_{wr} \cdot S(x, e) \cdot (x - e)^0 + \text{Caster2} \cdot S(x, e) \cdot (x - e)^0 - R_2 \cdot S(x, i) \cdot (x - i)^0 + C_1 \right]$$

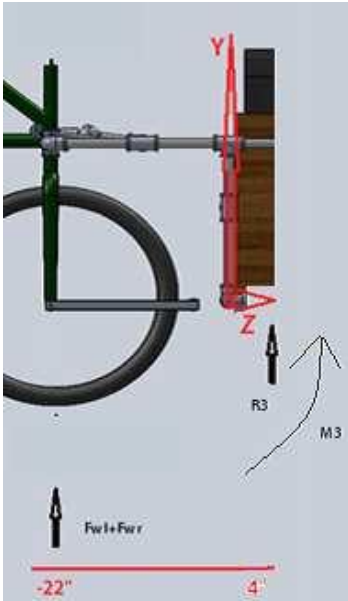
$$M_C(x) := F_{wr} \cdot S(x, e) \cdot (x - e)^1 + \text{Caster2} \cdot S(x, e) \cdot (x - e)^1 - R_2 \cdot S(x, i) \cdot (x - i)^1 + M_2 \cdot S(x, i) \cdot (x - i)^0 + C_1 \cdot x + C_2$$

$$\theta_C(x) := \frac{1}{E_{al} \cdot I} \left[ \frac{F_{wr} \cdot S(x, e) \cdot (x - e)^2}{2} + \frac{\text{Caster2} \cdot S(x, e) \cdot (x - e)^2}{2} - \frac{R_2 \cdot S(x, i) \cdot (x - i)^2}{2} + M_2 \cdot S(x, i) \cdot (x - i)^1 + C_1 \cdot \frac{x^2}{2} + C_2 \cdot x + C_3 \right]$$

$$y_C(x) := \frac{1}{E_{al} \cdot I} \left[ \frac{F_{wr} \cdot S(x, e) \cdot (x - e)^3}{6} + \frac{\text{Caster2} \cdot S(x, e) \cdot (x - e)^3}{6} - \frac{R_2 \cdot S(x, i) \cdot (x - i)^3}{6} + \frac{M_2 \cdot S(x, i) \cdot (x - i)^2}{2} + C_1 \cdot \frac{x^3}{6} + \frac{C_2 \cdot x^2}{2} \dots \right]$$



Side View-Section D



$$\sum F(y) = F_{wr} + F_{wl} + R_3 = 0$$

$$\sum M(f) = R_3 \cdot (j - f) + M_3 = 0$$

$$z := f, (f + 0.001in)..j$$

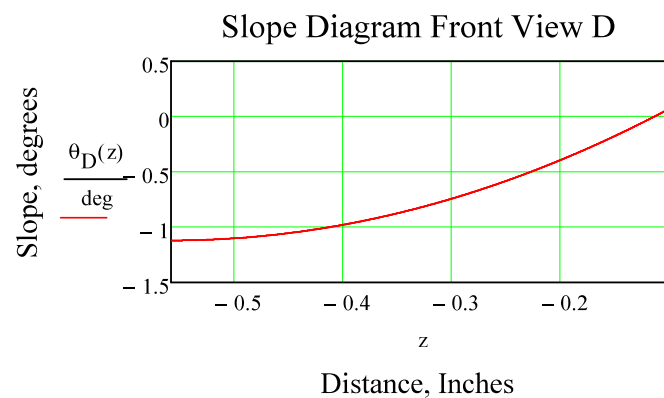
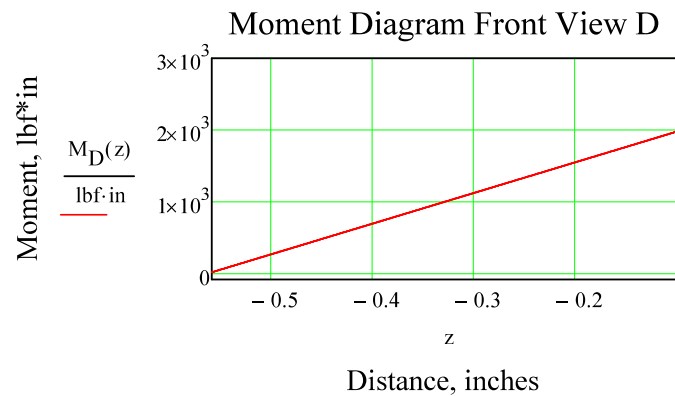
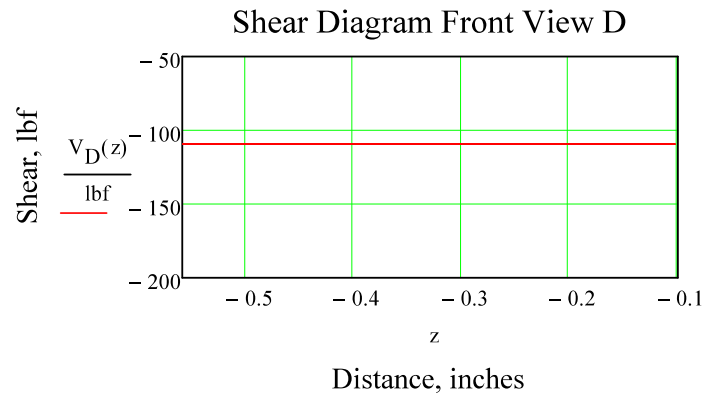
$$q_D(z) := F_{wr} \cdot S(z, f) \cdot (z - f)^{-1} + F_{wl} \cdot S(z, f) \cdot (z - f)^{-1} \dots \\ + R_3 \cdot S(z, j) \cdot (z - j)^{-1}$$

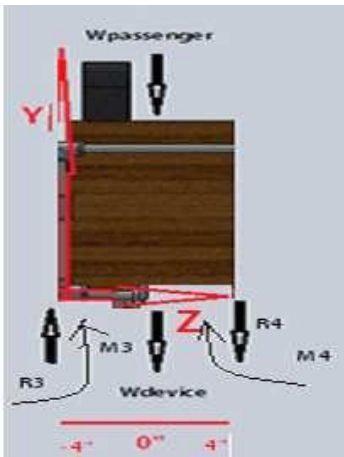
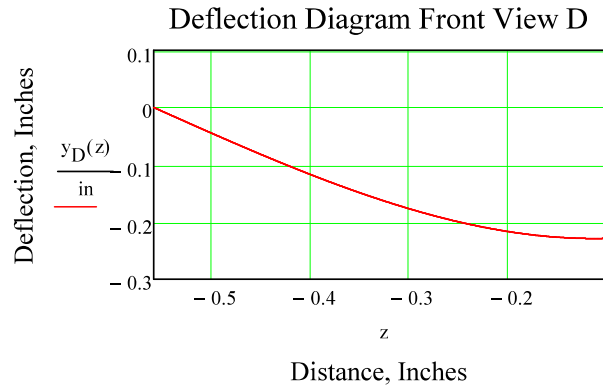
$$V_D(z) := \left[ \begin{array}{l} F_{wr} \cdot S(z, f) \cdot (z - f)^0 + F_{wl} \cdot S(z, f) \cdot (z - f)^0 \dots \\ + R_3 \cdot S(z, j) \cdot (z - j)^0 + C_1 \end{array} \right]$$

$$M_D(z) := F_{wr} \cdot S(z, f) \cdot (z - f)^1 + F_{wl} \cdot S(z, f) \cdot (z - f)^1 \dots \\ + R_3 \cdot S(z, j) \cdot (z - j)^1 + M_3 \cdot S(z, j) \cdot (z - j)^0 + C_1 \cdot z + C_2$$

$$\theta_D(z) := \frac{1}{E_{al} \cdot I} \left[ \begin{array}{l} \frac{F_{wr} \cdot S(z, f) \cdot (z - f)^2}{2} + \frac{F_{wl} \cdot S(z, f) \cdot (z - f)^2}{2} \dots \\ + \frac{R_3 \cdot S(z, j) \cdot (z - j)^2}{2} + M_3 \cdot S(z, j) \cdot (z - j)^1 + \frac{C_1 \cdot z^2}{2} + C_2 \cdot z + C_5 \end{array} \right]$$

$$y_D(z) := \frac{1}{E_{al} I} \left[ \begin{aligned} & \frac{F_{wr} \cdot S(z, f) \cdot (z - f)^3}{6} + \frac{F_{wl} \cdot S(z, f) \cdot (z - f)^3}{6} \dots \\ & + \frac{R_3 \cdot S(z, j) \cdot (z - j)^3}{6} + \frac{M_3 \cdot S(z, j) \cdot (z - j)^2}{2} + \frac{C_1 \cdot z^3}{6} + C_2 \cdot z^2 + C_5 \cdot z + C_6 \end{aligned} \right]$$





$$\sum F(y) = R_3 - W_{\text{Passweight}} - W_{\text{device}} - R_4 = 0$$

$$\sum M(j) = M_3 + W_{\text{device}}(g-j) + W_{\text{Passweight}}(g-j) - R_4(k-j) + M_4 = 0$$

$$z := j, (j + 0.001\text{in})..k$$

$$q_E(z) := R_3 \cdot S(z,j) \cdot (z-j)^{-1} - W_{\text{device}} \cdot S(z,g) \cdot (z-g)^{-1} - W_{\text{Passweight}} \cdot S(z,g) \cdot (z-g)^{-1} - R_4 \cdot S(z,k) \cdot (z-k)^{-1}$$

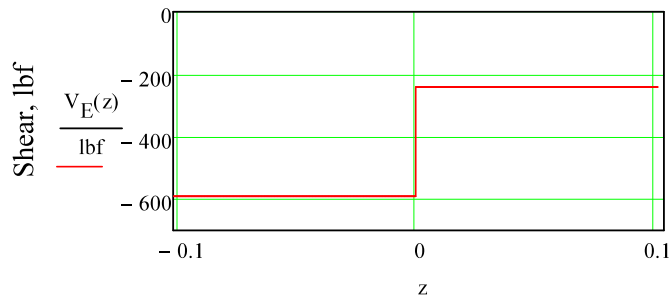
$$V_E(z) := \left[ R_3 \cdot S(z,j) \cdot (z-j)^0 - W_{\text{device}} \cdot S(z,g) \cdot (z-g)^0 - W_{\text{Passweight}} \cdot S(z,g) \cdot (z-g)^0 - R_4 \cdot S(z,k) \cdot (z-k)^0 + C_1 \right]$$

$$M_E(z) := R_3 \cdot S(z,j) \cdot (z-j)^1 - W_{\text{device}} \cdot S(z,g) \cdot (z-g)^1 - W_{\text{Passweight}} \cdot S(z,g) \cdot (z-g)^1 - R_4 \cdot S(z,k) \cdot (z-k)^1 \dots \\ + M_3 \cdot S(z,j) \cdot (z-j)^0 - M_4 \cdot S(z,k) \cdot (z-k)^0 + C_1 \cdot z + C_2$$

$$\theta_E(z) := \frac{1}{E_{al} \cdot I} \left[ \frac{R_3 \cdot S(z,j) \cdot (z-j)^2}{2} - \frac{W_{\text{device}} \cdot S(z,g) \cdot (z-g)^2}{2} - \frac{W_{\text{Passweight}} \cdot S(z,g) \cdot (z-g)^2}{2} - \frac{R_4 \cdot S(z,k) \cdot (z-k)^2}{2} \dots \right. \\ \left. + M_3 \cdot S(z,j) \cdot (z-j)^1 - M_4 \cdot S(z,k) \cdot (z-k)^1 + \frac{C_1 \cdot z^2}{2} + C_2 \cdot z + C_5 \right]$$

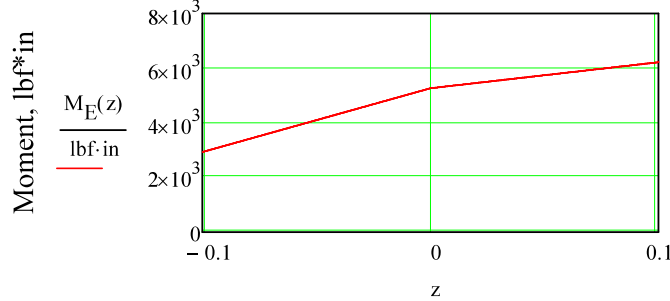
$$y_E(z) := \frac{1}{E_{al} \cdot I} \left[ \frac{R_3 \cdot S(z, j) \cdot (z - j)^3}{6} - \frac{W_{device} \cdot S(z, g) \cdot (z - g)^3}{6} - \frac{W_{Passweight} \cdot S(z, g) \cdot (z - g)^3}{6} - \frac{R_4 \cdot S(z, k) \cdot (z - k)^3}{6} \dots \right. \\ \left. + \frac{M_3 \cdot S(z, j) \cdot (z - j)^2}{2} - \frac{M_4 \cdot S(z, k) \cdot (z - k)^2}{2} + \frac{C_1 \cdot z^3}{6} + \frac{C_2 \cdot z^2}{2} + C_5 \cdot z + C_6 \right]$$

Shear Diagram Front View E



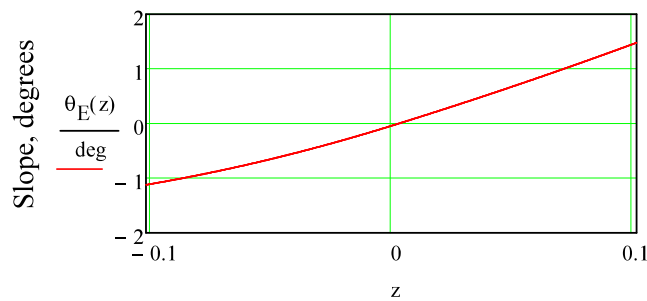
Distance, inches

Moment Diagram Front View E



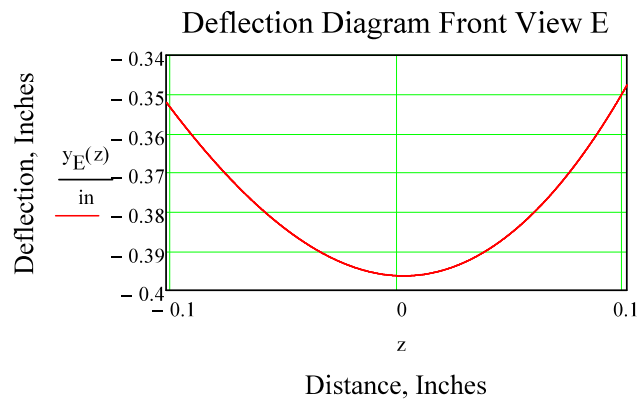
Distance, inches

Slope Diagram Front View E

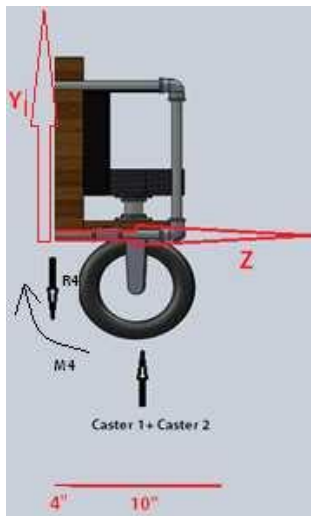


Distance, Inches





Section F



$$\sum F(y) = -R_4 + \text{Caster1} + \text{Caster2} = 0$$

$$\sum M(h) = R_4 \cdot k - M_4 = 0$$

$$\sum M(k) = \text{Caster1} \cdot (e - k) + \text{Caster2} \cdot (e - k) - M_4 = 0$$

$$z := k, (k + 0.001 \text{ in}) .. h + .1 \text{ in}$$

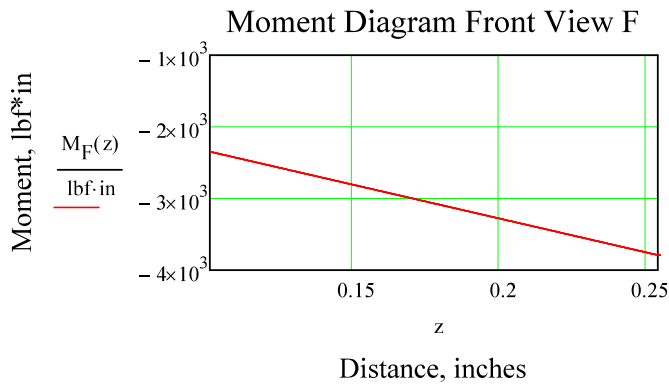
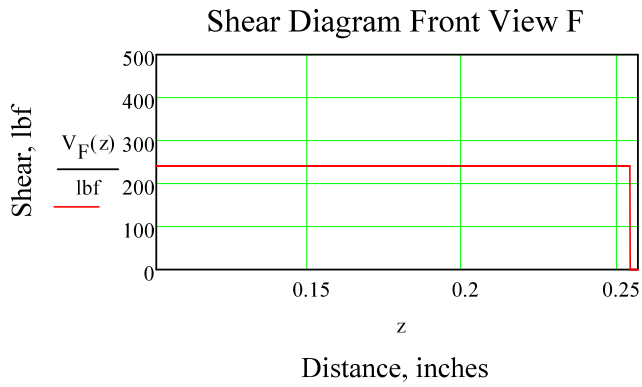
$$q_F(z) := \text{Caster1} \cdot S(z, h) \cdot (z - h)^{-1} + \text{Caster2} \cdot S(z, h) \cdot (z - h)^{-1} - R_4 \cdot S(z, k) \cdot (z - k)^{-1}$$

$$V_F(z) := \left[ \text{Caster1} \cdot S(z, h) \cdot (z - h)^0 + \text{Caster2} \cdot S(z, h) \cdot (z - h)^0 - R_4 \cdot S(z, k) \cdot (z - k)^0 + C_1 \right]$$

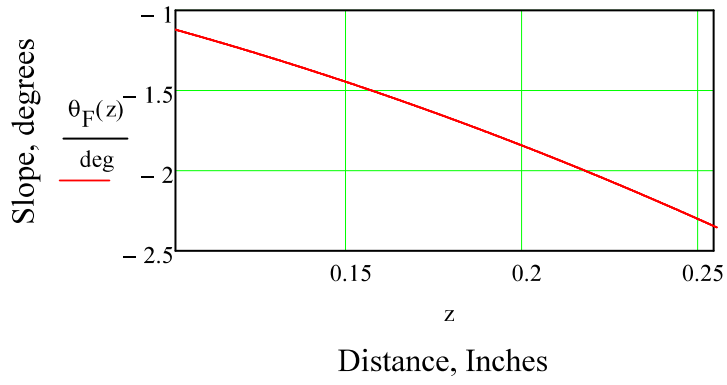
$$M_F(z) := \text{Caster1} \cdot S(z, h) \cdot (z - h)^1 + \text{Caster2} \cdot S(z, h) \cdot (z - h)^1 - R_4 \cdot S(z, k) \cdot (z - k)^1 - M_4 \cdot S(z, k) \cdot (z - k)^0 + C_1 \cdot z + C_2$$

$$\theta_F(z) := \frac{1}{E_{al} \cdot I} \left[ \frac{\text{Caster1} \cdot S(z, h) \cdot (z - h)^2}{2} + \frac{\text{Caster2} \cdot S(z, h) \cdot (z - h)^2}{2} - \frac{R_4 \cdot S(z, k) \cdot (z - k)^2}{2} - M_4 \cdot S(z, k) \cdot (z - k)^1 \dots \right. \\ \left. + \frac{C_1 \cdot z^2}{2} + C_2 \cdot z + C_5 \right]$$

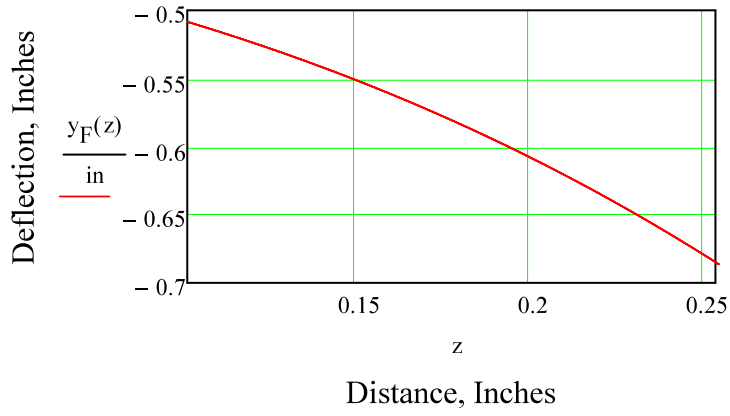
$$y_F(z) := \frac{1}{E_{al} \cdot I} \left[ \frac{\text{Caster1} \cdot S(z, h) \cdot (z - h)^3}{6} + \frac{\text{Caster2} \cdot S(z, h) \cdot (z - h)^3}{6} - \frac{R_4 \cdot S(z, k) \cdot (z - k)^3}{6} - \frac{M_4 \cdot S(z, k) \cdot (z - k)^2}{2} \dots \right. \\ \left. + \frac{C_1 \cdot z^3}{6} + \frac{C_2 \cdot z^2}{2} + C_5 \cdot z + C_6 \right]$$



Slope Diagram Front View F



Deflection Diagram Front View F



## **APPENDIX C: STEERING**

### **Details of Steering System Components**

Hardware:

Bolts:

1. Head Diameter – 0.43”, Thread Valley Diameter – 0.2”, Thread Length – 0.5”
  - a. Quantity – 28
2. Head Diameter – 0.43”, Thread Valley Diameter – 0.2”, Thread Length – 1.3”
  - a. Quantity – 1

Nuts:

1. Head Diameter – 0.43”, Head Height – 0.2”
  - a. Quantity – 45

Connection Rods:

- Material – 1/8” diameter, 7” length threaded steel rod
- Quantity - 3

Coupler Link:

- Material - 1/8” thickness, 0.5” width, 34” length steel bar
- Quantity – 2

Fork Arms:

- Material: 1/16” thickness, 1” x 1” square steel tubing
- Material cut lengthwise to produce two 0.5” x 1” C channels

L Brackets:

- Material: 1/8” thickness, 1” x 1” square steel tubing
- Material cut lengthwise at a 45 degree angle to produce two 1” x 1” Angle bars

- Cut to width required for application

Arm-Crossmember Connection:

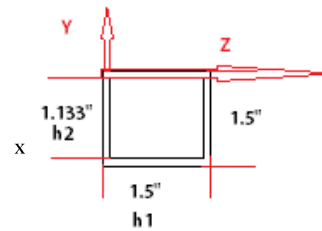
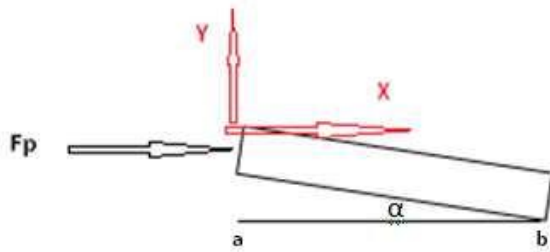
- Material: 1/8" thickness, 0.5" width, 34" length steel bar
- Material cut to length required, two holes drilled in proper position

# APPENDIX D: ATTACHMENT MECHANISM

New Attachment 1

FBD of the attachment mechanism connected to the head tube

F<sub>p</sub> = pushing force



$$Mpsi := 10^6 \text{ psi} \quad kpsi := 10^3 \text{ psi}$$

Material Properties of Aluminum

Youngs Modulus for Aluminum

$$E_{al} := 9.86 \cdot 10^6 \text{ psi} = 9.86 \times 10^3 \cdot kpsi$$

Yield Strength Aluminum

$$S_{yal} := 45 kpsi$$

Dimensions of the Square Tube

$$h_1 := 1.55 \text{ in} \quad h_2 := 1.33 \text{ in}$$

$$a := 0 \text{ in} \quad b := 6.42 \text{ in}$$

$$\alpha := 15 \text{ deg}$$

Area

$$A := h_1^2 - h_2^2 = 0.634 \text{ in}^2$$

I = the moment of inertia

$$I := \frac{(1.5 \text{ in})^4 - (1.33 \text{ in})^4}{12} = 0.161 \text{ in}^4$$

Integration Constants

New Attachment 2

$$C_1 := 0 \quad C_2 := 0$$

With singularity functions C1 and C2 are always zero, we will calculate for C3 and C4 after singularity functions are created

$$F_p := 100\text{lbf}$$

$$\sum F(y) = 0$$

$$\sum F(y) = F_p \cdot \sin(\theta) = 0$$

$$\sum F(x) = 0$$

$$\sum F(x) = F_p \cdot \cos(\theta) = 0$$

Establishing a step function

$$S(x, z) := \text{if}(x \geq z, 1, 0)$$

$$\text{Range of } x \quad x := a, (a + 0.001\text{in}).. b$$

To determine the singularity functions for shear, moment, slope and deflection we integrate in the following manner.

$$V(x) = \int -q(x) + C_1$$

$$M(x) = \int V(x) + C_1 \cdot x + C_2$$

$$\theta(x) = \int M(x) + \frac{C_1 \cdot x^2}{2} + C_2 \cdot x + C_3$$

$$y(x) = \int \theta(x) + \frac{C_1 \cdot x^3}{6} + \frac{C_2 \cdot x^2}{2} + C_3 \cdot x + C_4$$

for these integrations the following rules apply.

If  $n > 0$  and the expression inside the angular parenthesis is positive then  $f_n(x) = (x-a)^n$  the expression is a normal algebraic formula:

If  $n < 0$  then  $f_n = 1$  for  $x = a$  and  $f_n(x) = 0$  otherwise

If  $n = 0$  then  $f_n = 1$  for  $x \geq a$  and  $f_n(x) = 0$  otherwise

If  $n \geq 0$ , the integration rule is  $\int \langle x-a \rangle^n dx = \frac{\langle x-a \rangle^{n+1}}{(n+1)}$  This is the same for normal brackets

If  $n < 0$ , the integration rule is  $\int \langle x-a \rangle^n dx = \langle x-a \rangle^{n+1}$

Load Function

$$q(x) := F_p \cdot \sin(\alpha) \cdot S(x, a) \cdot (x - a)^{-1}$$

Shear Expression

$$v(x) := F_p \cdot \sin(\alpha) \cdot S(x, a) \cdot (x - a)^0 + C_1$$

Moment Expression

$$M(x) := F_p \cdot \sin(\alpha) \cdot S(x, a) \cdot (x - a)^1 + C_1 \cdot x + C_2$$

Slope Expression

$$\theta(x) := \frac{1}{E_{al} I} \left[ \frac{F_p \cdot \sin(\alpha) \cdot S(x, a) \cdot (x - a)^2}{2} + \frac{C_1 \cdot x^2}{2} + C_2 \cdot x + C_3 \right]$$

Deflection Expression

$$y(x) := \frac{1}{E_{al} I} \left[ \frac{F_p \cdot \sin(\alpha) \cdot S(x, a) \cdot (x - a)^3}{6} + \frac{C_1 \cdot x^3}{6} + \frac{C_2 \cdot x^2}{2} + C_3 \cdot x + C_4 \right]$$

Solving for integration constants 3 and 4

$$y(x) = 0$$

When

$$x = 6.42 \text{ in} \cdot \sin(\alpha)$$

and

$$x = d$$

at

$$x = 6.42 \text{ in} \cdot \sin(\alpha)$$

From the deflection expression we solve for C3

$$-C_3 = \frac{F_p \cdot \sin(\alpha) \cdot [(6.42 \text{ in} \cdot \sin(\alpha)) - a]^3}{6} + \frac{C_1 \cdot (6.42 \text{ in} \cdot \sin(\alpha))^3}{6} + \frac{C_2 \cdot (6.42 \text{ in} \cdot \sin(\alpha))^2}{2} + C_4$$

$$-C_3 = \frac{\phantom{F_p \cdot \sin(\alpha) \cdot [(6.42 \text{ in} \cdot \sin(\alpha)) - a]^3} + \phantom{C_1 \cdot (6.42 \text{ in} \cdot \sin(\alpha))^3} + \phantom{C_2 \cdot (6.42 \text{ in} \cdot \sin(\alpha))^2} + C_4}{6.42 \text{ in} \cdot \sin(\alpha)}$$



at

$x = b$

$$-C_3 = \frac{\frac{F_p \cdot \sin(\alpha) \cdot (b-a)^3}{6} + \frac{C_1 \cdot b^3}{6} + \frac{C_2 \cdot b^2}{2} + C_4}{b}$$

From the deflection equation we solve for C3

with  $x = 6.42 \text{ in} \cdot \sin(\alpha)$

$$-C_3 = \frac{\frac{F_p \cdot \sin(\alpha) \cdot (6.42 \text{ in} \cdot \sin(\alpha) - a)^3}{6} + \frac{C_1 \cdot (6.42 \text{ in} \cdot \sin(\alpha))^3}{6} + \frac{C_2 \cdot (6.42 \text{ in} \cdot \sin(\alpha))^2}{2} + C_4}{6.42 \text{ in} \cdot \sin(\alpha)}$$

We now substitute for C3 and solve for C4

$$C_4 \cdot (d - 6.42 \text{ in} \cdot \sin(\alpha)) = \frac{F_p \cdot \sin(\alpha) \cdot [(6.42 \text{ in} \cdot \sin(\alpha) - a)^3]}{6} + \frac{C_1 \cdot (6.42 \text{ in} \cdot \sin(\alpha))^3}{6} \dots$$

$$+ \frac{C_2 \cdot (6.42 \text{ in} \cdot \sin(\alpha))^2}{2} - \left[ \frac{F_p \cdot \sin(\alpha) \cdot (d-a)^3}{6} + \frac{C_1 \cdot d^3}{6} + \frac{C_2 \cdot d^2}{2} \right]$$

$$\left[ \left[ \frac{F_p \cdot \sin(\alpha) \cdot [(6.42 \text{ in} \cdot \sin(\alpha) - a)^3]}{6} + \frac{C_1 \cdot (6.42 \text{ in} \cdot \sin(\alpha))^3}{6} \dots \right] \cdot (6.42 \text{ in} \cdot \sin(\alpha)) \dots \right.$$

$$\left. + \frac{C_2 \cdot (6.42 \text{ in} \cdot \sin(\alpha))^2}{2} \right]$$

$$+ \left[ \frac{F_p \cdot \sin(\alpha) \cdot (b-a)^3}{6} + \frac{C_1 \cdot b^3}{6} + \frac{C_2 \cdot b^2}{2} \right] \cdot b$$

$$C_4 := \frac{\dots}{(b - 6.42 \text{ in} \cdot \sin(\alpha))}$$

$$C_4 = -5.919 \times 10^5 \frac{\text{in}^4 \cdot \text{lb}}{\text{s}^2}$$

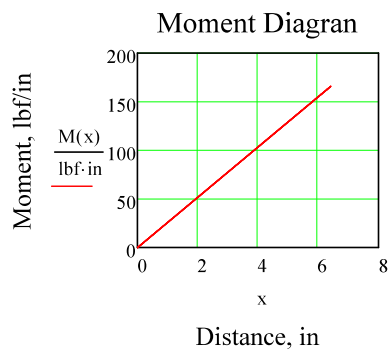
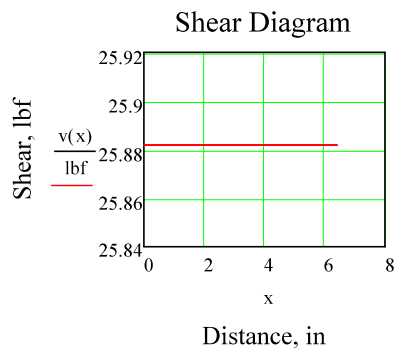
We now solve for C3

$$C_3 := \frac{\left[ \frac{F_p \cdot \sin(\alpha) \cdot (b-a)^3}{6} + \frac{C_1 \cdot b^3}{6} + \frac{C_2 \cdot b^2}{2} + C_4 \right]}{b} = 2.355 \times 10^4 \frac{\text{in}^3 \cdot \text{lb}}{\text{s}^2}$$

$$\theta(x) := \frac{1}{E_{al} \cdot I} \left[ \frac{F_p \cdot \sin(\alpha) \cdot S(x, a) \cdot (x - a)^2}{2} + \frac{C_1 \cdot x^2}{2} + C_2 \cdot x + C_3 \right]$$

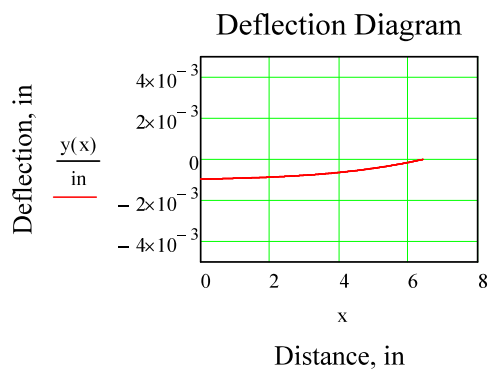
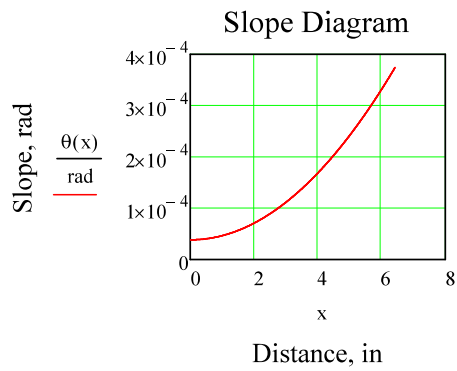
$$y(x) := \frac{1}{E_{al} \cdot I} \left[ \frac{F_p \cdot \sin(\alpha) \cdot S(x, a) \cdot (x - a)^3}{6} + \frac{C_1 \cdot x^3}{6} + \frac{C_2 \cdot x^2}{2} + C_3 \cdot x + C_4 \right]$$

We can now Graph the Shear, Moment, Slope and deflection Diagrams



Maximum Moment

$$M(6.42 \text{ in}) = 166.162 \text{ in} \cdot \text{lbf}$$



From these diagrams we can find the maximum shear and maximum moment

**Maximum Moment**

$$M_{b,max} := M(b) = 166.162 \text{ in}\cdot\text{lbf}$$

**Maximum Shear**

$$V_{b,max1} := v(b) = 25.882 \text{ lbf}$$

Now we can calculate the maximum bending stress

$$\sigma_y := \frac{M_{b,max} \cdot \left(\frac{h_1}{2}\right)}{I} = 799.23 \cdot \text{psi}$$

Maximum shear stress due to torsion stress

Q is a function of cross-sectional geometry

$$Q := 2 \cdot \left( \frac{1}{8} \text{ in} \right) \left[ 1.5 \text{ in} - \left( \frac{1}{8} \text{ in} \right) \right]^2$$

$$\tau_{.xy.} := \frac{M_{b,max}}{Q} = 351.549 \cdot \text{psi}$$

Axial Stress

$$\sigma_z := \frac{F_p \cdot \cos(\alpha)}{A} = 152.45 \text{ psi}$$

From this we can determine the principal stresses

$$\tau_{.max.} := \sqrt{\left( \frac{\sigma_y - \sigma_z}{2} \right)^2 + \tau_{.xy.}^2} = 477.669 \text{ psi}$$

$$\sigma_1 := \frac{\sigma_y + \sigma_z}{2} + \tau_{.xy.} = 827.389 \text{ psi}$$

$$\sigma_2 := 0$$

$$\sigma_3 := \frac{\sigma_y + \sigma_z}{2} - \tau_{.xy.} = 124.291 \text{ psi}$$

$$\sigma_{vmA} := \sqrt{\sigma_1^2 + \sigma_2^2 + \sigma_3^2 - \sigma_1 \cdot \sigma_2 - \sigma_2 \cdot \sigma_3 - \sigma_1 \cdot \sigma_3 + 3 \cdot \tau_{.xy.}^2} = 0.984 \cdot \text{kpsi}$$

Maximum Shear Stress Theory: Assumes that yield occurs when the shear stress exceeds the shear yield strength

$$T := \frac{\sigma_1 - \sigma_3}{2} = 351.549 \text{ psi}$$

For Aluminum shear yeild strength is approximatly 0.55\*tensile strength

Tensile strength of aluminum is minimum 75 kpsi

$$T_s := 75 \text{ kpsi}$$

$$S_{ys} := 0.55 \cdot T_s = 41.25 \cdot \text{kpsi}$$

Safety Factor, Maximum Shear Stress Theory

$$N_{MSSA} := \frac{.577 \cdot S_{yal}}{\tau_{.xy.}} = 73.859$$

Von Mises-Hencky theory

$$N_{\text{FOS}} := \frac{S_{\text{yal}}}{\left(\sigma_y^2 + 3 \cdot \tau_{.xy}^2\right)^{\frac{1}{2}}} = 44.787$$

## APPENDIX E

Tubing Number	Tubing Length	End 1	End 2
1	8.96	screw	slip
2	4.48	screw	slip
3	4.48	screw	slip
4	4.48	screw	slip
5	4.48	screw	slip
6	4.48	screw	slip
7	4.48	screw	slip
8	4.48	screw	slip
9	4.48	screw	slip
10	5	screw	none
11	3.27	screw	slip
12	9	screw	slip
13	2.59	screw	slip
14	2.59	screw	slip
15	9	screw	slip
16	7.5	screw	slip
17	3.27	screw	slip
18	7.5	screw	slip
19	9	screw	slip
20	2.59	screw	slip
21	2.59	screw	slip
22	9	screw	slip
23	9	screw	slip
24	9	screw	slip
25	9	screw	slip
26	9	screw	slip
27	9	screw	slip
28	9	screw	slip
29	10.77	screw	slip
30	8.96	screw	slip
31	10.77	screw	slip
32	8	screw	slip
33	17	screw	slip
34	10.77	screw	slip
35	8.96	screw	slip
36	10.77	screw	slip

37	17	screw	slip
38	8	screw	slip
39	8.96	screw	slip
40	12.52	screw	slip
41	8.96	screw	slip
42	12.52	screw	slip
43	3	screw	slip
44	9.5	screw	slip
45	9.5	screw	slip
46	4	screw	slip
47	22.5	screw	slip
48	4	screw	slip
49	3	screw	slip
50	9.5	screw	slip
51	9.5	screw	slip
52	30.5	screw	slip
53	30.5	screw	slip
54	4	screw	none
55	4	screw	none
56	22	screw	slip
57	17	screw	slip
58	22	screw	slip
59	17	screw	slip
60	3.52	screw	slip
61	3.52	screw	slip

Type Number	Piece Type	Piece Number	End 1	End 2	End 3	End 4
8	Elbow	11	screw	slip		
	Elbow	13	screw	slip		
	Elbow	17	screw	slip		
	Elbow	19	screw	slip		
	Elbow	24	screw	slip		
	Elbow	27	screw	slip		
	Elbow	40	slip	slip		
	Elbow	41	slip	slip		
8	Side Output	1	screw	screw	screw	

	Side Output	3	screw	screw	screw	
	Side Output	5	screw	screw	screw	
	Side Output	7	screw	screw	screw	
	Side Output	28	screw	screw	slip	
	Side Output	31	screw	screw	slip	
	Side Output	34	screw	screw	screw	
	Side Output	37	screw	screw	screw	
23	T	2	slip	screw	slip	
	T	4	slip	screw	slip	
	T	6	slip	screw	slip	
	T	8	slip	screw	slip	
	T	9	slip	screw	slip	
	T	10	slip	slip	screw	
	T	14	slip	slip	slip	
	T	15	slip	slip	screw	
	T	16	slip	slip	slip	
	T	20	screw	slip	slip	
	T	21	screw	slip	slip	
	T	22	screw	slip	screw	
	T	23	screw	slip	screw	
	T	25	slip	slip	slip	
	T	26	slip	screw	slip	
	T	29	slip	slip	screw	
	T	30	slip	slip	slip	
	T	32	screw	slip	slip	
	T	33	slip	screw	slip	
	T	35	slip	screw	screw	
	T	36	slip	screw	slip	
	T	38	screw	slip	slip	
	T	39	slip	screw	slip	
4	Cross	12	screw	slip	screw	slip
	Cross	18	screw	slip	screw	slip
	Cross	42	screw	screw	screw	screw
	Cross	43	screw	screw	screw	screw

